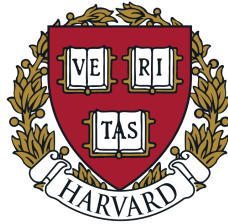


**Classification of Continuous Natural Human
Behavior Using Intracranial Field Potentials**



Jay Chandra

Department of Statistics and Molecular and Cellular Biology

Harvard University

Supervisor

Professor Gabriel Kreiman

In partial fulfillment of the requirements for the degree of

Bachelor of Arts in Statistics and Molecular and Cellular Biology

April 1, 2022

Statement of Research

The research described in this thesis was conducted at the Kreiman Lab in Boston Children’s Hospital from 2020 winter to the present (approximately 1.5 years). The Electrocorticography (ECoG) data used in this study was taken from neurosurgical procedures done by Dr. Joseph Madsen and his colleagues at Boston Children’s Hospital and Brigham and Woman’s Hospital in Boston. While I conducted the preprocessing steps for the raw ECoG, the code that I used was created by Jerry Wang (my direct graduate student advisor for the project). The code used to read in the voltage values from the large ECoG dataset and the code for detection of artifacts in the ECoG data was also produced by Jerry. In addition, a bulk of the behavior annotations for the three subjects studied in this thesis were done by a group of four volunteers. The annotations I did were primarily to correct errors in the annotations. Next, the code used to convert the annotations to a format that could be easily interpreted was written by Jerry. Finally, Jerry completed the process of converting the MRI and CT images of the brain to 3D coordinates with locations for the electrodes and brain area labels. The rest of the research was conducted by me with advice from Dr. Kreiman and Jerry. I aligned the behavior annotations with the ECoG, calculated all of the features, did analysis of the features, completed different types of classification of the behaviors using the features, did model selection and tuning, completed the analysis of brain areas and brain area interactions, generated all of the figures used in this thesis, and wrote the thesis.

Acknowledgements

I would like to thank everyone who supported me in my undergraduate journey. I would not have been able to have an enjoyable college experience without support from friends from my freshman roommates in Grays middle to my blocking group to my closest two friends who I spend almost all of my time with. In addition, I would like to thank the professors, advisors, and graduate students in the Statistics and MCB department who sparked my love of the intersection of quantitative disciplines and life sciences. More specific to this thesis project and my research, I appreciate the support that Professor Kreiman has given to me since freshman year when I started to do research with him. I would also like to thank Jerry Wang for the amount of time he spent with me, especially at the early phases of the project, helping me understand the complex dataset that was used in this thesis. Finally, above all, I want to express that this thesis and everything else that I have accomplished thus far would not have been possible without love and encouragement from my family.

Abstract

Classifying human behavior using voltage signals from the brain has primarily been accomplished in unnatural research environments where the patients are asked to do a specific movement or perform a specific task. However, in natural environments, it is very likely that brain signals are quite different than in controlled environments and decoding of the voltage data to identify behavior is more difficult. In this study, I show that it is possible to classify 12 naturally-performed behaviors (body movement, head movement, leg movement, arm movement, sleeping, eating, watching tv, playing video games, contact with the subject, patient speech, hearing speech, and quiet) using voltage data taken from Electrocorticography (ECoG) in three different subjects. I calculate many different features from the raw voltage data (time-domain features, mean power in six frequency bands, coherence in six frequency bands), and use them to classify the different behaviors (manually annotated using videos of the patient) by inputting them into a random forest classifier. I attempt classification in a binary manner (whether a behavior is occurring or not). Then, I attempt to do multi-class classification (which behavior is occurring out of a large set). Lastly, I determine whether it is possible to predict patient movement-based activities before they are physically initiated. I show that it is possible to decode movement and contact behaviors with an AUC ranging from 0.72 to 0.84, eating with an AUC from 0.86 to 0.95, patient speech and hearing speech with an AUC from 0.74 to 0.90, quiet with an AUC from 0.88 to 0.97, video games and watching TV with an AUC ranging from 0.87 to 0.95, and sleep with an AUC from 0.92 to 0.99 across the three subjects. In multi-class classification, five small scale behaviors with motor components in each subject are classified with accuracies that are 0.15 to 0.3 higher than the naive prediction. Next, I found that it was possible to do above chance prediction of patient speech, body movement, and head movement using voltage data from at least one second to two seconds before speech initiation. Finally, I conducted a thorough exploration of the brain areas (Desikan-Killiany parcellation) and brain area interactions that are important in distinguishing between whether a behavior is occurring and whether it is not. I found that the brain areas activated in this natural environment were generally similar to what is expected given previous brain studies.

Contents

1	Introduction	1
1.1	EEG and iEEG	1
1.2	Brain Computer Interfaces (BCI)	3
1.3	Neural Recording Data (ECoG)	4
1.4	Cortical Areas and Parcellations	6
1.5	Classifying Human Behavior	7
1.6	This Study	9
2	Methods	11
2.1	Human Subject Details	11
2.2	Electrode Details	11
2.3	Video Annotations	12
2.4	Signal Pre-processing	14
2.5	Feature Calculation and Validation	15
2.6	Time-Domain Features	17
2.6.1	Distribution of Signal	17
2.6.2	Amplitude	18
2.6.3	Trends	18
2.7	Frequency-Domain Features	19
2.7.1	Mean Power	20
2.7.2	Coherence	20
2.8	Choice of On and Off Time Points	20
2.9	Multi-Class Classification	21
2.10	Prediction of Future Behavior	21
2.11	Feature Scores and Significance Test	22

2.12 Model Building	23
2.12.1 Random Forest	23
2.12.2 Hyperparameter Search	25
2.12.3 Variable Selection	26
2.12.4 Sample Balancing Multi-class Classification	26
2.13 Behavior Classification	27
2.14 Mapping Electrodes to Brain Regions	28
2.14.1 Brain Region Importance	29
2.14.2 Brain Region Interaction Importance	29
3 Results	30
3.1 Video Annotations	30
3.2 Summary of Features	33
3.2.1 Time-Domain	33
3.2.1.1 Signal Distribution	33
3.2.1.2 Amplitude	35
3.2.1.3 Trends	35
3.2.2 Frequency-Domain	36
3.2.2.1 Mean Power	36
3.2.2.2 Coherence	39
3.2.3 Correlation Between Features	40
3.3 Association Between Features and Annotations	42
3.4 Overall Classification Results	44
3.4.1 Main Classification Results	45
3.4.2 Schema 2 for Off and On Timepoints	47
3.4.3 Other Classifiers	49
3.4.4 1s vs 2s Time Windows	50
3.4.5 Hyperparameter Optimization	51
3.5 Multi-Behavior Classification	55
3.6 Prediction of Future Events	55
3.7 Association with Brain Areas	57
3.8 Association with Brain Area Interaction	68

4	Discussion	82
4.1	Classification	82
4.2	Main Conclusions	82
4.2.1	Sources of Error in Classification	83
4.2.2	Training and Testing on Different Time Periods of the Day	84
4.2.3	Time Windows	85
4.2.4	Differentiating Between Multiple Behaviors	85
4.2.5	Prediction of Action Initiation	86
4.3	Implications of Classification Results	87
4.4	Association with Brain Areas and Interactions	87
4.4.1	Activities	87
4.4.2	Interpretation of Features	94
4.5	Future Directions	95
4.5.1	Patient Data	95
4.5.2	Behavior Labels	96
4.5.3	Change to the Classifier Type	96
4.5.4	Comparison of Results with Those from Non-Natural Behaviors	97
	References	98

Chapter 1

Introduction

1.1 EEG and iEEG

Over the past 100 years, the recording of electrical data in the brain through electroencephalograms (EEG) has been used to understand brain function associated with memory (Klimesch, 1999; Osipova et al., 2006; Weiss and Rappelsberger, 2000; Gärtner and Bajbouj, 2014), behavior (Mazher et al., 2015; Carus-Cadavieco et al., 2017; Armitage, 1995), cognition (Del Rio et al., 2019; Astolfi et al., 2009), movement (Seeber, Scherer, and Müller-Putz, 2016; Avanzini et al., 2012; D. Liu et al., 2018), etc. and to detect brain disorders (Aguiar Neto and Rosa, 2019; S. J. M. Smith, 2005; Atagün, 2016; Jáuregui-Lobera, 2012) by recording brain signals during resting states or during specific tasks. The neural recordings obtained from EEGs represent the summation of excitatory and inhibitory postsynaptic potentials in pyramidal cells oriented perpendicular to the surface of the brain (Rayi and Murr, 2021). These signals must pass through multiple layers including the meninges, cerebrospinal fluid, the skull, and the skin before being recorded by the EEG electrodes. As a result, this method has low spatial resolution and low signal to noise ratio, which are factors that prevent recording measurements needed for more precise assessments of brain function and circuitry (Burle et al., 2015; Schalk, 2010).

In more recent years, a technique called Electrocorticography (ECoG) has been used (Graf et al., 1984; Hill et al., 2012) to remedy this issue. The placement of electrodes is on the cerebral cortex, rather than the scalp as in the case of EEG measurements. This new arrangement in ECoG provides a unique opportunity for accessing electrical data (intracranial field potentials- IFPs) from the brain at a higher spatio-temporal resolution.

ECoG is one of the two types of intracranial EEGs (iEEG). The other type is stereotactic EEG (sEEG), which involves implanting electrodes into the brain and specific sites (Parvizi and Kastner, 2018). Due to the invasive nature of collecting ECoG (patients have their scalp and skull temporarily opened) and sEEG data (patients have small holes drilled through their scalp and skull), ECoG and sEEG have primarily been used in humans only when the procedure is medically necessary (Voorhies and Cohen-Gadol, 2013). Figure 1.1 shows the difference between EEG, ECoG, sEEG, and MEEG (similar to EEG but detects magnetic fields instead). Neurosurgeons primarily use ECoG and sEEG as a way to locate epileptogenic zones in patients with intractable epilepsy (Graf et al., 1984). Physicians will choose to use sEEG over ECoG when the location of the seizure zone is hypothesized to be in a deeper structure of the brain (not the cortex). ECoG is used over sEEG in cases where the extent of the seizure zone is not fully understood (Parvizi and Kastner, 2018). While data is being collected for epilepsy patients over multiple days, neuroscientists have begun to use the iEEG data to understand sensory pathways (Fauchon et al., 2020; Guo et al., 2021), cognition (Halgren et al., 1980; Miller, Weaver, and Ojemann, 2009), memory (Khursheed et al., 2011; Johnson et al., 2019), etc. In particular, the function and activity of the visual cortex has been extensively studied through iEEG recordings (H. Tang et al., 2014; Bansal et al., 2014).

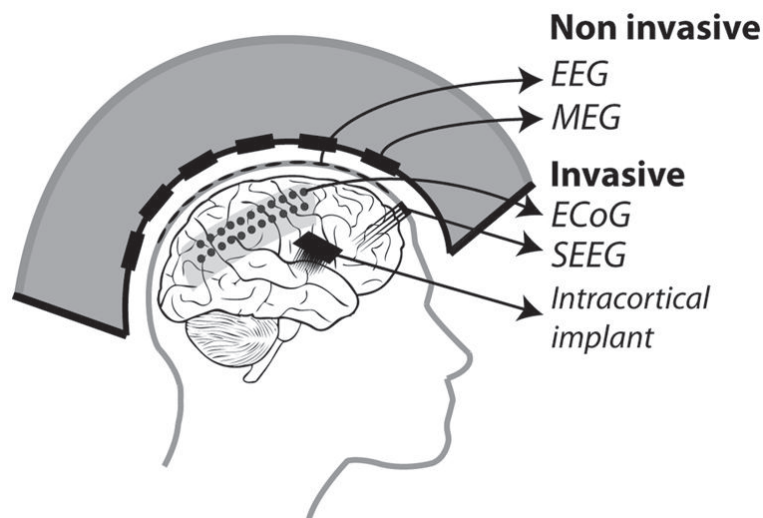


Figure 1.1 Visual Comparison of the Different Methods for Brain Activity Measurement Reprinted from Astrand et al. (Astrand, Wardak, and Ben Hamed, 2014). The Non-Invasive methods are EEG and MEG while the invasive methods are ECoG and sEEG.

1.2 Brain Computer Interfaces (BCI)

While iEEG is used to study brain processes and networks, the information that is gathered from iEEGs, particularly through ECoG, can be used in Brain-Computer Interfaces (BCIs). A BCI is a system that allows for a direct path of communication between the brain and an external device. This connection can be used to remedy disabilities downstream of the brain such as loss-of-limb, spinal chord injuries, stroke, and other neuromuscular disorders. If highly-accurate models can be trained to classify patient movements and behaviors using intracranial recordings, then this information can be translated into actions performed by prosthetics or into inputs for a tablet or smartphone (Wolpaw et al., 2002; Mak and Wolpaw, 2009). As a result, there has been extensive research into decoding human behavior such as speech (Angrick et al., 2019), arm movements (Nakanishi et al., 2013), foot movement (Satow et al., 2003), finger movements (Pistohl et al., 2012), face movement (Satow et al., 2003), perception (Tsuchiya et al., 2008), sleep vs wake (Pahwa et al., 2015), etc. In addition, deep brain stimulation (DBS), a treatment for movement disorders, epilepsy, obsessive-compulsive disorder, and other disorders, can be guided by BCIs. Currently, patients receive continuous DBS throughout the day that does not depend upon brain activity. However, DBS in response to specific brain activity recorded by electrodes has been shown to improve motor symptoms of Parkinson’s Disease patients better than continuous DBS (Little et al., 2013).

Since one of the primary use-cases for BCIs is remedying loss of limb and neuromuscular issues, it is clear why many studies are interested in decoding fine motor movements from brain activity. In fact, there have been studies that use brain signals to control prosthetics (Li et al., 2017; Yanagisawa et al., 2011; Hotson et al., 2016; Du et al., 2018). In the past year, there have been two studies that have demonstrated the potential of BCIs. Willett et al. describes decoding of attempted handwriting by one patient with spinal chord injury. The patient could not move his hand significantly due to the injury, but a grid of electrodes placed in the motor cortex was used to decode characters, words, and sentences, with high accuracy (Willett et al., 2021). Moses et al. decodes attempted speech in a patient with anarthria (inability to produce speech due to motor dysfunction) (Moses et al., 2021). A grid of electrodes was placed on the sensorimotor cortex, and the researchers used the neural recordings to detect the onset of speech and specific words.

Despite the promise of these works, they study a limited set of human actions and do

so in an incredibly controlled environment. In addition, while distinguishing individual finger movements, types of arm movements, and speech are incredibly important for BCIs since they can be used to remedy specific impairments, they largely ignore other activities performed outside of a controlled research environments. When patients undergo the ECoG procedure, often, video data of the patient is recorded, and this information can be made available for research purposes. Associating patient behavior from the video with neural recordings can allow researchers to assess the efficacy of BCIs in more natural circumstances. Wang et al. (N. X. R. Wang et al., 2017) used the video and pose estimation of patients to decode arm movements in four different subjects. While this study only analyzes arm movements, it demonstrates the need and also the difficulty of decoding natural human behavior. Derix et al. (Derix et al., 2014) similarly attempted to decode different types of speech in a natural environment using video recordings from three patients with epilepsy (results showed low very sensitivity for speech detection). Ruescher et al. (Ruescher et al., 2013) also classified speech, upper-extremity movement, and lower-extremity movement in a natural setting from videos again with very low sensitivity. Recently, a study attempted to decode movement, speech, and rest in an uncontrolled environment using computer-assigned behavior labels (N. X. Wang et al., 2016). However, the highly general activities and labeling errors limited this study. While these studies did demonstrate the ability to decode behavior in uncontrolled environments, they focused on a small subset of human activities and behaviors performed throughout the day. Preliminary work by the Kreiman group has explored natural and continuous human behavior that is labelled manually (to increase the accuracy of the labels) (Iaselli, 2018). However, the work is limited by the fact that only one subject was considered, the presence of errors in the behavior annotations, complete preprocessing of the voltage data was not completed, unexplained results for classification using specific features, and the lack of substantiation of results through associations with specific brain areas.

1.3 Neural Recording Data (ECoG)

As previously discussed, net voltage recorded by EEG and iEEG result from the postsynaptic potentials in pyramidal cells near the cortical surface. However, the levels of volt-

age are not constantly high or low throughout time. Instead, voltages oscillate throughout time at various frequencies that neuroscientists have linked to various types of human activities. The oscillatory nature results from a synchronization of neuronal excitation or inhibitions, which can drive forward specific bodily processes (Buskila, Bellot-Saez, and Morley, 2019). The amplitude of these waves are also unique to different human behaviors. Neuroscientists generally consider five different wave frequencies when characterizing and decoding brain signals: delta waves (0.5Hz - 3Hz), theta waves (3Hz-8Hz), alpha waves (8Hz-12Hz), beta waves (12Hz-30Hz), and gamma waves (30Hz-100Hz)(Posada-Quintero et al., 2019). Delta waves are generally associated with non-rapid-eye-movement sleep. However, other studies have also linked an increase in the delta content of EEG with various cognitive processes and motivation (Harmony, 2013). Theta waves are representative of the beginning of sleep but have also been associated in differentiation between emotional states, memory consolidation, and spatial navigation (Harmony, 2013; H. Zhang and Jacobs, 2015). On the sleep-wake scale, alpha waves are usually present when one closes their eyes or relaxes before going to sleep. While the source of alpha waves is not well known, alpha waves have been correlated with both inhibiting and increasing attention to a task (Klimesch, 2012). Beta waves are most prevalent in a fully awake state and are hypothesized to be involved in sensory processing, motor control, and stress(Posada-Quintero et al., 2019; Lalo et al., 2007). Finally, gamma waves (fastest waves) are associated with reaction time, attention, and working memory (Posada-Quintero et al., 2019; Kisley and Cornwell, 2006). It should be noted that these descriptions are over-generalizations and are also largely based on correlational studies. In addition, while many of these observations are based on EEG and ECoG data, some of these finding could not be made using EEG and ECoG because the waves were observed in deeper brain structures such as the hippocampus. The ultimate takeaway is, however, that while analyzing iEEG signals in the time-domain may be provide interesting insights, it is important to convert the signals to the frequency-domain and examine the delta, theta, alpha, beta, and gamma content in order to gain useful information about human behavior.

While the electrical information at each site in the cortex is important, the connectivity between brain areas and the flow of information between brain areas can also yield insights into human behavior. Anatomical connectivity is important in describing the

flow of information in the brain, but information on anatomical connectivity is difficult to gather and also differs between subjects (Burkhalter and Bernardo, 1989; Sparks et al., 2000). As a result, the correlation between brain activity in two areas has been used to provide information about the functional communication between brain areas. In addition, correlation of brain activity allows us to understand the strength of interactions and the timing of interactions (J. Wang et al., 2021). Coherence is the metric that quantifies the functional connectivity in each important frequency band listed above, and can be used as a predictor of behavior (Bowyer, 2016). For example, if one is attempting to determine when a person was playing a video game, one could observe the coherence in the beta and gamma range between electrodes in the visual cortex and electrodes in the auditory or motor cortex.

The voltage data recorded in iEEG and noninvasive EEGs in particular are subject to noise from other sources in the body and the environment. As a result, the voltage measurements at each location in the brain have a layer of noise that may obscure the brain waves that are interesting to researchers. As a result, there are different referencing methods that have been used to remove this noise (single-wire reference, common average reference, and bipolar reference). Single-wire referencing means that all voltage signals are taken in reference to one electrode. This can introduce bias if the one reference electrode is unreliable. Common average referencing takes the average signal from all electrodes and subtracts this from the electrodes. This removes noise common to all electrode sites. Bipolar referencing uses neighboring electrodes on the same electrode strips as reference. I will focus on bipolar referenced voltages throughout this study, because it produces highly local information for each electrode (Shirhatti, Borthakur, and Ray, 2016).

1.4 Cortical Areas and Parcellations

While specific areas of the the human cortex interact with many other areas of the cortex, neuroscientists have been interested in defining specific brain regions that closely interact functionally and/or anatomically. The largest divisions of the brain are four different lobes that are divided by the central sulcus (groove in the brain), the parieto-occipital sulcus, and the lateral fissure (Bui and J. Nguyen, 2019). The brain is also divided into the left and right hemisphere and is connected via the corpus callosum. Each region of the brain is

associated with different functions. For example, the prefrontal cortex in the frontal lobe is implicated in decision making, cognition, long-term memory, etc. The motor cortex in the frontal lobe controls contralateral body movements (Bui and J. Nguyen, 2019). The occipital lobe contains the visual cortex, the temporal lobe contains Wernicke’s area, which is responsible for language processing, and the parietal lobe contains the somatosensory cortex, which controls sensory information from the contralateral portion of the body. Figure 1.2 provides an illustration for these areas. Again, these are gross generalizations that have been sourced from correlation studies like lesion studies and may not be accurate. Since the primary purpose of ECoG is to identify the precise location and extent of epileptogenic zones, electrodes do not cover the entire brain and may not cover regions that are associated with a particular human behavior. This can make decoding activities particularly difficult. The few ECoG studies based on non-medically necessary procedures do not face this problem because they choose to implant the electrodes in more useful areas of the brain (Willett et al., 2021; Moses et al., 2021).

There are more granular divisions of the cortex beyond lobes and cortices. A commonly-used parcellation of the brain is the Desikan-Killiany parcellation, which subdivides the brain into 36 areas defined by gyri (ridge of the brain). There are many other parcellations including Brodmann (52 areas) (Zilles and Amunts, 2010), Destrieux (74 areas) (Destrieux et al., 2010), etc. While there is biological relevance to these divisions, the primary utility is that they can allow us to combine information across patients and combine electrodes in a single patient. There is no overlap between the precise location of the electrodes between the patients. However, if the electrodes are grouped in the different areas, then patients can be compared and the importance of a particular brain area in a particular activity can be determined.

1.5 Classifying Human Behavior

In BCIs, the main objective is to classify a set of intentions or behaviors by the patient using neural recordings. The question then becomes: How does one take a time series of voltage data from multiple patients and use this information to label a human behavior at a particular time point? As mentioned previously, this becomes a classic supervised learning task in machine learning. The common approach to classifying behavior demon-

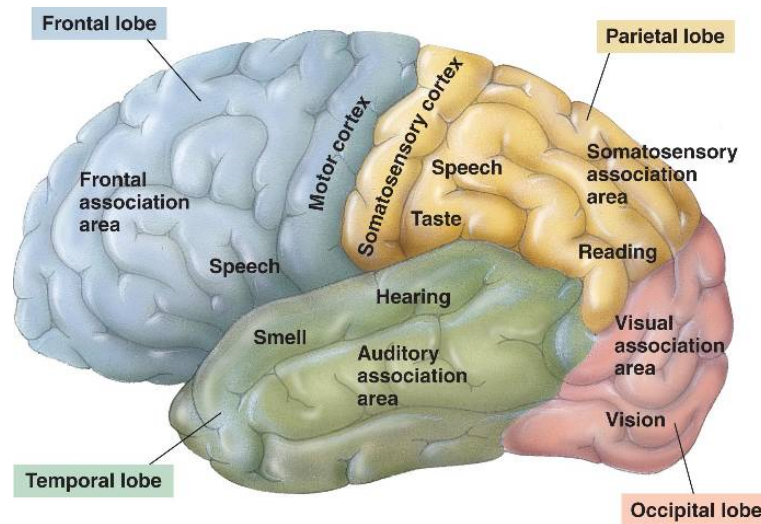


Figure 1.2 Visualization of Brain Lobes and human senses or abilities generally associated with that region. Reprinted from (*brain-lobes.html 49_15CerebralCortex-L.jpg* 2021)

strated in previous studies is to calculate spectral features outlined in section 1.3 from each electrode and use these variables to understand a particular behavior or particular set of behaviors that are occurring. Depending on the type of classifier, raw voltage values can also be used as inputs. There are many different types of existing classifiers that can be useful for this task (and have been previously used for this task). The simplest method, that has in some circumstances been found to outperform more complex classifiers in human movement classification based on ECoG data, is logistic regression (Marjaninejad, Taherian, and Valero-Cuevas, 2017). Logistic regression creates predictions that are functions of the probability of an event based on a linear combinations of predictors. In this case, the event is whether a behavior is occurring or whether a behavior is not occurring. This model type, especially after regularization techniques are applied, is more generalizable, interpretable, and overfits less to the training data in comparison to other classifiers. Logistic regression is also parametric in nature because it fits specific values that describe a distribution or the relationship between the input variable and the output variable. Other simple parametric classifiers that have been used in classifying human behavior include naive bayes (Chestek et al., 2013), which uses bayes rule to calculate the posterior probability of a particular class for a test data point given the training data. Linear discriminant analysis (LDA) (Bleichner et al., 2016) is somewhat similar to naive bayes but one major advantage is that it doesn't assume independence between features. LDA attempts to project the multidimensional data into a smaller dimension

that maximizes the linear separation between data samples with different class identities. An extension of LDA is Quadratic Discriminant Analysis, which finds a non-linear boundary between classes. Finally, linear support vector machines (SVM) (Ryun et al., 2014) find optimal hyperplanes that separate behaviors from each other based on a set of features. An SVM can have a radial kernel function. Instead of finding a hyperplane of separation, two classes can be distinguished by a "curved" surface. This method is especially prone to overfitting. Other non-parametric models include k-nearest neighbors (KNN) (Chin et al., 2007), which calculates the distance between a new point and the known training point and decision tree based models (Kennedy and Adams, 2003), which splits groups based on the values of predictors, and the best split is chosen based on the split that maximizes class purity in each node. I will be experimenting with all of the above methods while trying to classify behaviors based on ECoG data.

The above methods have been the most popular when decoding brain signals. However, these algorithms largely ignore the time series nature of the data. The voltage data and the labels for human behaviors occur in a specific order. In the above methods, if the data were shuffled in time, there would be no difference in the model and classification accuracy. However, it is possible that neural information before a behavior is performed would be important for classification. While they have not been widely applied in the context of BCIs, time series classification algorithms such as KNN with dynamic time-warping could be useful (Bagnall et al., n.d.) (these methods are quite computationally intensive). There are ways to avoid these methods based on the way that the classification problem is constructed and the types of features included, however.

1.6 This Study

BCI studies have primary only been done in controlled environments and on a specific set of behaviors. In this study, I will be using neural recordings from ECoG to decode many large-scale natural behaviors that a patients performs repeatedly throughout the day (rather than directed activities that a patient performs in a research setting). Also, I will show that it is possible to differentiate between multiple similar behaviors such as arm movement, leg movement, head movement, and speaking. In addition, in Wang et al. (N. X. R. Wang et al., 2017), they showed it was possible to predict finger/arm

movement well before the movement initiation. For highly repetitive activities such as body movement, head movement, arm movement, leg movement, and patient speech, I will show that there is an above chance ability to detect these activities even before the initiation of the movement. Classification will be accomplished using multiple different features and methods listed in section 1.5, and the results will be compared to choose a classifier with the best accuracy and related metrics. Finally, I will describe the brain areas and the connections between brain areas that are associated with different human behaviors.

Chapter 2

Methods

2.1 Human Subject Details

I analyzed data from 3 subjects with pharmacologically intractable epilepsy who were undergoing a neurosurgical procedure to treat the epilepsy. Demographic details on each subject and the number of implanted electrodes are provided in Table 2.1. In addition, it is important to note that all of the electrodes were implanted on the right hemisphere of the brain.

To identify the specific epileptogenic zones, these patients underwent ECoG. The intracranial field potentials (IFP) that were collected during this procedure were made available for research purposes and this was approved by the Institutional Review Boards at Boston Children’s Hospital. Procedures and data usage were conducted with the subjects’ informed consent.

Subject	Age	Gender	Ethnicity	Electrodes	Bipolar Electrodes
1	32	Male	White	40	35
2	11	Male	White	104	91
3	16	Female	White	176	154

Table 2.1: Subject Details

2.2 Electrode Details

As described in (J. Wang et al., 2021), subjects were implanted with platinum electrodes (Ad-Tech, Racine, WI, USA; 2.3 mm diameter exposed area, with inter-electrode dis-

tances of 10 mm, impedance $\leq 1\text{k}\Omega$). All electrodes were implanted in the subdural cavity in a grid or strip pattern. Each of the three patients had a different arrangement of electrodes and location of electrodes according to the needs of the neurosurgeon. The number of electrodes and the arrangement of the electrodes are provided in Table 2.1 and Figure 2.1 respectively.

In addition, as described in (J. Wang et al., 2021), the neurosurgeons took T1-weighted magnetic resonance imaging (MRI) images of the brain before electrodes were implanted. In order to get the structure of each individual brain, we used the freesurfer package (Dale, Fischl, and Sereno, 1999). It is able to take the MRI images and provide the coordinates of the surface of the brain. Then, the implanted electrodes were imaged through computed tomography (CT), and they were lined up with the MRI images using the iELVis package (“iELVis: An open source MATLAB toolbox for localizing and visualizing human intracranial electrode data” 2017).

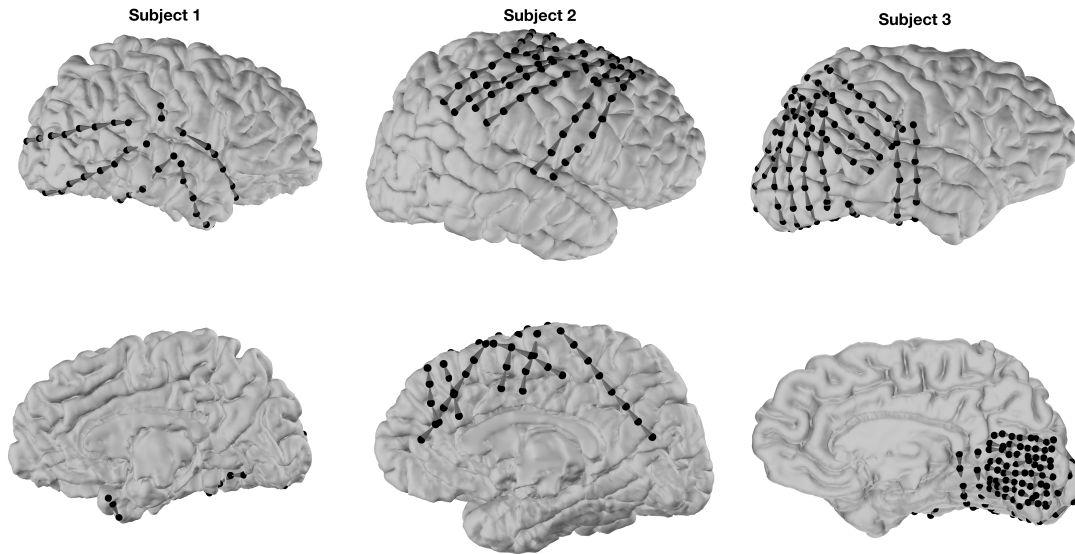


Figure 2.1 Location of the electrodes in the 3 subjects. The black spheres are the electrodes and the grey cones are the grid/strip connections between electrodes

2.3 Video Annotations

The video annotations (ten behaviors/activities that the patient was doing) were manually added for the three different subjects. These annotations were based on the audiovisual recordings of the patients. The behaviors were annotated in the Natus Neuroworks

software with a custom-made interface for selecting when an activity was happening and when it was not. The "on" and "off" time points for each activity were recorded on a millisecond timescale so that they could be aligned with the electrical data. All three patients had eight of the same behaviors labelled:

1. **Contact:** Someone else is physically coming into contact with the subject. This includes both activities in which the patient initiates the contact with the other person and when another person initiates contact with the patient. This does not include contact with inanimate objects such as blankets or pillows or a game controller as the patient would then be in physical contact with something at every time point.
2. **Eating:** The patient is actively consuming food or drinking. This does not include the time points where the food is in front of the patient or when the food is being cut, for example. It only includes the time when the patient is chewing, swallowing, or bringing food to the mouth.
3. **Head Movement:** The patient is moving their neck to create movement to their head. Any movements of the face itself including chewing, smiling, or raising eyebrows are not included in this behavior type.
4. **Patient is Talking:** The patient is actively producing speech. Simply producing sound from the mouth is not included in this class. Therefore, humming, burping, or other general sounds are not included.
5. **Sleep:** The patient is sleeping. It is important to note that it is difficult to determine precisely when the patient had fallen asleep. We used cues such as closing of the eyes to label sleeping. This would therefore include all of the classical stages of sleep.
6. **Someone is Talking:** Someone else in the room is talking. The patient does not need to be a part of the conversation (although they could be). The nurse could be talking to the mother in the room or the patient could be directly talking to their mother.
7. **Video Games:** The patient is playing games on the computer or doing a specific experiment (created by researchers) on the computer

8. **Watching TV:** The patient is watching the television actively. If the TV is on and the patient is not paying attention to, then this activity is not valid.

Annotations for patient 1 also include two motor based actions:

1. **Arm Movement:** Any type of movement of the arm, forearm, or hand.
2. **Leg Movement:** Any type of movement of the thigh, lower leg, or foot.

Annotations for patient 2 and 3 also include two more behaviors:

1. **Body Movement:** Any type of movement excluding head movements. This includes arm movement, leg movement, hip movement, etc.
2. **Quiet:** The level of noise excluding human talking is low or zero. The patient is usually resting during this time with minimal interactions with others.

Four people were assigned to the task of labelling the behaviors given the video of the patients. The sheer length of the recordings and the slow speed at which one must watch the video to get correct labels means that this labelled dataset took many days to create. Errors are inevitable in such a labelling schema. However, I manually corrected many of these errors at later time points to ensure the robustness of the labels. Any major errors especially for the large scale events like sleep or watching TV were corrected. In addition, there were time points in which we were unable to see or hear the patient. I considered these regions as unlabelled/undefined.

2.4 Signal Pre-processing

The voltage signal was pre-processed as described in Wang et al. (J. Wang et al., 2021). I did bipolar re-referencing of the electrode potentials in relation to the nearest electrode. As explained in the introduction, bipolar re-referencing allows for the reduction of bulk neural signals that are present in the brain and emphasizes the smaller, local changes. With this method, there is more region-specific information. However, with this re-referencing method, there is a loss of useful information that may be the same everywhere. For example, if a constant voltage throughout a region is representative of a certain activity, then this value will be subtracted off from each electrode and we will see no

signal. Ultimately, I believe that the the information gained is much more important the information lost. Bipolar referencing is defined simply by the following expression: $V_{jt} = V_{it} - V_{(i+1)t}$ where j denotes the index of the bipolar electrode, i denotes the index of the true electrode and t is the time point.

There are a few different sources of error in recording the voltage signals that can be systematically removed. One example is DC offset caused by the interface between the electrodes and the fluid in the area. The recording method removed the DC offset so that we could observe changes on the scale of μV (the DC offset can be on the scale of mV). Another source of error is power noise from the alternating current in the recording instrument. There are multiple different ways to remove this noise (Akwei-Sekyere, 2015) but the most common method is notch filtering at harmonics of 60Hz. While this can lead to distortion in the signal, it does ensure that there is less noise in the gamma frequency. A fifth-order butterworth notch filter with a bandwidth of 3Hz was used to remove the power noise in the harmonics of 60Hz. The final source of noise that was explicitly accounted for was from other medical devices. It was removed with a fifth-order butterworth notch filter with a bandwidth of 4Hz at 20Hz.

All the voltage signals were sampled at 250Hz or down-sampled to 250Hz.

2.5 Feature Calculation and Validation

While the annotations were recorded at a millisecond level, it would be incorrect to think that a person could record patient activity at that temporal resolution even if the video is slowed down. Therefore, I binned the labeled activities and the calculations of features at the one second level (and two second level as a sensitivity analysis). As long as more than 50% of the time window had the activity label, it was considered as "on" for the activity. If not, the activity was considered as "off". This approach also allows for the calculation of higher order features beyond just the raw bipolar voltages at a particular time point. In addition, when binning into specific time periods, it is important to identify the set of artifacts and noise in the data that are not physiologically significant but are instead caused by the recording methods. As described in Wang et al. (J. Wang et al., 2021), there are five different artifacts that were searched for in the voltage signal:

1. **Large Amplitude:** Range of voltage was greater than 2000 μV in the chosen time

interval (main analysis uses a time interval of one second).

2. **Large Slope:** $|\frac{dV}{dt}| > 100\frac{\mu V}{ms}$. This would represent a large jump in voltage that is not feasible in physiological circumstances.
3. **Small Amplitude:** There is not substantial variation in the voltage in the chosen time period. This could be representative of incorrect detection of the changing voltage in that particular bipolar electrode.
4. **Seizure Events and Interictal Discharges:** Seizure events and the surrounding fifteen minutes are marked by clinicians. In addition, Interictal Discharges, which are characterized by a set of abnormal electrical events in between epileptic events that are not as severe as seizure events (E. H. Smith et al., 2022), are also marked by clinicians.
5. **Cortical Stimulation:** In order to determine the region of the brain primarily responsible for the epilepsy, electrical stimulation was provided to the brain. These time points would not be valuable for our analysis and were therefore marked as artifacts.

The first three artifacts were calculated per bipolar electrode and per time point. However, the last two were calculated per time point only (all electrodes were not usable during those time points). This distinction is important in the classification step, because in the case of artifacts 1-3, there is no need to completely remove a time point. Instead, only one electrode would not be included in the analysis. Overall, 0.09%, 0.28%, and 0.98% of the one second time intervals and bipolar electrodes combinations contained any of the artifacts 1-3 for subjects 1-3 respectively. 0.69%, 0.81%, and 0.0% of the one second time intervals contained artifacts 4 and 5 for subjects 1-3 respectively.

Overall, there are many different features that can be calculated given a time series of data in a window of one second or two seconds (where there are 250 and 500 data points due the 250Hz sampling rate). These features can be separated into two major categories: Time-Domain and Frequency-Domain.

2.6 Time-Domain Features

Time-Domain features are calculated from the raw voltage signals during the time window. There are many different options for these features including those that describe the distribution of the voltage, the amplitude, signal complexity (entropy), and long-term trends (Boonyakitanont et al., 2020). Here, I chose seven different features from the raw voltage signals that were minimally correlated, so that each feature provides unique information for classification. The overall goal was to choose features that were biologically relevant, provided good separation between on and off states of the behaviors, and were not highly correlated with other features.

2.6.1 Distribution of Signal

Features included in this group include the classic statistical measures of a distribution including the mean, mode, median, standard deviation, interquartile range, moments (skewness, kurtosis, etc.). To be conservative in the possible features included, I chose the mean absolute value (MAV), the minimum value (MIN) the maximum value (MAX) of the waveform, and shannon entropy of the signal (ENT). The extremes of the distribution will tell us about spikes in the data that may be informative. Mean absolute value will capture the true value of the voltage without information being lost through negative and positive voltages averaging out. In other words, it is the mean magnitude of the signal. It is difficult to detect whether there is a net inhibitory postsynaptic potential or excitatory postsynaptic potential just by the sign of the voltage due to the organization of the pyramidal neurons and the many locations to create an inhibitory or excitatory effect. However, the MAV feature may hold some of this information. The shannon entropy feature is not firmly rooted in biology but instead quantifies the variation in the distribution of the signal. High entropy can be interpreted as a lot of different values with equal probabilities (uniform distribution). Instead, if there is little variation in the signal over time, and there is a lot of probability density at a particular voltage, the entropy will be low. Overall, here are the definitions of these features:

- **MAV:** $\frac{1}{n} \sum_{i=1}^n |v_i|$
- **MIN:** $\min(v_1, v_2, \dots, v_n)$

- **MAX:** $max(v_1, v_2, \dots, v_n)$
- **ENT:** $-\sum_{i=1}^n P(v_i) \log(P(v_i))$

where v_1, v_2, \dots, v_n are the voltage values in a particular time window

2.6.2 Amplitude

As described in the introduction, there is an oscillatory nature in iEEGs that represent the synchronous excitations and or inhibitions. The strength of these synchronizations can be quantified by the root mean square (RMS) voltage, which captures the amplitude of the waves. Our definition may be different than those used in other works.

RMS: $\sqrt{\frac{1}{n} \sum_{i=1}^n (v_i - \bar{v})^2}$ where i is the i th time point in the time window of size n

2.6.3 Trends

When visualizing the voltage signals in the one minute and two minute windows, there seemed to be a few overall patterns. One is a signal where there is pseudo-random variation around an overall mean or overall pattern. Another is where there are local trends in the data where the overall mean or pattern is not returned to easily. A way to differentiate between these two patterns is the Hurst Exponent (HE). An HE of 0.5 indicates a random walk, an HE less than 0.5 indicates a time series that reverts to the mean, an HE greater than 0.5 indicates a time series that has a high positive auto-correlation where high values will be followed by high values and vice versa. Biologically, high values of HE could represent a positive feedback system where positive or negative voltage signals are amplified. Low values of HE could represent a negative feedback system where signals are dampened. The exact calculation of HE is provided in the following algorithm:

HE: Divide the overall time series of length N into segments of size N/m where $m = 1, 2, \dots, 20$ (the maximum value of 20 is arbitrary). This is done by taking every m th element of the overall time series starting for the 1 through m th element of the time series. Then follow this procedure for each segment of length q .

$$vmean_i = v_i - \bar{v} \text{ (mean centering)}$$

$$cmean_i = \sum_{j=1}^i vmean_j \text{ where } i \text{ is } 1, 2, \dots, q \text{ (cumulative values the mean)}$$

$$R = max(cmean_1, cmean_2, \dots, cmean_q) - min(cmean_1, cmean_2, \dots, cmean_q)$$

$$S = \sqrt{\frac{1}{q-1} \sum_{i=1}^q cmean_i - cm\bar{e}an}$$

$$D = \frac{1}{m} \sum_{i=1}^m R/S \text{ for all different ordered time series of length } q.$$

Once D is calculated for all values of m, we can fit the following curve and solve for H to determine the Hurst exponent for a particular time series:

$$D(q) = H \log(q) \text{ The OLS estimate of the slope can be used to estimate H.}$$

2.7 Frequency-Domain Features

As discussed in the introduction, brain voltages have cyclic patterns due to synchronous excitations or inhibitions. The relative amount of the signal in different frequency bands is relevant and linked to different behaviors. As a result, I studied six major frequency ranges that have been previously described in the literature: Delta (0.5Hz-3Hz), Theta (3Hz-8Hz), Alpha (8Hz-12Hz), Beta (12Hz-30Hz), Gamma (30Hz-100Hz), Broadband (0.5Hz-125Hz). All frequency-domain features depend on the estimate of the power spectral density for the wave in a particular time window. There are a few ways to estimate the power spectral density including the fast fourier transform, maximum entropy spectral estimation, and Welch's method. Welch's method tends to be the most reliable (although computationally intensive) because of the averaging over multiple smaller time periods within the signal. The parameters for the Welch's method (we used the *welch* function in MATLAB) includes the number of divisions of the original signal, the amount of overlap, and the windowing method to use (due to the sampling of the signal, spectral leakage occurs where peaks of frequency can be spread across surrounding frequencies). Here, I used an overlap of 50% and a hamming window. Generally, lower window sizes are ideal as you can average over more samples. However, the spectral resolution (spectral resolution = $\frac{1}{window \ size}$) will lower if the window size is lower. This is why I use a window size of 0.5 seconds (spectral resolution = 2Hz) for the delta, theta, and alpha frequencies and 0.2 seconds (spectral resolution = 5Hz) for the beta, gamma, and broadband frequencies. Once the power spectral density is calculated, we can then calculate a few different features. It should be noted that in my calculations, I excluded information from frequencies within 4Hz of the 20Hz medical instrument noise and within 3Hz of the 60Hz power line noise.

2.7.1 Mean Power

The mean power is a basic feature of the power spectral density. It tells us the relative amount of content in each frequency band. While simple, this feature has proved to be quite useful in decoding tasks. The final result is one feature for each electrode and frequency band.

2.7.2 Coherence

Coherence is a metric of the power transfer between two systems. It can also be thought of as correlation in the frequency domain and is a proxy for the functional connectivity in the brain. Notably, the coherence does not provide information on the direction on power transfer. Here, I calculated the coherence between the voltage signals in all possible pairs of bipolar electrodes. As a result, for each patient and each frequency band, there were $\binom{n}{2}$ features where n is the number of bipolar electrodes. Coherence is defined as follows:

$C_{xy}(f) = \frac{|P_{xy}(f)|}{\sqrt{P_{xx}(f)P_{yy}(f)}}$ where f is a particular frequency, x is the first signal, y is the second signal, P_{xy} is the cross spectral density, P_{xx} is the power density of signal x, and P_{yy} is the power density of signal y

$P_{xy} = \frac{1}{2\pi} \sum_{-\infty}^{\infty} R_{xy}(\tau)e^{-if\tau}$ where $R_{xy}(\tau) = \sum_{t=1}^T v_x(t)v_y(t + \tau)$ where T is the length of the time window and $v(t)$ is the voltage at time t.

I used the *mscohere* function to calculate the coherence with the same power spectral density estimate method described at the beginning of this section. All feature calculations were performed in MATLAB and more computationally intensive calculations (coherence features) were parallelized on the FAS cluster.

2.8 Choice of On and Off Time Points

For almost every behavior, there is a severe class imbalance where there are more times in the day where the patient is not performing the behavior in comparison to when they are. There are many different ways to deal with class imbalance (one way is to not deal with it- there are metrics for classification performance that are robust to class imbalance). If the number of time points that are considered on is N, then we could randomly sample N time points from all of the off time points. The issue with this is when behaviors are done at certain times of the day, then we are instead decoding the time of day rather than

the activity itself. This would result in an inflated accuracy of decoding. An alternative approach would be to sample the time points that surround the on points. This is an attractive choice because it solves the problem of auto correlation in the signal being used for prediction and also more closely mimics a real scenario where a brain computer interface would want to detect the start of a behavior and the end of the behavior. In practice, this means I iterated through each section when the behavior was occurring and when the behavior was not occurring. If the on length was N , then I tried to find $N/2$ length off periods surrounding the on segment. If there was not enough off time points surrounding the on segment, I would then have asymmetrical off segments surrounding the on segments to ensure that the total length of the off segments was equal to the on segment. Lastly, there are a few cases where there are not long enough off time segments surrounding the on segment to create a balanced dataset. This results in a situation where the length of off segments is strictly less than or equal to the that of the on segments. To remedy this, I provide results where I sub-sample the on segments.

2.9 Multi-Class Classification

Instead of detecting whether a specific activity is occurring or not, I also attempt to determine if the short time-span activities that had a physical component to them could be classified with above chance probability. For subject 2 and 3, the activities that satisfied this condition are body movement, contact, eating, head movement, and patient is talking. For subject 1, the activities that satisfied this condition are arm movement, contact, eating, head movement, and leg movement. Note that patient is talking was not included because for subject 1, the patient is talking behavior happened for long stretches of time and had more than 50 times the samples as some of the other activities. For the selection of the time points for each class, I took all of the samples in each class and removed the samples that overlapped with the other classes for that subject.

2.10 Prediction of Future Behavior

Prediction of future behavior would be valuable only for activities that are initiated by the subject. For subjects 2 and 3, this includes body movement, head movement, and

patient is talking behaviors. For subject 1, this includes arm movement, leg movement, head movement, and patient is talking. I defined the on time points as the one-second sample t seconds before the actual starting point of the behavior and the off time points as the one-second sample $t - 1$ seconds before the actual starting point of the behavior. If the off timepoint corresponding to the on timepoint overlaps with the another on timepoint, then the pair of off and on timepoints is discarded. The t s considered are 1s, 2s, 3s, and 4s.

2.11 Feature Scores and Significance Test

In the case of subject 3, who has the highest number of features since there are 154 bipolar electrodes, there are $154 * 12 + 11781 * 6 = 72534$ features. Even in the case of subject 1, who has the lowest number of features since there are only 35 bipolar electrodes, there are $35 * 12 + 595 * 6 = 3990$ features. Therefore, it is valuable to get a simple estimate of the importance of each feature in distinguishing between the on and off states for each behavior both from a variable selection stand point and biological importance stand point. In signal processing, the discriminability index (d') is used to determine whether a feature is useful in distinguishing between two different signals. This metric is also the same as the two-sample t-statistic.

$$d' = \frac{\bar{on} - \bar{off}}{\sqrt{\frac{s_{on}^2}{N_{on}} + \frac{s_{off}^2}{N_{off}}}}$$

where s is the sample standard deviation

In determining the statistical significance for each electrode, I considered many possible tests. Ultimately, I used the wilcoxon rank sum non-parametric test because of the strong right-skew in many of the feature distributions. While the sample size of each feature was nearly 1000 at minimum, I thought that this test would still be more reliable. The test of significance was applied for every bipolar electrode. Therefore, there was risk for an inflated type II error rate. To mitigate this, I used the conservative bonferonni correction. The new confidence level was 0.05 divide by the number of electrodes times the number of features.

2.12 Model Building

As discussed in the introduction, there are many methods for accomplishing supervised learning (especially binary classification). Simpler methods (but not necessarily less effective) for binary classification includes logistic regression, naive bayes (*fitcnb* in MATLAB), QDA (*fitcdiscr* in MATLAB), and KNN (*fitcknn* in MATLAB). More cutting edge methods include random forest and SVM with a radial kernel (*fitcsvm* in MATLAB). Ultimately, there is no good way to decide which classifier to use other the heuristics provided in section 1.5. I trained many of these classifiers and evaluated their performance in an unseen test set. Results will be provided for multiple classifiers in one subject as a comparison. However, for most of the classification problems, I decided to use the random forest model (specifically the *TreeBagger* or *fitcensemble* MATLAB implementation of the random forest model) as it is quite robust in high dimensional datasets, is complex enough to model intricacies in the data, overfits much less to the training data due to the bootstrap sampling and feature subsetting at each split, and the robust approach to dealing with missing data through surrogate splits (stores the next best split if the feature is missing). Surrogate splits are important here as about 3% of the data is missing for any given feature. If I try to train a classifier on multiple features, then I will have to throw out anywhere from 5%-60% of the data depending on the subject.

2.12.1 Random Forest

I will focus on the theory and algorithm of the random forest here as it is the primary classifier used in classification. Random forest models are made of a set of decision trees. The key difference between the random forest and classical decision trees is the bootstrap resampling of the main dataset to create many different datasets and the consideration of only a subset of features at each split of the tree. For one of the bootstrap resampled datasets, the following steps occur until the maximum number of splits is reached, all leaves are pure (only one class in the leaf), or the minimum leaf size is reached in all cases:

1. A set of features are randomly sampled from the larger set of features.
2. All possible splits (thresholds) are considered for these features. The best possible split is defined (for classification problems) by an impurity score. The impurity

score is a measure of the abundance of the classes in the leaf. Ideally, there would be a 0 impurity, which means all observations are of one class. Here, I used the gini index, which is defined by the follow function $Gini = 1 - \sum_{j=1}^C p_j^2$ where p is the proportion of observations in class j and C is the total number of classes. Notice how the Gini Index is 0 (optimal) if one p_j is 1. The maximum value is 0.5, when the classes are equally present in the node.

3. The impurity score is calculated for every possible split. Note that the impurity score is a weighted average (proportional to the number of samples in each resulting node) of the impurity of the two resulting nodes. The lowest impurity split is picked. If there is missing data for a particular feature, then the that sample is not included in the impurity score calculation. However, the classifier will search for the next best split based on another variable for each sample missing the feature.
4. For each node created, repeat steps 1-3 unless the maximum number of splits or the minimum leaf size is reached for a resulting node.
5. Steps 1-4 are repeated for each bootstrap sample
6. Finally, for each observation, there is a single vote from each decision tree that is created. The final class probabilities for each observation is based on the proportion of votes from each tree and the predicted class is the majority class predicted.

The purpose of a random forest is to reduce the variance in final predictions, thereby reducing overfitting. It will do so first by bootstrap resampling. If \hat{Y}_1 are the class predictions of decision tree one, then the variance will be $Var(\hat{Y}_1)$. If I then add N trees, the variance will be $Var(\frac{1}{N}(\hat{Y}_1 + \dots + \hat{Y}_N))$ which becomes $\frac{1}{N^2} \sum_{j=1}^N Var(\hat{Y}_j) + \frac{1}{N^2} \sum_{i \neq j} Cov(\hat{Y}_i, \hat{Y}_j)$. The variance of the average predictions is less than or equal to the individual variance (especially evident in the case than $N = 2$). However, through bootstrap sampling, the trees will be very similar and the covariance terms will be high, causing the variance drop to be small. The trees can be forced to have lower covariance by randomly sampling predictors at each split. The higher the number of variables sampled at each split, the more the algorithm is simply a bagging algorithm rather than a random forest. As the number of variables goes to 1, there may be increased bias in predictions.

2.12.2 Hyperparameter Search

Once a model type is decided upon, the hyperparameters in the model still need to be selected. There are a number of heuristics to decide on these values. Alternatively, a popular method is to separate the data into a train, validation, and test set. For each behavior and for each patient, I would train a model with a specific set of hyperparameters on the train set and calculate the error rate in the validation set. This would be done for all shuffles of the train and validation sets (in this case- 5-fold cross validation). Then, I would repeat this with another set of parameters and finally the model with the lowest average error rate would be finally used on the test set. This would be the final result used. While this procedure is rigorous it is also very computationally intensive given that there are many different classification problems (ten behaviors for three subjects and multiple classification schemas).

The way to choose the hyperparameters to assess, can be done in a few different ways: random search, grid search, Bayesian model-based selection. Grid search and random search does not use the results from previous hyperparameter tests. However, grid search does use parameters that would seem plausible (the range of hyperparameter search is specified). The method used in this manuscript is the Bayesian approach. A distribution of the model score given the hyperparameters is created, then I sample the best parameters from it, evaluate the hyperparameters on the true objective function, and then update the distribution of the model score given this information. Then a new set of hyperparameters are selected based on the new distribution of the model score given the hyperparameters. This procedure was implemented using the *bayesopt* function in MATLAB.

The cost function used as the objective function is the sum of the misclassification cost: $L(\mathbf{X}) = \sum c_{y_j \hat{y}_j}$ where c is the cost of classifying sample j in predicted class \hat{y}_j when the true class is y_j . \mathbf{X} is the set of hyperparameters.

To choose the next point to evaluate to better estimate the surface of the objective function, the minimum mean of the posterior distribution is chosen. In the MATLAB implementation, the next point is also chosen based on the time cost of evaluating the next point. In addition, if a particular set of hyperparameters is being oversampled, then noise is added to the estimated surface to coax the original next point algorithm to pick another point away from that set.

As presented later in the results section, the AUC of the classifier does not increase by much (and sometimes decreases) through hyperparameter search. Therefore, hyperparameter search was not conducted in the main classification results.

2.12.3 Variable Selection

Finally, while for a random forest, having a large amount features (even greater than the number of samples) generally doesn't cause issues, I decided to reduce the number of features by only taking the top 50% off the electrodes for each feature based on the discriminability index. For the coherence features, I chose the square root of the total number of electrode pairs as the number of electrode pairs to include in the classifier.

2.12.4 Sample Balancing Multi-class Classification

In order to produce class probabilities that aren't biased towards the more abundant class in multi-class classification, there needs to be a change to the classifier and/or the samples given for the classifier. As defined before, the Gini index is $Gini = 1 - \sum_{j=1}^C p_j^2$ where p is the proportion of observations in class j and C is the total number of classes. Here, the smaller classes will influence the Gini impurity index much less because their proportions will be small compared to the abundant class. Therefore, the decision tree will attempt to classify the abundant class better with little regard to the small sized class. This can be mitigated through re-weighting the classes so that correctly classifying the minority class is equally important as classifying the majority class. Alternatively, the bootstrap sample can favor the minority class so that each decision tree sees more of the minority class. The MATLAB *TreeBagger* implementation of Random Forests allows for input of a cost matrix which specifies the cost of misclassifying a particular class. I defined the cost of misclassification as the inverse of the number samples in that class. Therefore, the cost of misclassifying majority classes is low while the cost of misclassifying minority classes is high. The aforementioned weights for each class and the bootstrap sampling are adjusted based on these costs to ensure that the decision tree equally weights the minority and majority classes.

2.13 Behavior Classification

There are two goals related to classification: what is the highest performance model that I can build and what brain areas and electrode locations yield the most information for classification? As a result, I did classification using a combination of all features and classification using a single feature (ie. bipolar electrode 27- mean alpha frequency content or bipolar electrode 89- RMS). For the single feature classification, I only used an LDA classifier since with only one feature, it makes sense to just draw one boundary. Any value above the boundary would be considered as on/off and anything below would be considered the other behavior state.

The metric that I used to determine the binary classification performance is AUROC (Area Under the Receiver Operating Characteristic), which I will refer to as AUC for simplicity. The AUC is the area under a graph of the true positive rate plotted against the false positive rate for various cutoffs for the class assignment. The AUC is a difficult metric to interpret but is much more robust to class imbalance and properly summarizes the model output since models output a probability (or a similar value) that an observation is in a particular class. An interpretation for AUC would be the probability that a random on behavior sample has a more extreme feature combination than that of a random off behavior sample. Metrics like accuracy, sensitivity, and specificity all use a specific cutoff of probability and are also heavily influenced under class imbalance.

AUC does not translate well to a multi-class scenario. Instead, classical metrics that use cutoffs will be used: accuracy, precision, recall, and f1 score. The first three metrics are not robust to class imbalance (as is faced in the multi-class classification) while the f1 score is because it can be interpreted as a weighted average of precision and recall. Accuracy, precision, recall, and f1score are defined as follows for a multi-class situation:

$Accuracy = \frac{\sum_{j=1}^n I_{\hat{y}_j=y_j}}{n}$ where j is the j th sample, \hat{y} is the class prediction and y is the true class.

$Precision = \frac{1}{N} \sum_{i=1}^N \frac{TP_i}{TP_i+FP_i}$ where TP_i is the true positive count for class i and FP_i is the false positive count for class i . The individual precision for each group is being averaged over all classes where each class is given the same weight.

$Recall = \frac{1}{N} \sum_{i=1}^N \frac{TP_i}{TP_i+FN_i}$ where TP_i is the true positive count for class i and FN_i is the false negative count for class i . The individual recall for each group is being averaged over all classes where each class is given the same weight.

$F1 = \frac{1}{N} \sum_{i=1}^N \frac{2*TP_i}{2*TP_i+FN_i+FP_i}$ where TP_i is the true positive count for class i and FN_i is the false negative count for class i , and FP_i is the false positive count for class i . Again, the individual f1 score for each class is being averaged over all classes where each class is given the same weight.

In addition, to get a sense of the variation in the AUC, I conducted 10-fold cross validation to split the train + validation set and the final test set. As a result, I received 10 final AUC values and calculated the standard deviation and mean of those 10 values. In addition to 10-fold cross validation, which splits the train and test set at random, I attempted to mimic the task of a brain-computer interface more closely. Instead of splitting randomly, I split the dataset into ten approximately equal sized portions that are not at the same time of day. This simulates a situation where the brain-computer interface is trained during a portion of the day and is then tested in a different portion of the day (which is what is done in practice). This task is also harder than the other tasks as it requires that voltage signals at one time of day from an activity are also present at another time. This would be particularly difficult for body movement decoding especially if there are minimal electrodes on the motor cortex for that subject.

2.14 Mapping Electrodes to Brain Regions

As described in Wang et al., 2021, the structure of the brain for the three patients was determined before surgery through MRI scans. The *freesurfer* software was used to translate the images to a coordinate space defining the edges and ridges of an individual’s brain (Dale, Fischl, and Sereno, 1999). CT images taken after the electrodes were implanted were used to map the electrodes on the brain surface. This process was carried out by the *iElvis* package (“iELVis: An open source MATLAB toolbox for localizing and visualizing human intracranial electrode data” 2017). In an attempt to combine information across patients, I visualize electrodes on a common brain that is an average of the 48 subjects for which voltage data is available (3 subjects have labelled behavior data).

There are many different types of brain parcellations as described in the introduction. I decided to use the Desikan-Killiany parcellation primarily because it had a moderate number of regions (36 areas). This would allow for enough electrodes to be in each region so that an average importance of the region would be valuable. It also ensures that there

is enough spatial resolution beyond the four major lobes, for example.

For the brain region importance and brain region interaction importance, I used the AUC and discriminability index to quantify importance. I did not consider variable importance in the classifier as it may provide misleading information. For example, if there are two very useful, highly correlated electrodes, then one electrode would show a very low importance even though it may be strongly associated with the behavior. Instead, an electrode that is mildly associated with the behavior may be considered the second most important since it provides new information.

2.14.1 Brain Region Importance

In all, there were 12 behaviors that were studied across the three subjects. Arm movement and leg movement were only available in subject 1 while body movement and quiet were only included for subject 2 and 3. I calculated the AUC and discriminability index and averaged over the region that the electrode belonged to. I considered all electrodes from all three patients together to increase the number of electrodes in each region. Overall, this analysis would provide information about the importance of different brain regions in the various activities. It could also provide insights into the function of each brain region.

2.14.2 Brain Region Interaction Importance

The coherence metric represents a functional association between brain areas defined by the electrode positions. There are $\binom{36}{2} = 630$ possible pairs of brain region interactions. While a single brain region can have different signals for on and off states for behavior, it is possible that the functional interaction between two brain areas is more indicative of a behavior. Again, I calculated the AUC and discriminability index for all electrode pairs, and I averaged those values for the brain areas that they belonged to. All subjects were included in this analysis.

Chapter 3

Results

3.1 Video Annotations

Tables 3.1-3.3 provides summary statistics for the different behaviors across the three patients and Figure 2.1 is a visual representation of the behaviors throughout time. Note that there are time points when the label could not be determined accurately. This could be because the video/audio was not available during those time points, the patient was out of view, or it was difficult for the annotator to determine whether the action was happening or not happening. Accounting for the undefined regions, there are approximately 24 hours, 24 hours, and 8 hours annotated for subjects 1-3 respectively.

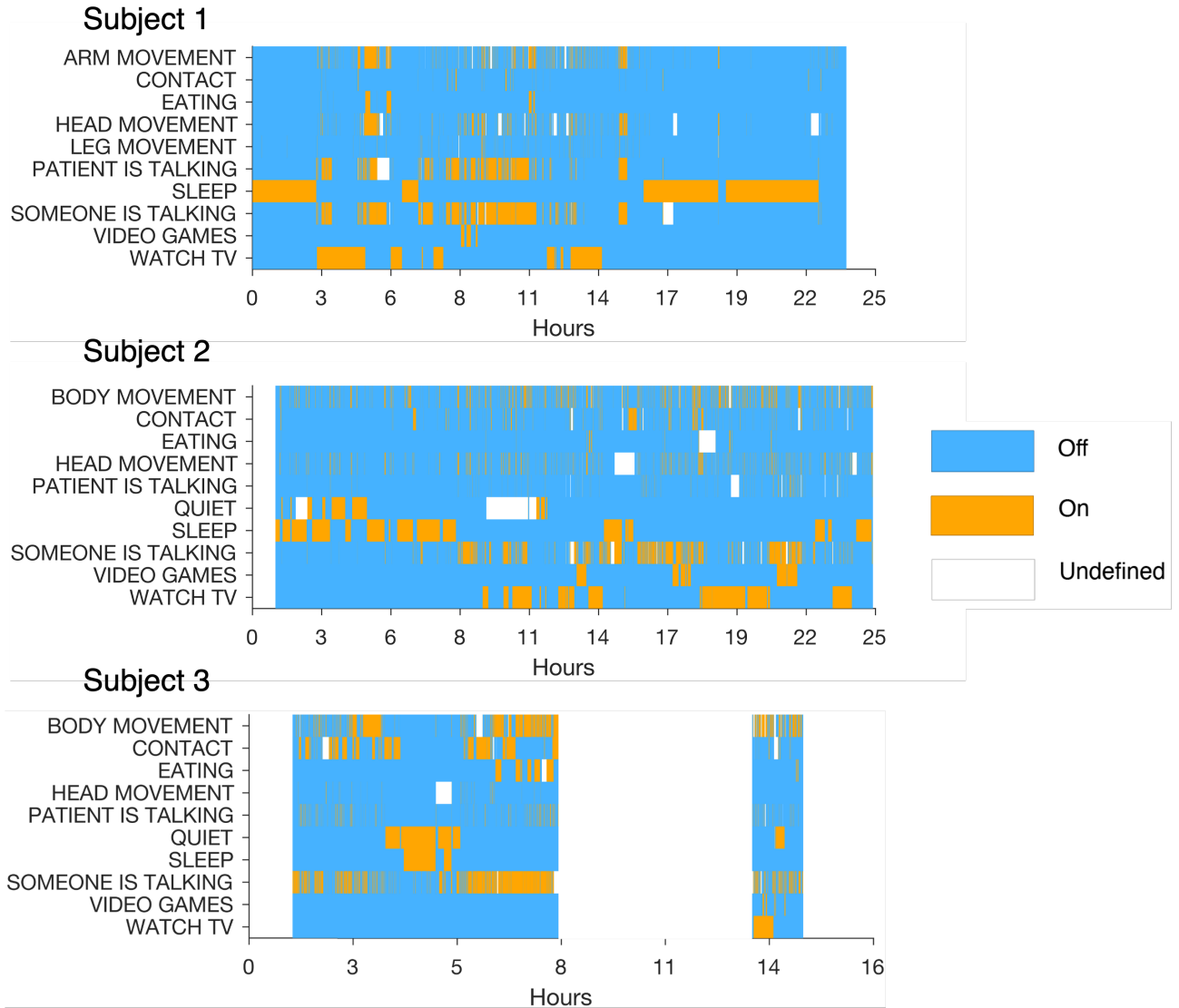


Figure 3.1 State of the Different Behaviors throughout the Time for which Behaviors were labeled for subject 1-3. The blue regions represent time periods where the activity was not performed. Orange regions indicate time periods where the behavior was happening. White areas were not labelled due to various difficulties.

The summary information for each behavior gives us a better sense for the activities that are being done by each patient. Across all subjects, physical movements, physical contact, patient is talking, and someone is talking are activities that are short in time. These activities also tend to be quite frequent. The distribution for the duration of these smaller scale activities are highly right-skewed. Many instances of the activity occur for a short period of time but there are a few cases where the activity occurs for a long period of time. This is why the mean time is much greater than the median time in these cases. In contrast, there are few large scale activities that are infrequent yet occur for a long period of time. This includes sleep, quiet, video games, and watching TV. These

3.1 Video Annotations

Behaviors	Median Time (s)	IQR Time (s)	Mean Time (s)	SD (s)	Event Count
ARM MOVEMENT	20.3	6.6	89.6	9.5	447
CONTACT	20.8	10.7	26.9	24.1	43
EATING	103.7	3.3	223.3	24.6	20
HEAD MOVEMENT	20.6	4.5	103.5	10.4	343
LEG MOVEMENT	7.8	4.7	12.3	6.4	153
PATIENT IS TALKING	74.4	20.6	201.7	44.8	211
SLEEP	8941.1	9995.3	4704.3	6295.4	4
SOMEONE IS TALKING	170.5	27.7	412.3	84.7	122
VIDEO GAMES	449.9	470.3	180.9	270.1	3
WATCH TV	2046.3	1279.3	2455.5	2815.5	8

Table 3.1: Subject 1 Label Summaries

Behaviors	Median Time (s)	IQR Time (s)	Mean Time (s)	SD (s)	Event Count
BODY MOVEMENT	12.6	6.7	19.2	10.4	1024
CONTACT	21.1	6.4	60.5	12.5	239
EATING	31.9	16	36.7	40.4	26
HEAD MOVEMENT	7.3	3.4	12.2	5.8	1030
PATIENT IS TALKING	4	2.6	4.8	3.4	385
QUIET	672	453.7	758	518.8	10
SLEEP	1583.5	1638.3	977.7	1717.8	16
SOMEONE IS TALKING	30.9	8.6	89.2	19.1	678
VIDEO GAMES	925.6	873.3	520.2	916.3	7
WATCH TV	1189.3	675	1333.5	1875.3	18

Table 3.2: Subject 2 Label Summaries

Behaviors	Median Time (s)	IQR Time (s)	Mean Time (s)	SD (s)	Event Count
BODY MOVEMENT	36.9	9.9	104.7	21	290
CONTACT	90.3	17.2	170.3	81.2	90
EATING	229.8	58.1	250.6	435.8	12
HEAD MOVEMENT	6.1	3.4	7	5.2	59
PATIENT IS TALKING	5	2.5	6.5	4.3	399
QUIET	1239.1	1037.2	1080.7	662.6	6
SLEEP	1842.4	1842.4	1618	2288.2	2
SOMEONE IS TALKING	28.4	8.6	72.3	21.2	514
VIDEO GAMES	84.6	85.3	40.7	67.7	5
WATCH TV	1859.3	1859.3	0	0	1

Table 3.3: Subject 3 Label Summaries

activities tend to have a distribution of duration that is either symmetric or left skewed. In other words, there are many longer duration instances of the behavior but there are a few low duration events.

3.2 Summary of Features

To ensure that features were both useful and represented the intended aspect of the voltage waveform, I visualized the particular feature for the top two electrodes as determined by the discriminability index. The degree to which a visual separation between the on and off states for the behavior is seen in this figure will would indicate the success of a classifier using only those two features. In addition, I plotted three raw voltage data waveforms corresponding to the levels of the different features. The specific examples are chosen randomly from any of the three subjects and any of the twelve different behaviors for demonstration purposes.

3.2.1 Time-Domain

For time-domain features, it is possible to observe the actual values of the voltage data to understand the feature rather than having to analyze the periodicity of a waveform or the correlation of the periodicity as in subsequent sections.

3.2.1.1 Signal Distribution

As discussed in the methods section, the features that are included in this category are **MAV**, **MAX**, **MIN**, **ENT**. Figure 3.2 shows the corresponding feature value for the one-second of raw voltage data. The MAV figure is simple to interpret as it is essentially the mean of the signal. As the center of the distribution becomes more extreme, the MAV increases. The MAX figure and MIN figure are also simple to interpret. However, there are two situations that would create a more extreme MAX or more extreme MIN. One is if there is a "spike" of voltage downwards or upwards. While the center of the distributions may be the same, the spikes can produce different feature values. This is shown in the bottom-most and top-most subplot for the MAX and MIN features respectively. Alternatively, a MAX and MIN feature may just be more extreme because it's average is lower or higher. If this is the case, then the MAX and MIN features will be highly correlated with the MAV feature. For ENT (negative of the shannon entropy as displayed in the figure), the highest entropy figure in the top subplot is characterized by a lot of "movement" of the signal in the range of 500 and -1000. This movement means that their is more randomness in the signal and therefore greater entropy. As we move downwards,

3.2 Summary of Features

as expected, the signal becomes more ordered with small variations around a center value, which indicates low entropy.

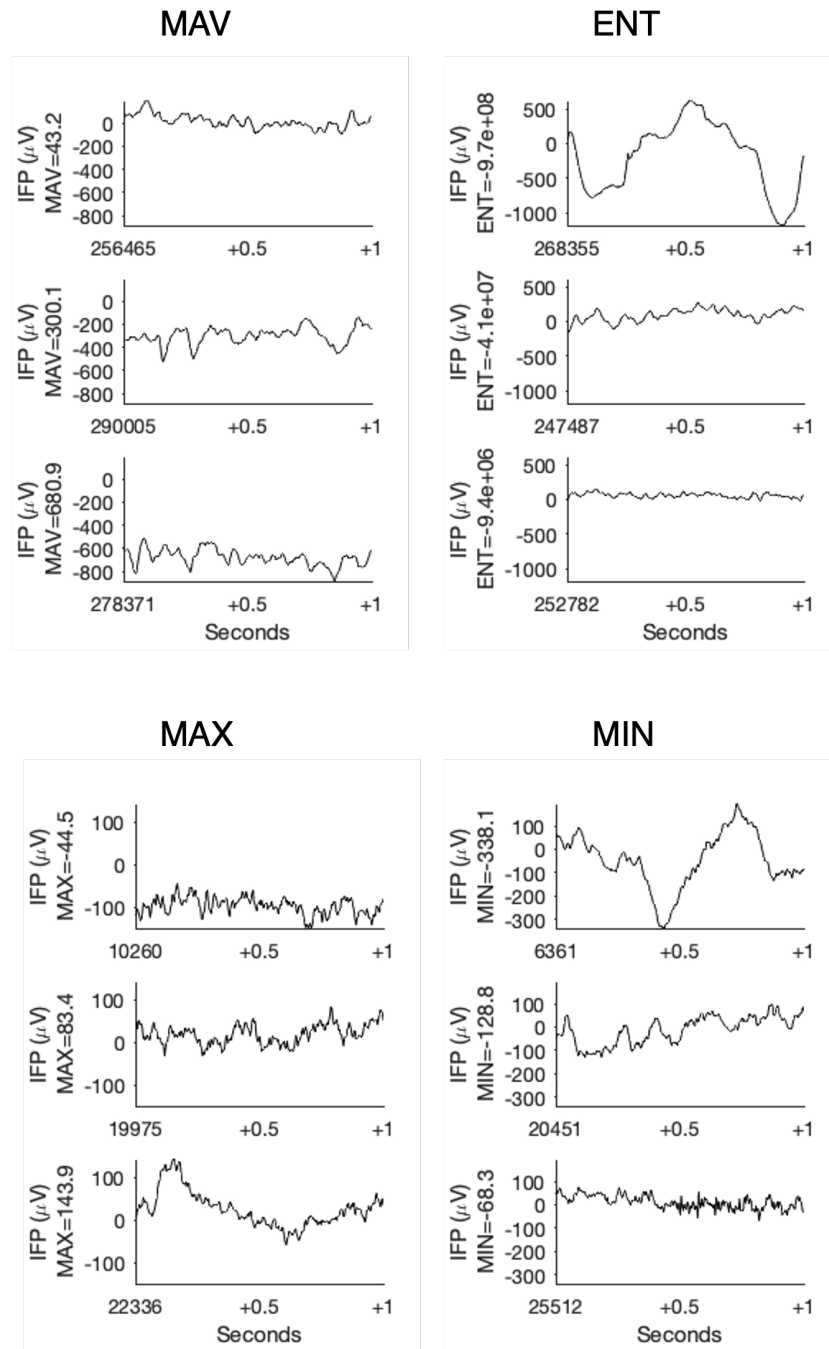


Figure 3.2 Example Voltage Signals and their associated feature values for MAV, ENT, MIN, and MAX features. The MAV figure (top left) was taken from the arm movement activity for Subject 1. The ENT figure (top right) was taken from the someone is talking behavior for Subject 1. The MAX figure (bottom left) was taken from the patient is talking behavior for Subject 3. The MIN figure (bottom right) was taken from the patient is talking behavior for Subject 3. The x-axis first provides information about the number of seconds that have elapsed since the beginning of the patient recordings followed by the additional number of partial seconds. All of the figures represent one second segments and feature values are provided on the y-axis ranked lowest to highest.

3.2.1.2 Amplitude

Figure 3.3 provides a visual representation of the RMS feature, which essentially tells us about the amplitude of a signal. As the RMS increases from the top-most subplot to the bottom-most subplot, there is greater variability around the mean signal value. This makes sense, as greater variability around the mean, means that there is a greater amplitude for the wave.

3.2.1.3 Trends

Figure 3.3 also provides a visual representation of the HE feature. As expressed in the methods section, the HE is a measure of a signals tendency to return to the long term trend of the mean. As the HE increases from the top-most subplot to the bottom-most subplot, there is more "travel" of the signal. In the first subplot, we see some noise around a central value while in the bottom subplot, there is large movement upwards and downwards before returning to the mean value. Because of this, the HE feature encapsulates some of the information from the RMS feature.

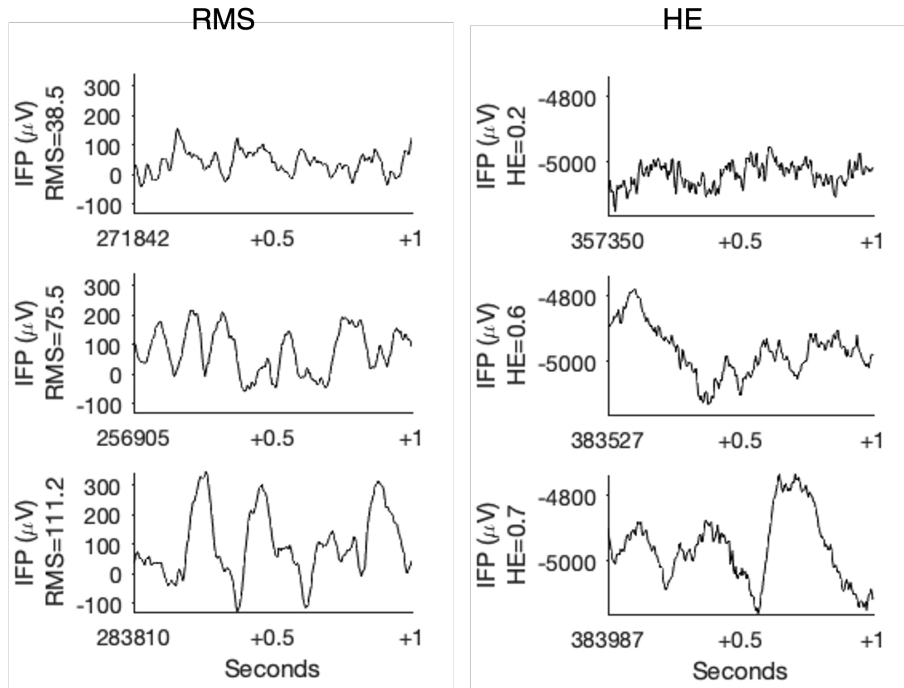


Figure 3.3 Example Voltage Signals and their associated feature values for RMS and HE features. The RMS figure (left) was taken from the arm movement Activity for Subject 1. The HE figure (right) was taken from the quiet behavior for Subject 1. The x-axis first provides information about the number of seconds that have elapsed since the beginning of the patient recordings followed by the additional number of partial seconds. All of the figures represent one second segments and feature values are provided on the y-axis ranked lowest to highest.

3.2.2 Frequency-Domain

The following visualizations relate to the periodic aspects of the voltage signals and the frequency of the waves. The format of the figure is the same as those in the time-domain section.

3.2.2.1 Mean Power

Figures 3.4-3.6 provide the voltage signal visualizations with their corresponding mean frequency content. Figure 3.4 shows the delta and theta waves, which are the slower waves of the voltage data. Higher delta content is signified by waves with very large periods. In the bottom-most subplot, there is a large peak between +0.5 and +1 seconds, which must be responsible for this. In contrast, the others have relatively flat waveforms. For the theta visualizations, more theta content means that there are around 5 or so full waves in the signal rather than a stationary time series that is stable at a specific mean.

3.2 Summary of Features

In figure 3.5, the same overall observations hold from in figure 3.4. Since alpha waves and beta waves still do not encompass the very high frequency ranges, high values are associated with visible waves that have higher frequencies than the delta and theta cases. In the bottom-most alpha power subplot, there are relatively high amplitude waves that have a greater frequency than those in the highest theta and delta wave examples. the same is seen in the bottom-most beta subplot. The low beta and alpha contents do not have prominent waves.

In figure 3.6, the example voltage signals for the broadband and gamma feature are displayed. For the mean gamma power figure, very high frequency waves have the highest gamma feature value. These waves also have a relatively low amplitude in comparison to lower gamma content waves. The broadband feature takes the average over the entire spectrum. Since the lower frequencies have much greater power values, the broadband feature value will favor lower frequency waves over higher frequency ones. However, the highest broadband mean power feature will have components of both. This is what is seen in the bottom-most subplot of the broadband figure. There are large and slow waves with smaller noisy waves on them.

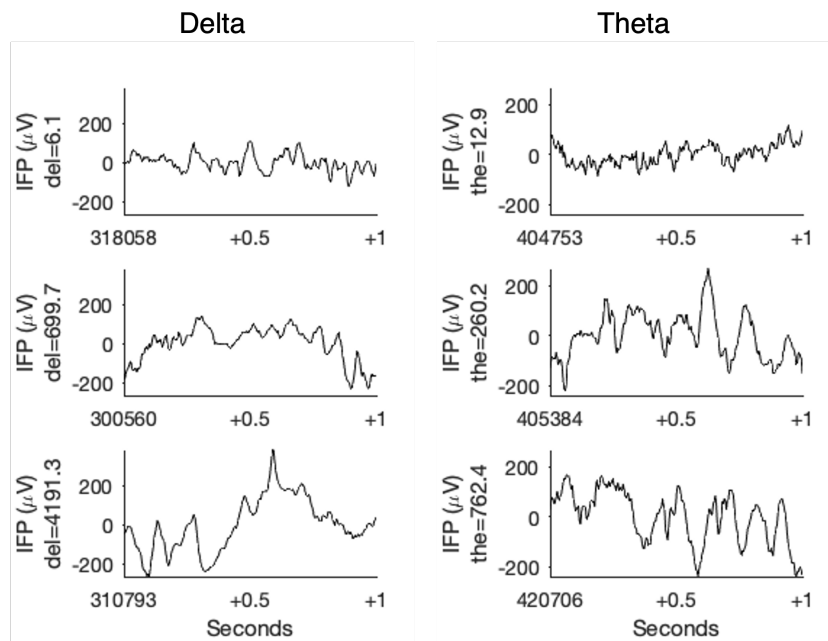


Figure 3.4 Example Voltage Signals and their associated feature values for Delta and Theta features. The Delta figure (left) was taken from the sleep activity for Subject 1. The Theta figure (right) was taken from the video game activity for Subject 2.

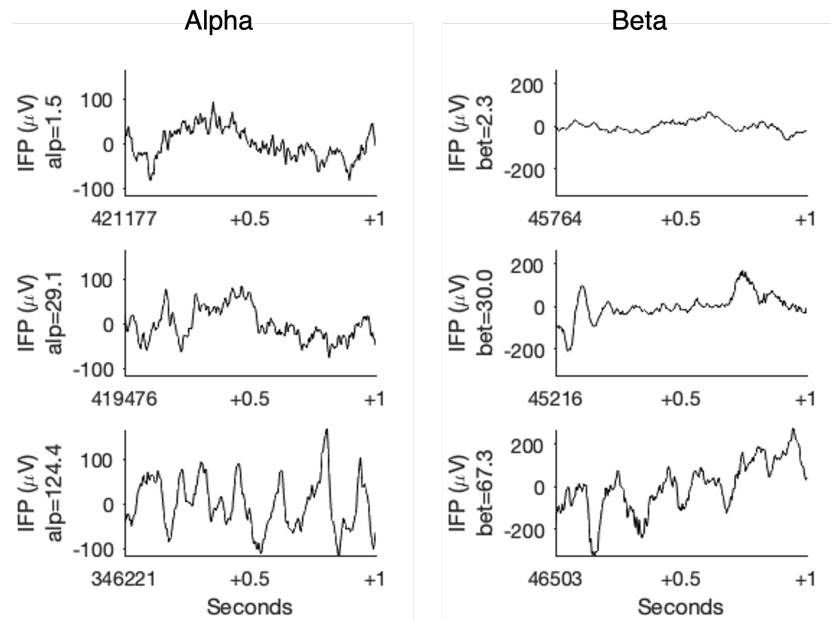


Figure 3.5 Example Voltage Signals and their associated feature values for Alpha and Beta features. The Alpha figure (left) was taken from the patient is talking behavior for Subject 2. The Beta figure (right) was taken from the video games behavior for Subject 3.

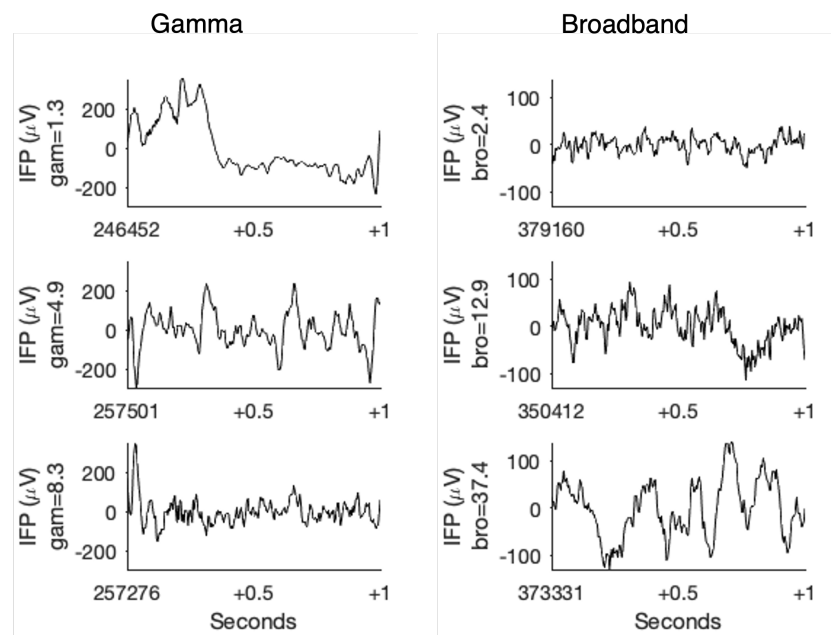


Figure 3.6 Example Voltage Signals and their associated feature values for Gamma and Broadband features. The Gamma figure (left) was taken from the arm movement behavior for Subject 2. The Broadband figure (right) was taken from the quiet behavior for Subject 2.

3.2.2.2 Coherence

While it is even more difficult to visualize the coherence (power transfer) between two signals in various frequency bands, it is easier to distinguish between coherence in all of the frequency ranges considered (broadband). The lowest broadband coherence usually occurs, as displayed here, in situations where the waves are not readily apparent and there is no visual pattern to the waves. This is what is seen in the top-most subplots. There just seems to be random noise around zero voltage. In contrast, for the highest broadband coherence, there will be a clear periodic structure and the waves will be associated with each other. For example, in the bottom-most subplot on the left, there is a starting peak that is associated with but is slightly delayed from the peak on the right. Then, there is another peak in the left subplot, which once again comes after the second peak on the right subplot. In addition, there is a decrease in voltage between around 0.1s and 0.5s in both figures, which could be representative of a slow wave in both. Finally, there are higher frequency features between 0.5s and 1s in both signals. One could interpret this as the brain area of the electrode on the left taking input from the area electrode on the right (or electrode areas associated with the electrode on the right).

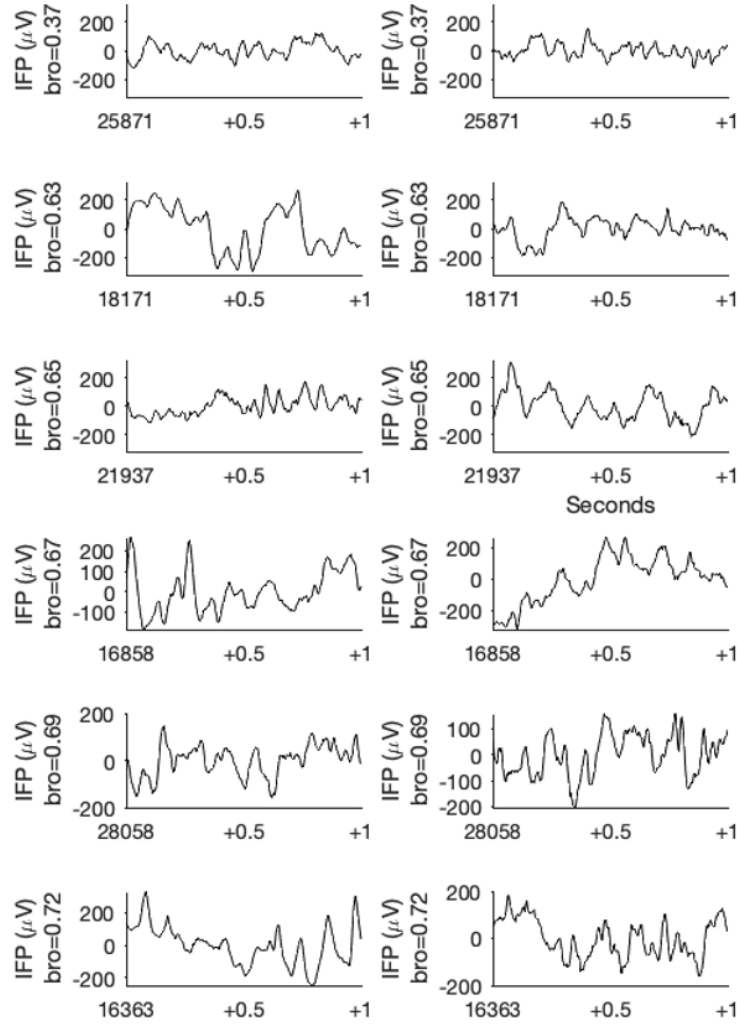


Figure 3.7 Example Voltage Signals and their associated feature values for the Broad-band Coherence Feature. This was taken from the watching movie for Subject 1. The left column of subplots represents one electrode and the right column of subplots represents another electrode.

3.2.3 Correlation Between Features

As has been hinted in the previous subsections, features may be correlated with each other based on the structure of the voltage signal and the construction of the features. Ideally, there would be zero correlation between features, because then each feature would be providing new information to the classifier. However, this of course is not the case in any real situation. Figure 3.8 shows the correlation matrix for the 12 single-electrode

features (excluding coherence) averaged over all of the electrodes from the three subjects. The most concerning correlations are between the mean broadband power and RMS and entropy and MAV. As mentioned earlier, broadband power is the amount of periodic content in the signal while RMS is the amplitude of the waves. Naturally as wave amplitude increases the amount of periodic content will increase. The relationship between ENT and MAV is less obvious. However, after further inspection, it is possible to conclude that signals with high magnitude generally have higher variability. This is because the signals will not be centered at 0 but will fluctuate to higher or lower values, which will increase both MAV and ENT. Other than these two, the correlation between the features is reasonable.

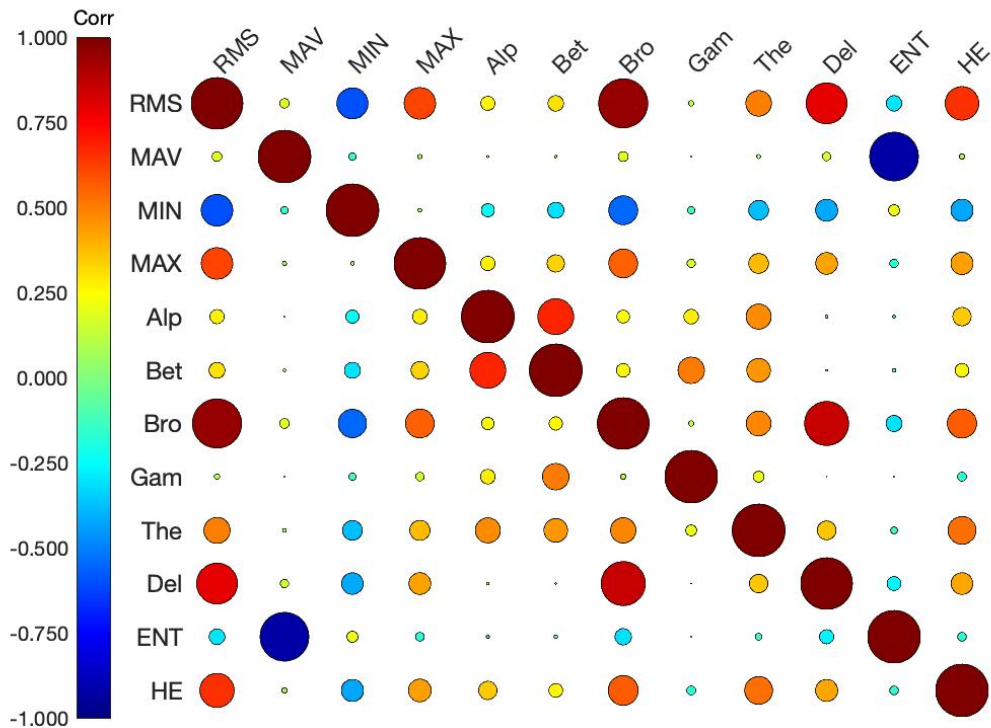


Figure 3.8 Visualization of Correlation Matrix for the 12 single-electrode features averaged over subjects and electrodes. The size of the circle represents the magnitude of the correlation and the color of the circle represents the value of the correlation. The diagonal of the figure has a 1.0 correlation as it represents the correlation of the same vectors of data

3.3 Association Between Features and Annotations

Using a rank sum test and a confidence level of $0.05/(total\ comparisons) = 0.05/((154 + 35 + 91\ electrodes) * (12\ features)) = 1.48 * 10^{-5}$, table 3.4 presents the percentage of the total number of electrodes studied for each behavior that are significantly different between the off and on states of the activity based on the given feature.

Behaviors	RMS	MAV	MIN	MAX	Alp	Bet	Bro	Gam	The	Del	ENT	HE
BODY MOVE- MENT	56	34	47	52	55	60	56	58	62	39	38	56
CONTACT	49	46	50	53	39	48	48	56	47	40	51	44
EATING	36	13	28	23	26	37	36	43	35	23	14	30
HEAD MOVE- MENT	28	14	23	23	23	31	28	31	30	23	14	28
PATIENT IS TALKING	17	12	15	17	15	14	17	24	18	15	13	23
QUIET	74	67	71	70	64	72	74	78	71	75	69	83
SLEEP	99	73	94	91	72	71	99	77	99	97	77	97
SOMEONE IS TALKING	50	37	46	46	41	44	51	51	51	40	40	39
VIDEO GAMES	44	19	35	37	41	48	44	53	47	28	19	61
WATCH TV	71	48	69	66	65	71	71	58	68	57	53	64
ARM MOVE- MENT	69	31	57	54	26	37	69	34	49	60	37	63
LEG MOVE- MENT	6	11	14	14	0	3	6	0	0	6	14	6

Table 3.4: Percent of the Electrodes that are Significant for Each Feature Type and Behavior

Table 3.4 allows us to do a crude comparison of the differences in the distributions of the on and off states of an activity for different features. Lower percentages mean that less of the electrodes may be useful for differentiating between when a behavior is occurring and when it is not. Note that this does not tell us the strength of the associations. Instead it tells us whether there may be a global change in the brain associated with a particular activity. Strikingly, for sleep, we see that for all of the features, greater than 70% of the electrodes are significant and for 3 of the features, this number is 99%. In contrast, patient is talking and leg movement behaviors both have relatively small percentages of electrodes that are significant. This could signify poor ability to classify these activities or may signify that the cortical representation of these activities is only available at a few sites. In addition, while one feature may not be useful, another for the same behavior

3.3 Association Between Features and Annotations

may be good at differentiating the on and off state for a behavior. A good example of this is the arm movement behavior where for the RMS feature, 69% of the electrodes are significant while for the mean alpha content feature, only 26% of the electrodes are significant.

Next, I will quantify the strength of the association using the discriminability index (DI). I will assume that the strength of the association between a feature and a behavior is defined by the maximum discriminability index for all of the electrodes across all three patients. Table 3.5 presents these values.

Behaviors	RMS	MAV	MIN	MAX	Alp	Bet	Bro	Gam	The	Del	ENT	HE
BODY MOVEMENT	0.45	0.43	0.30	0.30	0.38	0.43	0.34	0.38	0.46	0.22	0.33	0.76
CONTACT	0.31	0.44	0.40	0.38	0.26	0.32	0.29	0.39	0.33	0.19	0.39	0.37
EATING	0.54	0.47	0.45	0.39	0.69	0.92	0.48	1.27	0.62	0.54	0.42	1.47
HEAD MOVEMENT	0.43	0.56	0.60	0.55	0.40	0.44	0.36	0.52	0.40	0.37	0.54	0.63
PATIENT IS TALKING	0.71	0.50	0.58	0.66	0.50	0.60	0.65	0.37	0.55	0.36	0.43	0.59
QUIET	0.80	0.77	0.90	0.80	0.41	0.75	0.64	0.74	0.69	0.62	0.71	0.85
SLEEP	0.82	0.76	0.70	0.84	1.05	1.57	0.65	1.05	0.93	0.55	0.74	0.92
SOMEONE IS TALKING	0.88	0.76	0.81	0.73	0.54	0.65	0.76	0.37	0.70	0.45	0.61	0.87
VIDEO GAMES	0.84	0.90	0.84	0.87	0.74	0.74	0.76	0.85	0.74	0.50	0.82	0.96
WATCH TV	0.58	0.50	0.60	0.62	0.57	0.67	0.52	0.46	0.55	0.43	0.43	0.48
ARM MOVEMENT	0.34	0.30	0.23	0.31	0.12	0.17	0.33	0.20	0.26	0.26	0.26	0.39
LEG MOVEMENT	0.18	0.50	0.40	0.47	0.23	0.30	0.17	0.19	0.18	0.17	0.41	0.33

Table 3.5: Maximum Discriminability Index (DI) for Each Feature Type and Behavior

Table 3.5 proves that while the ability to find a significant difference for a behavior based on a feature might be easy because the signal is distributed through the cortex, that does not mean that the strength of the signal is high. An example of this is the RMS feature for the patient is talking behavior. While only 17% of the electrodes are significant, the maximum DI is 0.71, which is much higher than the DI of arm movement (0.34) when arm movement has 69% of electrodes as significant. Overall, sleep has the highest DI value of 1.57 for the mean beta content feature. The next highest DI is for the eating behavior and the mean gamma content (1.27). This DI is substantially higher than the other DIs for eating. The movement behaviors generally seemed to have

3.4 Overall Classification Results

lower DIs across all of the features.

Before conducting formal classification experiments, it is important to show that there is easy to identify separation between the on and off states of behavior based on one or two features alone. Figure 3.9 shows that the sleep activity is one where there is clear separation between the two states based on just one feature (HE) from two electrodes. There are two clear separate clusters for sleep and not sleeping. For the eating activity, while there is not as good visual separation, higher gamma content in both electrodes is indicative of the eating activity. In the last example (leg movement), the MAV features is does provide mild separation between the groups, however, it is much less than the other two examples. This likely means it will be difficult to classify leg movement.

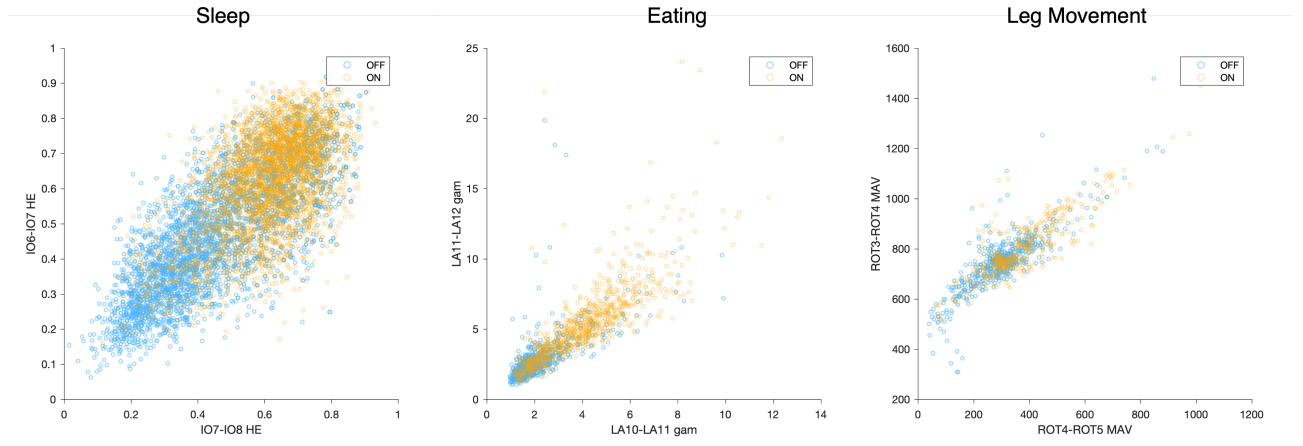


Figure 3.9 Separation Between the On and Off States of Activities Based on one Feature from Two Electrodes. The left-most figure is for the sleep activity for subject 3. The middle figure is for the eating activity for subject 2. The right-most figure is for the leg movement activity for subject 1. The orange points represent the on points for the activity and the blue points represent the off points for the activity.

3.4 Overall Classification Results

In this manuscript, the main analysis is considered to be for one second time intervals and for the schema in which the control (off) time points were taken from the regions surrounding the main on time points. The main classifier I used was a random forest classifier with 100 trees, a minimum leaf size of 1, maximum number of splits as the number of samples, the square root of the number of samples to sample at each split, full sampling with replacement for each bootstrap sample, and the gini diversity index as the split criterion. Unless otherwise noted, these are the hyperparameters and data

setup used. When combining features into a single classifier, 50% of the electrodes for each features were used and the square root of each coherence feature was used. The best features were selected using the discriminability index.

3.4.1 Main Classification Results

Figure 3.10 provides the main results for this manuscript. For all 10 behaviors for 3 subjects, there is an above chance classification AUC (one standard deviation below the mean does not include 0.5). For subject 1, the movement behaviors and contact have an AUC around 0.70-0.75. The rest of the behaviors have much higher AUCs in the range of 0.87-0.98. Sleep has a remarkably high AUC of 0.98 and a very low variation between train and test splits. For subject 2, the movement behaviors and contact have an AUC around 0.82 while the patient is talking behavior has a lower AUC at 0.74. The rest of the behaviors (as in the first subject) have much higher AUCs in the range of 0.90-0.94. Finally, for subject 3, the movement behaviors and contact have an AUC around 0.81 while the patient is talking behavior has a lower AUC at 0.73. Then, eating and someone is talking have AUCs of 0.87. Video games, quiet, and sleep have AUCs ranging from 0.94 to 0.99. Once again, the high AUC and low variability is notable. For all of the subjects, most of the unique information for classification is contained within the time-domain features (RMS, MAV, MIN, MAX, ENT, HE). This is because there is a negligible improvement in AUC when the mean power and coherence features are added to the classifier. The exceptions to this are eating, sleeping, and watching tv for subject 1, video games for subject 2, and eating and contact for subject 1. Also, across all activities and subjects, the mean power and coherence features did not outperform the time-domain features except for sleep in subject 1 and video games and head movement in subject 3.

3.4 Overall Classification Results

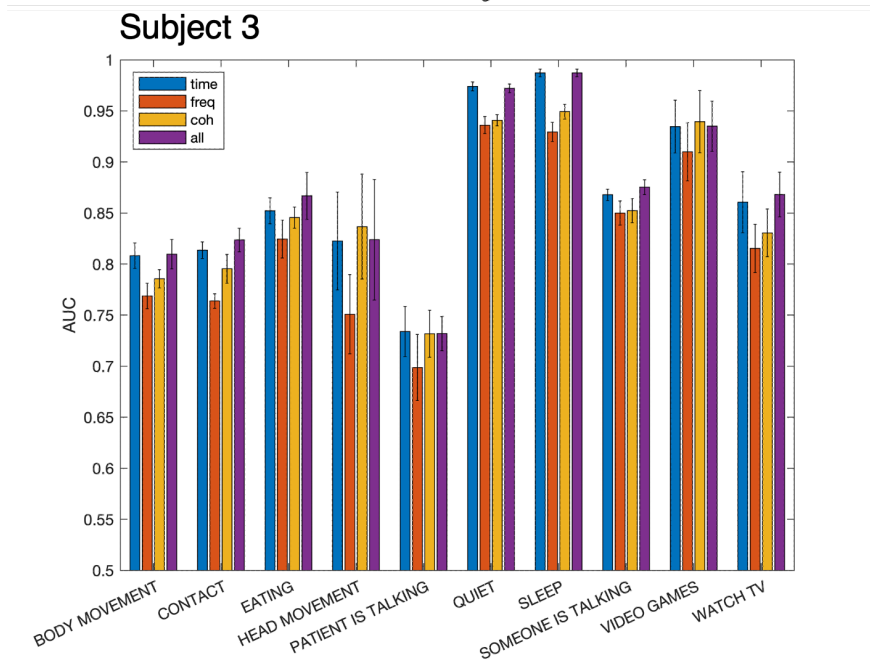
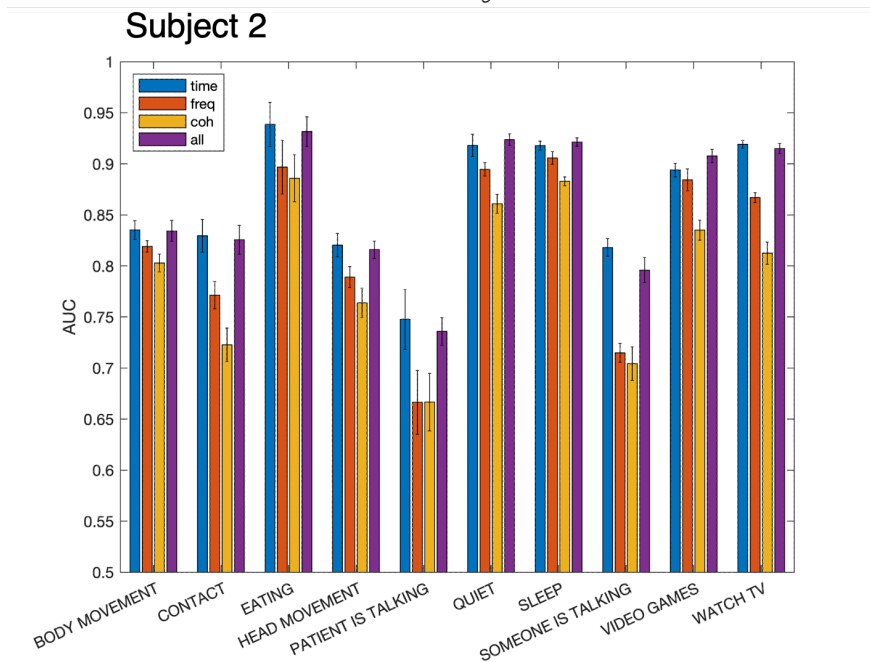
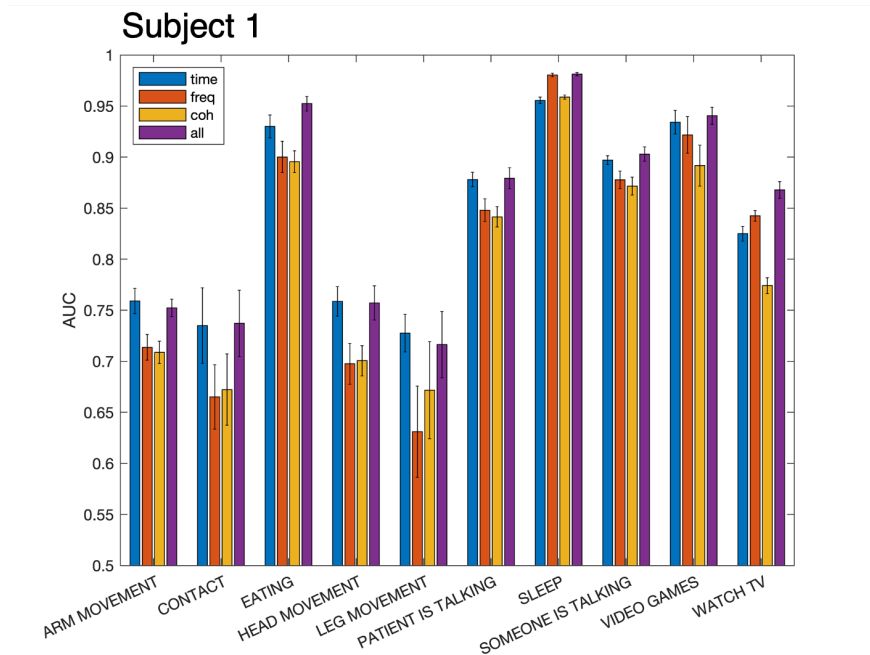


Figure 3.10 Classification AUC for 3 Subjects with Different Feature Sets. The mean classification AUC for 10 different activities, 4 different feature sets, and 3 subjects is presented here. The blue bars are for time-domain features (RMS, MAV, MIN, MAX, ENT, HE), the red bars are the mean power features, the orange bar is for the coherence features, and the purple bar is for all features combined. The error bars indicate the standard deviation of the AUC across the 10 divisions of the train and test set.

3.4.2 Schema 2 for Off and On Timepoints

Schema 2 is where the train and test sets are not randomly distributed throughout time. Instead, the data used to train comes from a separate time of day than the test data. Figure 3.11 provides the results for this schema. In comparison to the results provided for the main schema of selecting the train and test sets, the AUC across all activities for all subjects decreases by a substantial amount. In addition, the variation in the AUC across the different train and test splits is much higher. The movement and contact behaviors for subject 1 now have an AUC of 0.57-0.66 (in comparison to 0.70-0.75 from the main results). Sleep is the only larger scale activity that is robust to this new schema. The AUC for sleep is still high at 0.97. Eating and someone is talking only decreases by about 0.05 in AUC to 0.90 and 0.86 respectively. Video games, watching tv, and patient is talking drops by 0.06-0.12 in AUC to 0.88, 0.74, and 0.75 respectively. For subject 2, again, the more robust behaviors are sleep, eating, and video games. They only drop to a mean AUC of 0.87, 0.89, and 0.85 respectively. However, for the other behaviors, there is a much higher drop. For body contact, quiet, someone is talking, and watching tv, there is a drop of mean AUC in the range of 0.19 to 0.25. The body movement has a more moderate drop in AUC of 0.83 to 0.76. In addition, the standard deviation in AUC for contact and watching tv is very high. Finally, there are similar decreases in AUC for subject 3. However, the only semi-robust behaviors to this new schema are eating, video games, and head movement. The rest of the behaviors have larger decreases in AUC. The largest decreases is seen in sleep (0.25 drop) and someone is talking (0.2 drop). Across all three subjects, the standard deviation of the AUC goes below 0.5 for the contact behavior in subject 1 and subject 2. In addition, the someone is talking behavior for subject crosses 0.5 in subject 2.

3.4 Overall Classification Results

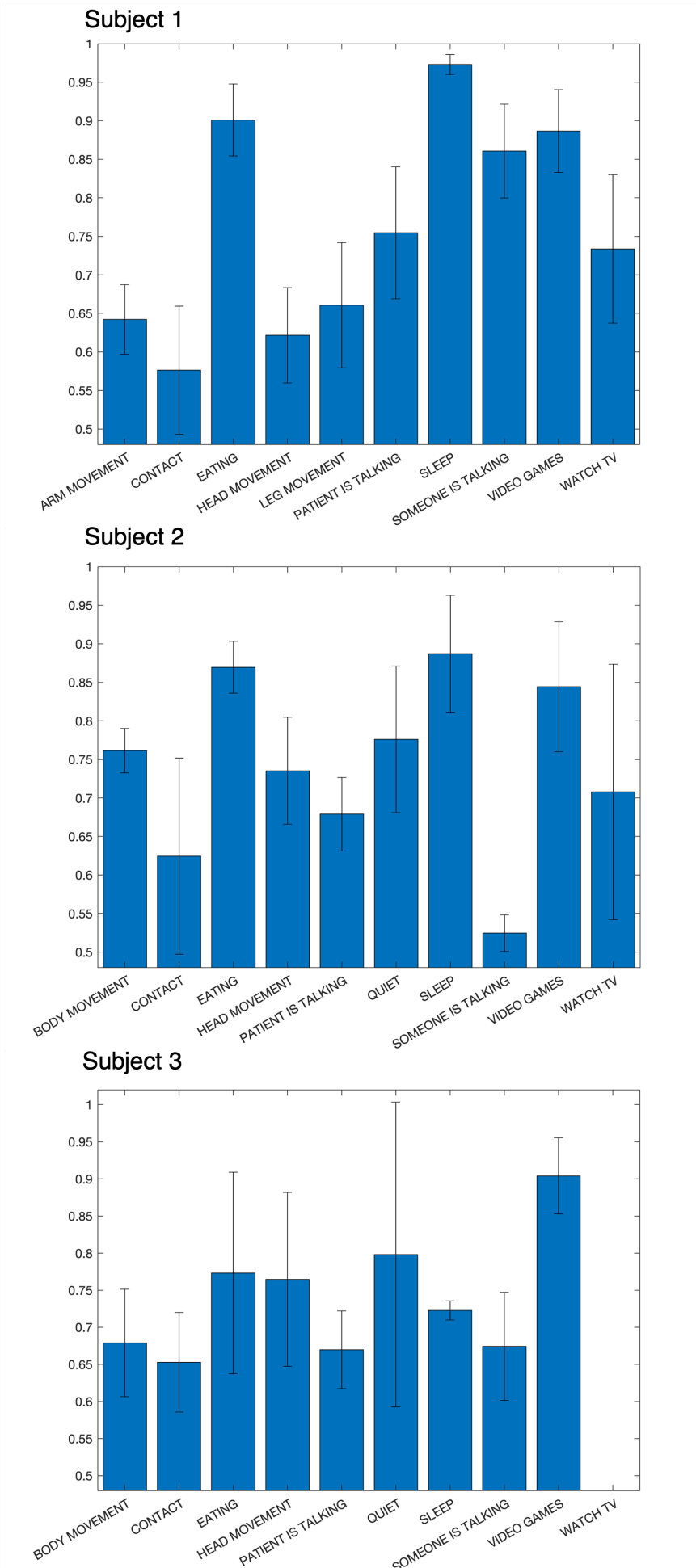


Figure 3.11 Classification AUC for 3 Subjects for Schema 2 of Test and Train Split. The classification AUC for 10 different activities and 3 subjects is presented here. The error bars indicate the standard deviation of the AUC across the 10 divisions of the train and test set. Note that for Subject 3, there is only one instance of tv watching, so it is not possible to separate the data into train and test sets.

3.4.3 Other Classifiers

To justify the choice of the random forest model, five other popular machine learning models were considered and compared to the random forest. These models include gradient boosting decision trees, Quadratic Discriminant Analysis (QDA), Support Vector Machines (SVM), Naive Bayes, and Logistic Regression. The comparison between classifier is show in figure 3.12. Across all behaviors, the random forest has the higher mean AUC (by as much as a 0.06 increase) except for the video games activity where the mean AUC of the gradient boosting decision tree has a higher AUC by 0.005 (standard deviations overlap). The AUC of classifiers tends to follow this order: Random Forest, Gradient Boosting Decisions Trees, QDA, SVM, Naive Bayes, and then Logistic Regression. As discussed in the methods section, the number of features used in these tasks can be very high. Therefore, the performance of the classifiers is mostly dictated by their ability to handle high-dimensional data. Note that data only for subject 1 is included for brevity purposes but the same trends hold in subject 2 and subject 3.

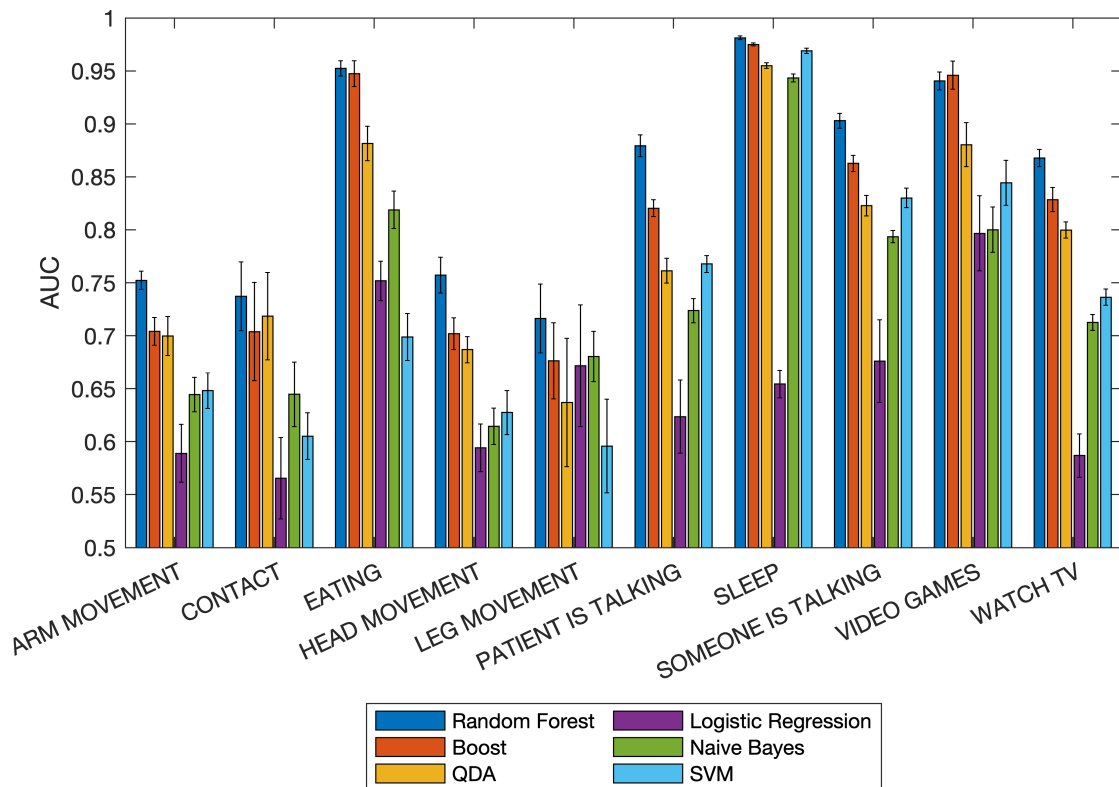


Figure 3.12 Comparison Between Classifiers on the basis of AUC for the Behaviors Labeled for Subject 1. All feature types are used to train these classifiers and the behaviors are labelled in 1s time windows. The random forest classifier is the same as the one presented in figure 3.10. QDA is Quadratic Discriminant Analysis, SVM is Support Vector Machines, and Boost is Gradient Boosting Decision Trees

3.4.4 1s vs 2s Time Windows

To determine whether classification performance changed between 1s and 2s behavior labelling windows, the same models were trained on the two types and the classification performance was recorded. In most cases, as depicted in figure 3.13, there was a slight increase in AUC when moving to the 2s window. However, only in sleep and video games was there enough of an increase that the standard deviations from the mean did not overlap. Only in the case of eating was there a decrease in mean AUC for the 2s windows. The exact same patterns were seen in subjects 1 and 3 (not shown in the figure) except for in the contact activity, there was decrease in mean AUC for 2s windows.

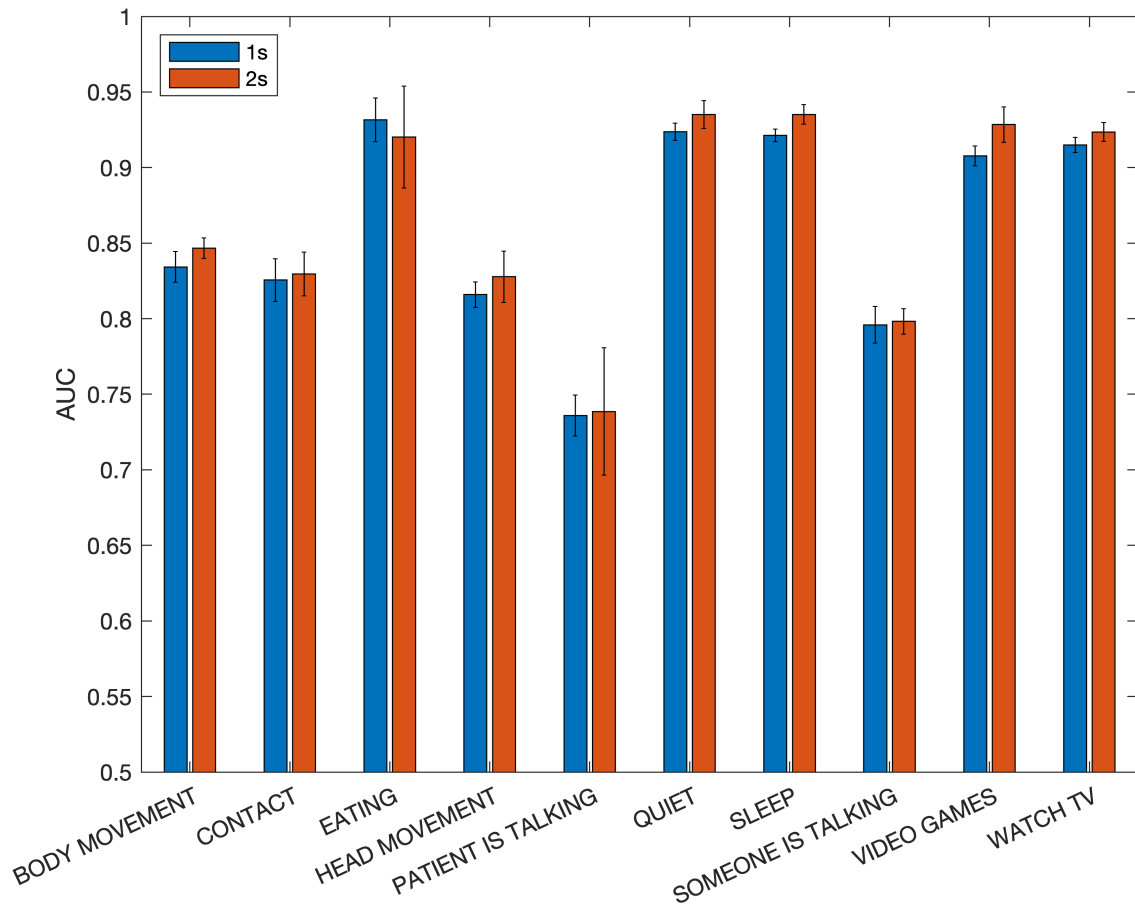


Figure 3.13 Comparison Between Classifier Performance for 1s and 2s Time Windows for Subject 2. All feature types are used to train the classifiers. The blue bars are the 1s windows and the red bars are the 2s windows.

3.4.5 Hyperparameter Optimization

All of the above results are for the fixed hyperparameters described at the beginning of the results section. Figure 3.14 shows the classification AUC for subject 1 using the normal hyperparameters and the hyperparameters found through Bayesian hyperparameter search. The AUCs are quite similar across all of the behaviors. For 8 out of 10 behaviors, the fixed hyperparameters have a greater AUC. Only for video games and contact, does the hyperparameter search provide a better AUC on the test set. This shows that there is only a minor improvement if any when conducting hyperparameter search.

3.4 Overall Classification Results

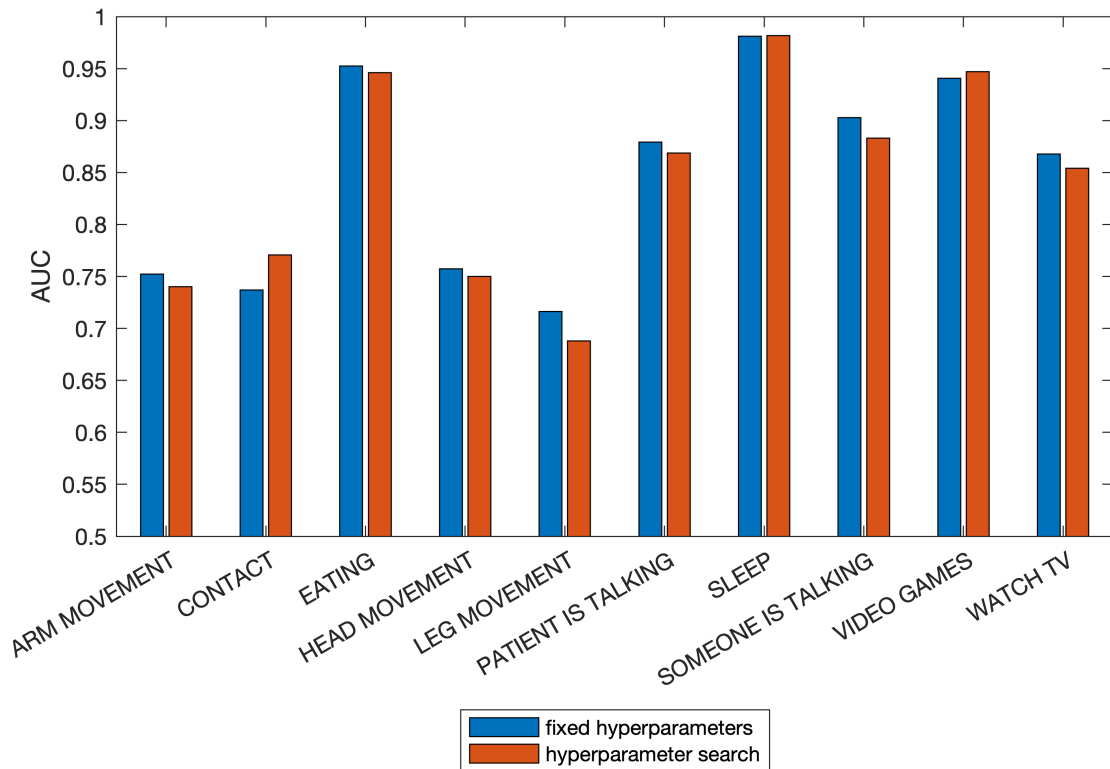


Figure 3.14 Comparison Between Classifier Performance for fixed hyperparameters (described at the beginning of the results section) and hyperparameters selected post Bayesian hyperparameters search for Subject 1. All feature types are used to train the classifiers. Note that there are no error bars provided because there was a single holdout set used. The blue bars are for fixed hyperparameters and the red bars are for post Bayesian hyperparameter search.

It is worthwhile to study situations where the hyperparameter search yielded better AUCs, when the fixed hyperparameters yielded better results, and when both yielded the same results. The below figure (3.15) provides this visualization.

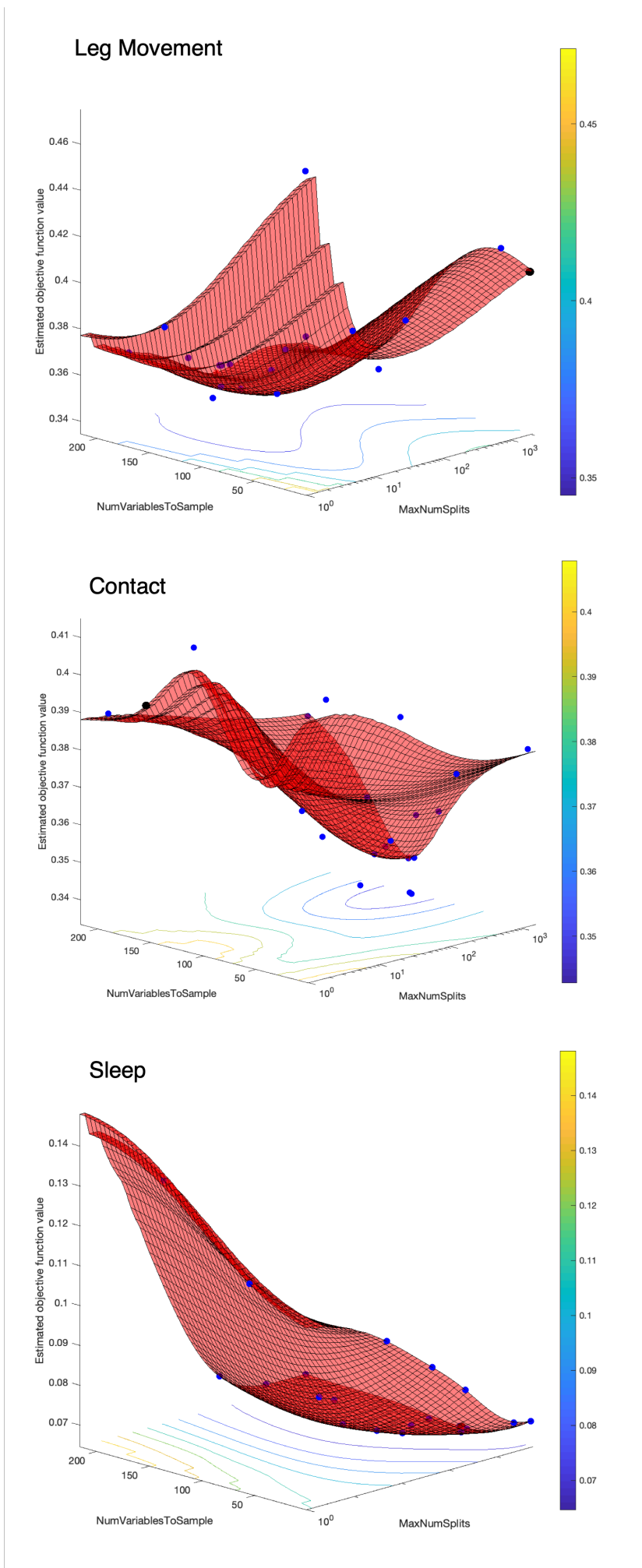


Figure 3.15 Estimated Objective Function Surface for the Number Variables to Sample and Maximum Number of Splits as Hyperparameters. The red surface is the estimated objective function (sum of classification cost) value given the hyperparameters. The blue points are the points that were actually evaluated and the true value of the objective function was found. The contour map below the surface provides the topology of the objective surface. The colorbar provides the value of the objective function corresponding displayed in the contour lines.

Figure 3.15 provides a visualization of the estimated objective function (sum of classification cost) for the number of variables to sample at each split and the maximum number of splits in the tree as the independent variables. Leg movement was the activity in which the fixed hyperparameters outperformed the model after hyperparameter search. As expressed earlier, the square root of the number total features was the number of variables to consider at each split in the fixed case and the number of training samples was the maximum splits. The number of variables to samples was 14 and the maximum number of splits varied by the activity. The hyperparameter search had a minimum cost at 107 maximum splits of the possible 2126 splits and 215 of the possible 216 variables to sample. In the sub-figure for leg movement, there is not a sharp drop in the objective function at any point, so the objective function may not be estimated properly. This may be why the model converged to hyperparameters that performed much worse. It is also worth noting that if 215 of 216 predictors are considered at each split, the model is no longer a random forest. The contact activity is the example where hyperparameter search was useful. Here, 1529 of 1582 maximum splits and 120 of 216 number of variables to sample were selected. In this example, there is a steep drop at the optimal hyperparameter set, so these hyperparameters may be considered more trustworthy. Finally, for sleep, the AUC was the same in both cases for hyperparameters. 56644 of 56927 maximum splits and 59 of 216 number of variables to sample were selected. While the number of variables to sample was higher than the 14 used in the fixed model, the signal in the data for sleep may have been so strong that hyperparameter optimization would have little effect.

3.5 Multi-Behavior Classification

As discussed in the methods section, small time-scale behaviors with many repetitions and that had a motor component to them were selected for multi-class classification. The random forest classifier attempted to find the correct class, not just from one alternative, but from four other alternatives. The metrics for the multi-class classification are presented in table 3.6. For all metrics except for accuracy, classification of behaviors for subject 2 performs better than that of subject 3. Classification of behaviors for subject 3 also performs better than that of subject 1. The recall for subject 2 is 0.65, which means there is a 65% chance of correctly predicting a class label averaged over all of the different classes. This value is much lower for subject 1 and 3. The baseline accuracy in table 3.6 is the accuracy when the most abundant class is always predicted. All three subjects have accuracy well above the baseline accuracy. The increase over the baseline accuracy is approximately 0.15, 0.2, and 0.3 for subject 1, 2 and 3 respectively. Overall, the lower variability in estimates for subject 2 is a result of more samples to train and test on.

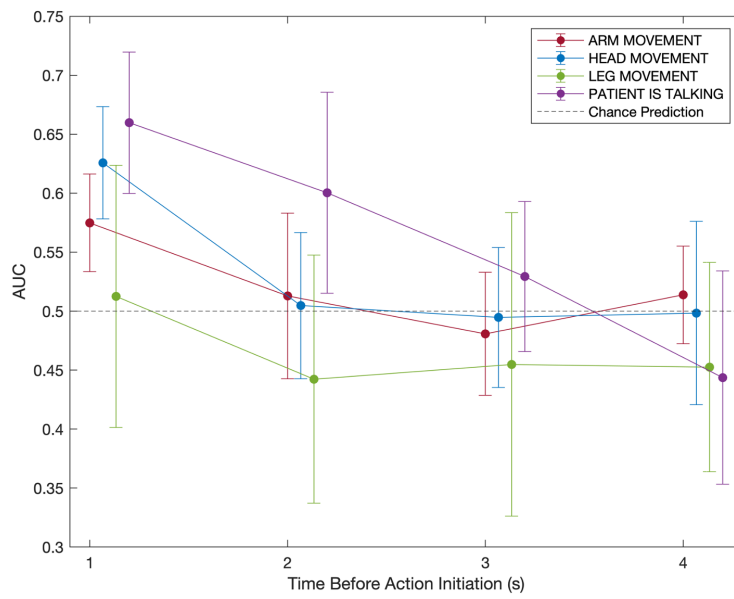
Subject	Precision	Recall	F1	Accuracy	Baseline Accuracy
1	0.51 (0.04)	0.44 (0.04)	0.43 (0.04)	0.55 (0.03)	0.39
2	0.65 (0.01)	0.65 (0.02)	0.65 (0.02)	0.68 (0.01)	0.47
3	0.61 (0.08)	0.49 (0.04)	0.51 (0.04)	0.75 (0.01)	0.46

Table 3.6: Multi-class Classification Mean and Standard Deviation of Metrics

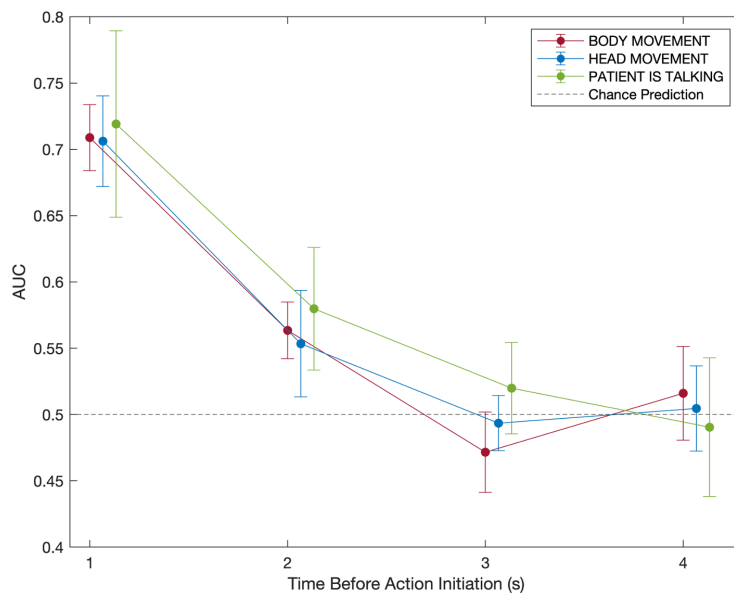
3.6 Prediction of Future Events

I attempted above-chance classification for repetitive movement-based activities that are clearly initiated by the subject. For 1s, 2s, 3s, and 4s before the start of an activity, I calculated the AUC for classification in all three subjects. Figure 3.16 provides these results. All behaviors except leg movement in all subjects could be classified above chance (AUC of 0.5) one second before action initiation. In subject 1 and 2, even at two seconds before action initiation, there could be above chance classification of patient talking. In subject 2, two seconds before, both body movement and head movement could be classified above chance as well. As a sanity check, for both three second and four seconds, all signal was lost and the AUC was distributed seemingly randomly around 0.5 AUC.

Subject 1



Subject 2



Subject 3

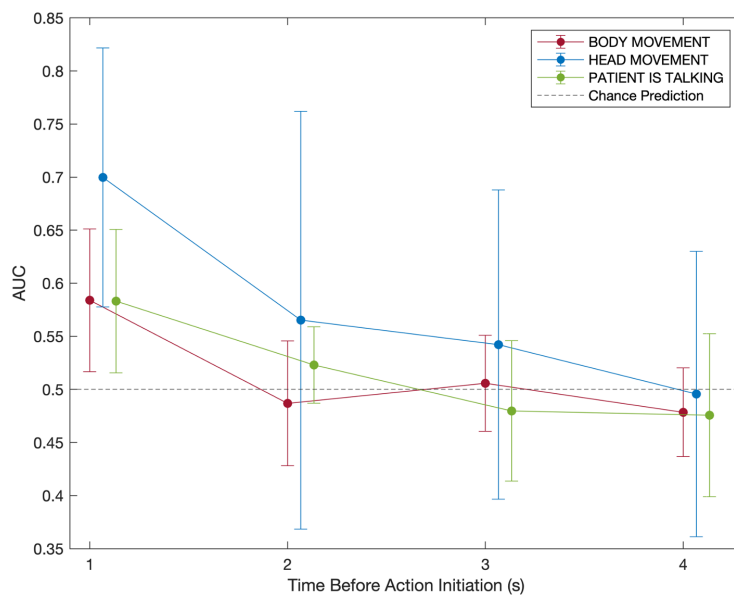


Figure 3.16 Prediction of Behaviors Before their Initiation. The x-axis is the timepoint of the last data point used in classification (1s means that data from 1/250s to 1s was used). The y-axis is the AUC with the chance prediction line at 0.5. Each subplot is for a different subject and each line is for a different behavior. The error bars represent the standard deviation in AUC over ten shuffles of the train-test split.

3.7 Association with Brain Areas

Even given the ability to classify the ten behaviors for 3 subjects, it is important to consider where the information for classification is coming from. In the following subsections, I will show the top electrodes and interaction between electrodes and their associated brain areas that provide the best separation between the on and off state for an activity. It is important to note that these are simple associations and there is no causation being implied here.

In the following tables (Tables 3.7-3.9), I show the brain areas from which the top 5 electrodes (based on the discriminability index- DI) are from. While I did calculate the AUC for individual electrodes, the results are not included here due to the greater interpretability of the DI metric. The AUC results generally follow the DI results. I only show information from three features (RMS, Gamma, and HE) that are not highly correlated to try to capture the complete information brain signals without providing information for all 12 features. The values in parentheses for each table indicate the DI value that is associated with the electrode in that region of the brain. A negative sign indicates that the feature had a lower value in the on state than the off state. Note that arm movement and leg movement are only for subject 1, which has only 35 electrodes to compare across.

- **BODY MOVEMENT:** For body movement, across all three features, the post-central gyrus and the precentral gyrus dominate the most important features. In the gamma frequency, while the DIs are lower in magnitude, they have positive values in contrast to the negative values seen for HE and RMS. Another important area shown by the gamma results is the precuneus area.
- **CONTACT:** There is more variation in the top ranked brain areas for contact but generally, contact is associated with the inferior parietal area. The lingual, supramarginal, and precentral are also highly associated with contact.

- **EATING:** Eating has similar patterns as body movement. The postcentral and precentral gyrus are the important regions for differentiation between eating and no eating. There are negative DIs for RMS and Hurst and positive DIs for gamma.
- **HEAD MOVEMENT:** Again, the postcentral and precentral gyrus are important across all three features but now the paracentral area has less RMS and HE during head movement while the precuneus and lingual area have higher gamma activity.
- **PATIENT IS TALKING:** The top ranked area in all three features is the pars opercularis. All three features have lower values when the patient is talking. Other important areas are the inferior parietal, precentral, and fusiform areas.
- **QUIET:** For the RMS feature, the inferior parietal area dominates the quiet activity. There is a higher RMS in the inferior parietal area during quiet in comparison to non-quiet. In HE and gamma, the lateral occipital and inferior temporal are very important as well. Again, HE and gamma have opposite signs for the DI. This time there is higher HE content for quiet than non-quiet.
- **SLEEP:** There doesn't seem to be a specific brain region that has an especially high magnitude of DI. There is more of a uniformly high DI throughout many brain areas. Sleep also has the highest DIs in which the DI is negative for gamma and positive for RMS and HE.
- **SOMEONE IS TALKING:** Similar to the patient is talking and quiet activities, the inferior parietal area is best for distinguishing between times when someone is talking and when there is no one talking. The pars opercularis region and fusiform region are also important. For HE and RMS, the feature values are always lower during the activity.
- **VIDEO GAMES:** The inferior parietal area is again found as the top region across all three features. In addition, the fusiform and lingual area represent many of the top electrodes for the HE and gamma features while the cuneus has a high DI for RMS.
- **WATCH TV:** The lingual area is the dominant region for all features and curiously the DI is positive for all three features.

3.7 Association with Brain Areas

- **ARM MOVEMENT and LEG MOVEMENT:** These two behaviors were only performed by subject 1 and there was sparse coverage of the brain. For both arm movement and leg movement, the supramarginal gyrus, the superior temporal gyrus, and the postcentral gyrus are the most important. Again, the DIs were positive for gamma and negative for RMS and HE.

Behavior	Rank 1	Rank 2	Rank 3	Rank 4	Rank 5
BODY MOVEMENT	postcentral (-0.45)	postcentral (-0.42)	precentral (-0.38)	postcentral (-0.37)	postcentral (-0.35)
CONTACT	lingual (-0.31)	inferior- parietal (0.30)	supra- marginal (-0.29)	lingual (-0.28)	perical- carine (-0.27)
EATING	postcentral (-0.54)	precentral (-0.52)	postcentral (-0.47)	postcentral (-0.46)	precentral (-0.45)
HEAD MOVEMENT	inferior- parietal (0.43)	inferior- parietal (0.41)	superi- orfrontal (-0.40)	paracen- tral (-0.40)	precentral (-0.40)
PATIENT IS TALKING	parsop- ercularis (-0.71)	inferior- parietal (-0.65)	precentral (-0.61)	inferior- parietal (-0.61)	supra- marginal (-0.53)
QUIET	inferior- parietal (0.80)	inferior- parietal (0.79)	inferior- parietal (0.76)	inferior- parietal (0.75)	inferior- parietal (0.73)
SLEEP	precentral (0.82)	precentral (0.80)	postcentral (0.78)	superi- orfrontal (0.77)	superi- orfrontal (0.76)
SOMEONE IS TALKING	inferior- parietal (-0.88)	inferior- parietal (-0.84)	parsop- ercularis (-0.79)	supra- marginal (-0.77)	precentral (-0.69)
VIDEO GAMES	inferior- parietal (-0.84)	parsop- ercularis (0.82)	inferior- parietal (-0.74)	precentral (0.71)	cuneus (0.67)
WATCH TV	lingual (0.58)	precentral (-0.56)	paracen- tral (-0.55)	precentral (-0.52)	precentral (-0.50)
ARM MOVEMENT	supra- marginal (-0.34)	postcentral (-0.30)	inferior- parietal (-0.26)	lateraloc- cipital (-0.22)	inferior- parietal (-0.21)
LEG MOVEMENT	superi- ortemporal (-0.18)	supra- marginal (-0.18)	inferior- parietal (-0.16)	lateraloc- cipital (-0.16)	inferior- parietal (-0.15)

Table 3.7: RMS Feature Top Electrodes Based on the Discriminability Index

3.7 Association with Brain Areas

Behavior	Rank 1	Rank 2	Rank 3	Rank 4	Rank 5
BODY MOVEMENT	postcentral (-0.76)	postcentral (-0.71)	postcentral (-0.71)	postcentral (-0.69)	precentral (-0.68)
CONTACT	inferior- parietal (0.37)	superi- ortemporal (0.36)	lateraloc- cipital (0.34)	precentral (0.33)	postcentral (0.30)
EATING	postcentral (-1.47)	postcentral (-1.36)	precentral (-0.92)	supra- marginal (-0.87)	postcentral (-0.83)
HEAD MOVEMENT	precentral (-0.63)	paracen- tral (-0.63)	postcentral (-0.56)	postcentral (-0.55)	superi- orfrontal (-0.53)
PATIENT IS TALKING	parsop- ercularis (-0.59)	inferior- parietal (-0.55)	fusiform (- 0.52)	precentral (-0.51)	inferi- ortemporal (-0.47)
QUIET	inferi- ortemporal (0.85)	lateraloc- cipital (0.84)	superior- parietal (0.83)	inferior- parietal (0.82)	lateraloc- cipital (0.82)
SLEEP	superior- parietal (0.92)	lateraloc- cipital (0.92)	precentral (0.78)	precentral (0.78)	lateraloc- cipital (-0.78)
SOMEONE IS TALKING	inferior- parietal (-0.87)	fusiform (- 0.82)	inferi- ortemporal (-0.76)	parsop- ercularis (-0.72)	inferior- parietal (-0.70)
VIDEO GAMES	inferior- parietal (-0.96)	inferior- parietal (-0.89)	fusiform (- 0.89)	inferior- parietal (-0.83)	fusiform (- 0.82)
WATCH TV	lingual (0.48)	lingual (0.47)	superi- orfrontal (-0.43)	lingual (0.43)	lingual (0.42)
ARM MOVEMENT	supra- marginal (-0.39)	postcentral (-0.28)	lateraloc- cipital (-0.20)	lateraloc- cipital (-0.19)	inferior- parietal (-0.19)
LEG MOVEMENT	superi- ortemporal (-0.33)	superi- ortemporal (-0.20)	superi- ortemporal (-0.19)	supra- marginal (-0.18)	lateraloc- cipital (-0.13)

Table 3.8: HE Feature Top Electrodes Based on the Discriminability Index

3.7 Association with Brain Areas

Behavior	Rank 1	Rank 2	Rank 3	Rank 4	Rank 5
BODY MOVEMENT	postcentral (0.38)	precuneus (0.30)	paracentral (0.29)	posteriorcingulate (-0.29)	precuneus (0.27)
CONTACT	inferior-parietal (-0.39)	inferior-parietal (-0.37)	superior-temporal (-0.37)	inferior-parietal (-0.32)	supramarginal (-0.30)
EATING	postcentral (1.27)	postcentral (1.14)	postcentral (0.88)	supramarginal (0.88)	superior-temporal (0.84)
HEAD MOVEMENT	precuneus (0.52)	lingual (0.43)	postcentral (0.42)	superior-parietal (0.42)	lateralocipital (0.41)
PATIENT IS TALKING	parsopercularis (-0.37)	precentral (-0.34)	middletemporal (0.26)	inferior-parietal (-0.25)	postcentral (0.24)
QUIET	lateralocipital (-0.74)	inferior-temporal (-0.72)	lateralocipital (-0.68)	lateralocipital (-0.68)	superior-parietal (-0.67)
SLEEP	superior-temporal (-1.05)	middletemporal (-0.90)	inferior-temporal (-0.90)	inferior-parietal (-0.89)	middletemporal (-0.86)
SOMEONE IS TALKING	lateralocipital (0.37)	parsopercularis (-0.37)	middletemporal (-0.34)	fusiform (0.33)	inferior-temporal (0.33)
VIDEO GAMES	fusiform (0.85)	inferior-parietal (0.74)	lingual (0.73)	lingual (0.72)	inferior-parietal (0.69)
WATCH TV	lingual (0.46)	lingual (0.42)	lingual (0.42)	lingual (0.42)	lingual (0.38)
ARM MOVEMENT	supramarginal (0.20)	postcentral (0.17)	superior-temporal (0.13)	lateralocipital (0.13)	lateralocipital (0.11)
LEG MOVEMENT	superior-temporal (0.19)	superior-temporal (0.14)	temporalpole (0.14)	lateralocipital (0.11)	fusiform (-0.08)

Table 3.9: Mean Gamma Power Feature Top Electrodes Based on the Discriminability Index

The following figures show the DIs of the electrodes and the average DI of brain areas on the brain itself to get an understanding of the crucial areas, their relation to each other in space, and also their relation to regions that may not be as useful for decoding. While it is not possible to include every feature and behavior combination, I provide 9 of the 12 behaviors sorted based on theme and a selection of a feature with relatively high

3.7 Association with Brain Areas

DI values for each of the 9 behaviors. Note that I did not consider the arm movement and leg movement behaviors here because of the low amount of electrodes available (35) and the resulting lack of coverage of a substantial area of the brain.

I also adapted a figure showing the Desikan-Killany parcellation of the brain for reference. The different regions referenced later can be found easily on this map.

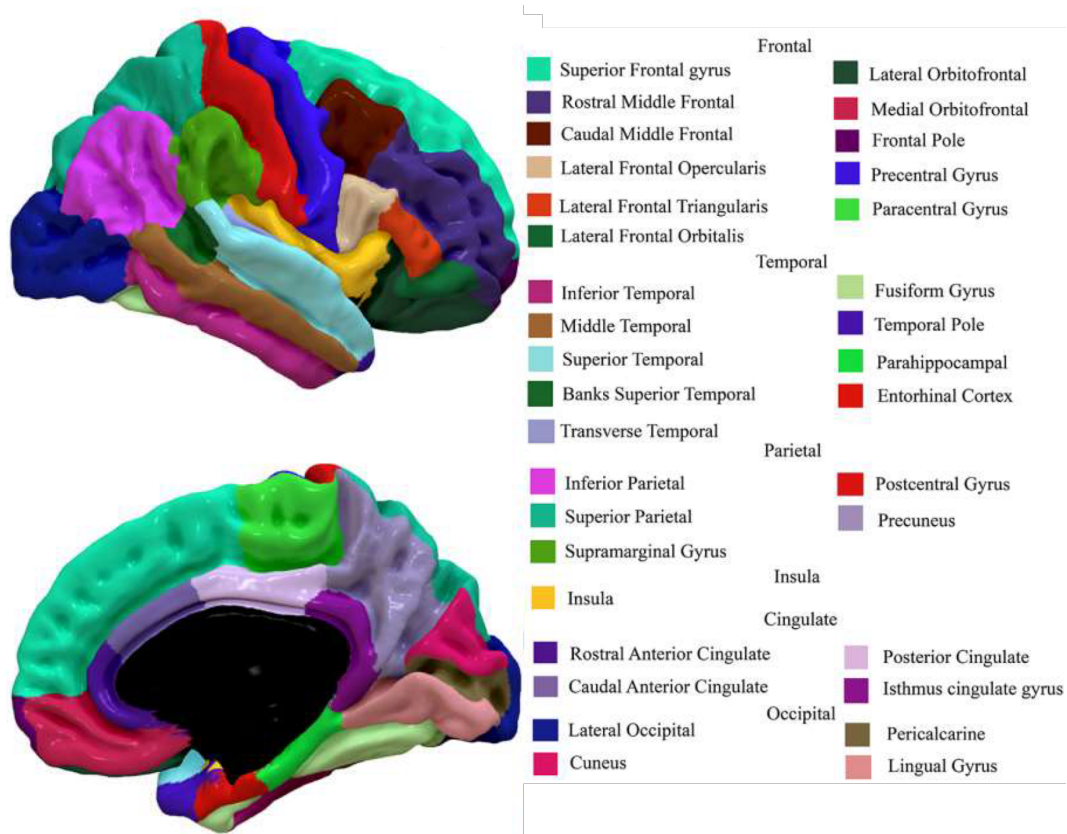
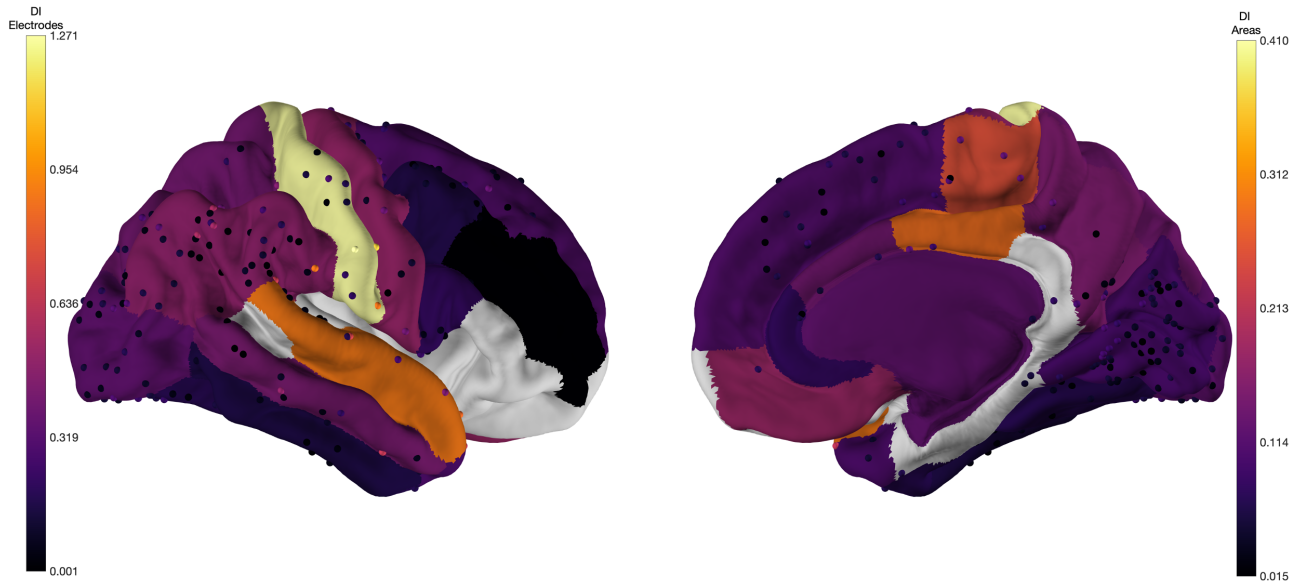
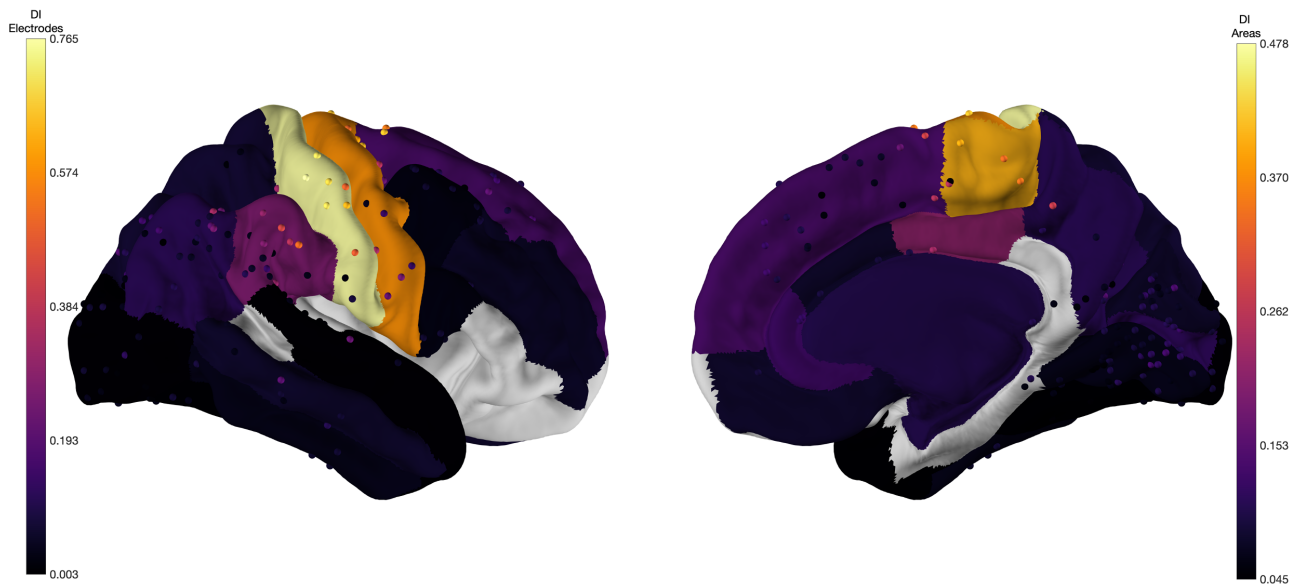


Figure 3.17 Desikan-Killany Parcellation on the Right Hemisphere of the Brain. Each Region is colored differently and the corresponding name is included in the legend on the right. This visualization is adapted from Dong et al. (Dong et al., 2021)

Eating-Gamma



Body Movement- HE



Head Movement- MAV

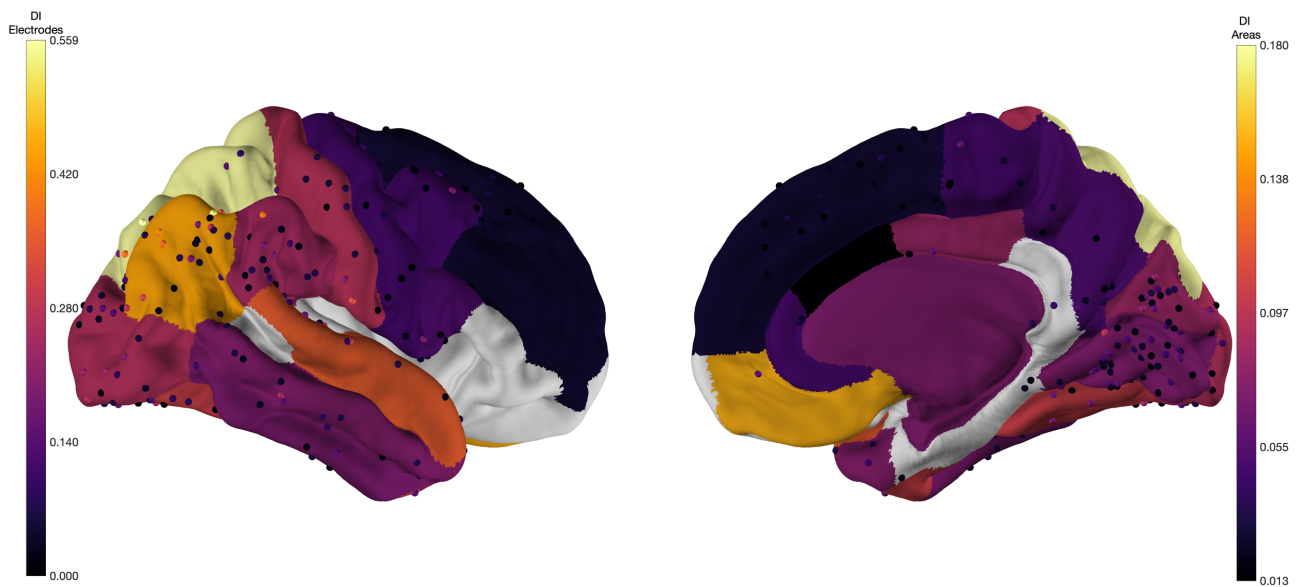
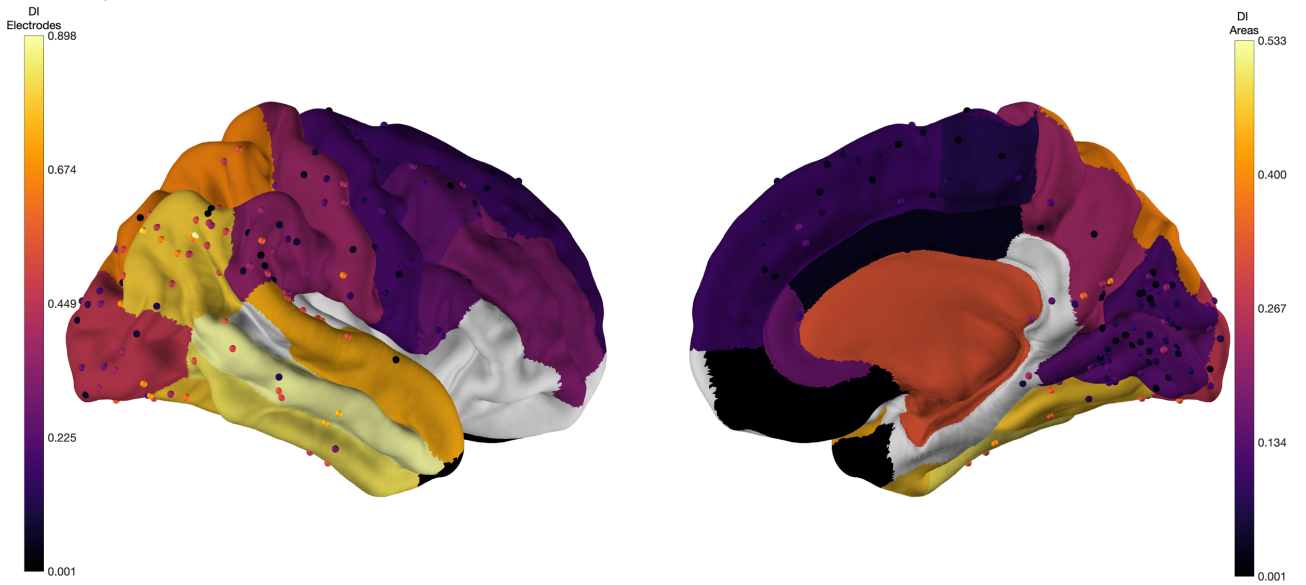


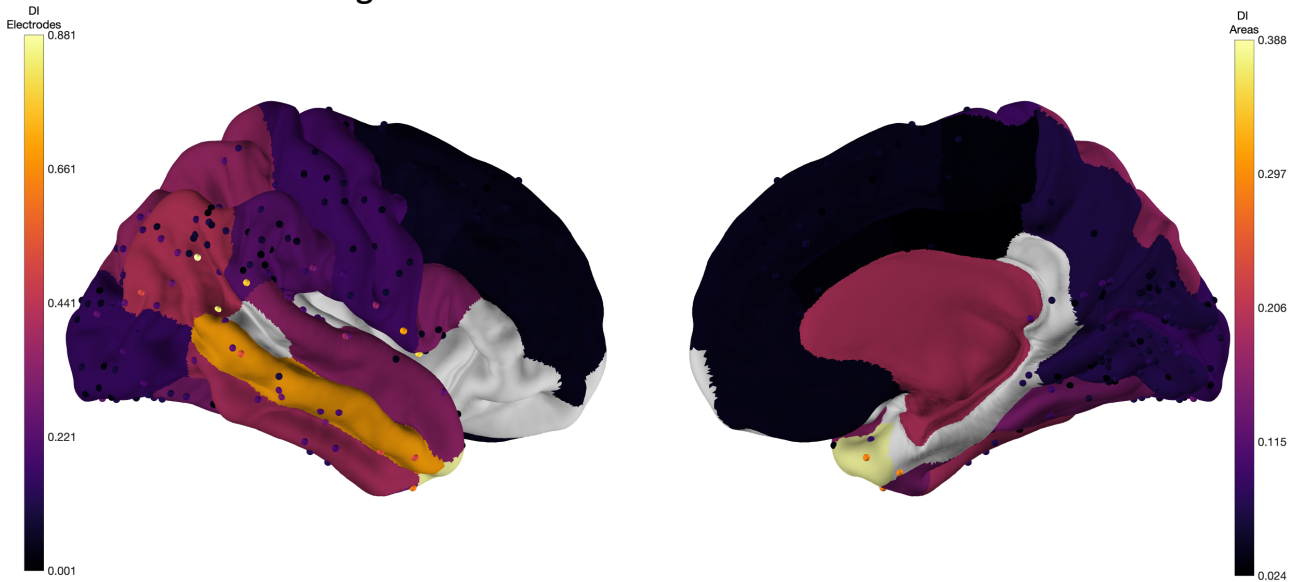
Figure 3.18 Magnitude of Discriminability Index (DI) Visualized for Three Activities with Movement Components (Eating, Body Movement, Head Movement) on an Average Brain for the 280 electrodes and 36 Brain Areas. The top figure is for eating and the mean gamma power is the feature. The middle figure is for body movement and the feature is HE. The bottom figure is for head movement and the MAV feature. The brain areas with at least one electrode are colored while the brain areas not covered are in gray. Each dot is an electrode and they are colored based on DI. The brain areas are also colored based on average DI. The color bar on the left is for electrodes and the color bar on the right is for brain areas.

In figure 3.18, for eating and gamma there is a very similar pattern of important regions and important electrodes. For both activities, the most light region (region with highest average DI) is the postcentral gyrus followed closely by the precentral gyrus (the region located more towards the front the of the brain) for body movement. It is important to notice that for eating, the electrodes with highest DI are located towards the bottom of the postcentral gyrus. Instead the most important electrodes for body movement are towards the middle and top of the postcentral gyrus. For body movement, this pattern is the same for the precentral gyrus. Head movement doesn't follow the same pattern as the others. Instead, the inferior and superior parietal regions have the highest average DIs and electrodes with the highest DIs. In addition, there is an electrode at the bottom off the postcentral gyrus with relatively high DI. Across all figures, there is little importance from the frontal areas of the brain (although there is not a lot of coverage on the frontal lobe).

Quiet- MIN



Someone is Talking- RMS



Patient Speaking-RMS

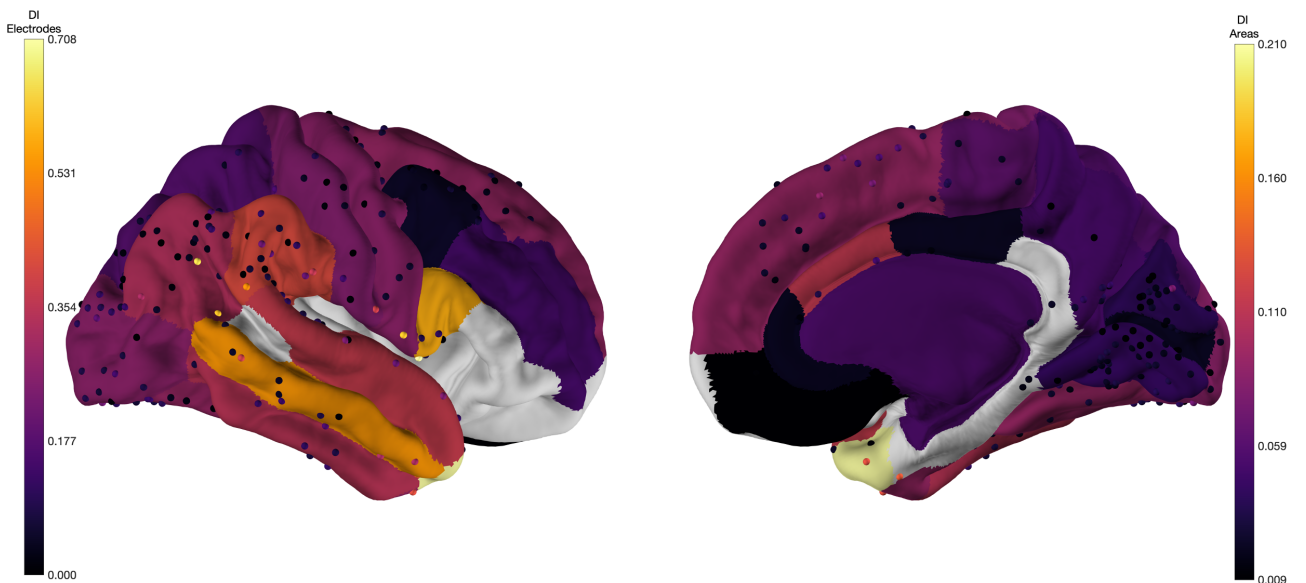
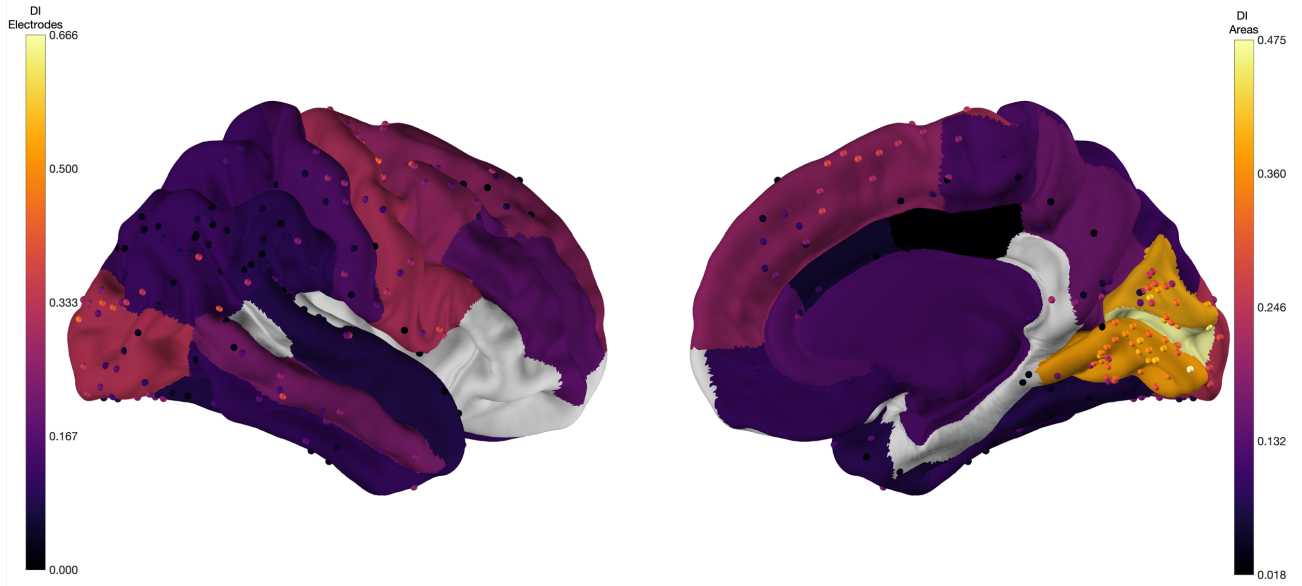


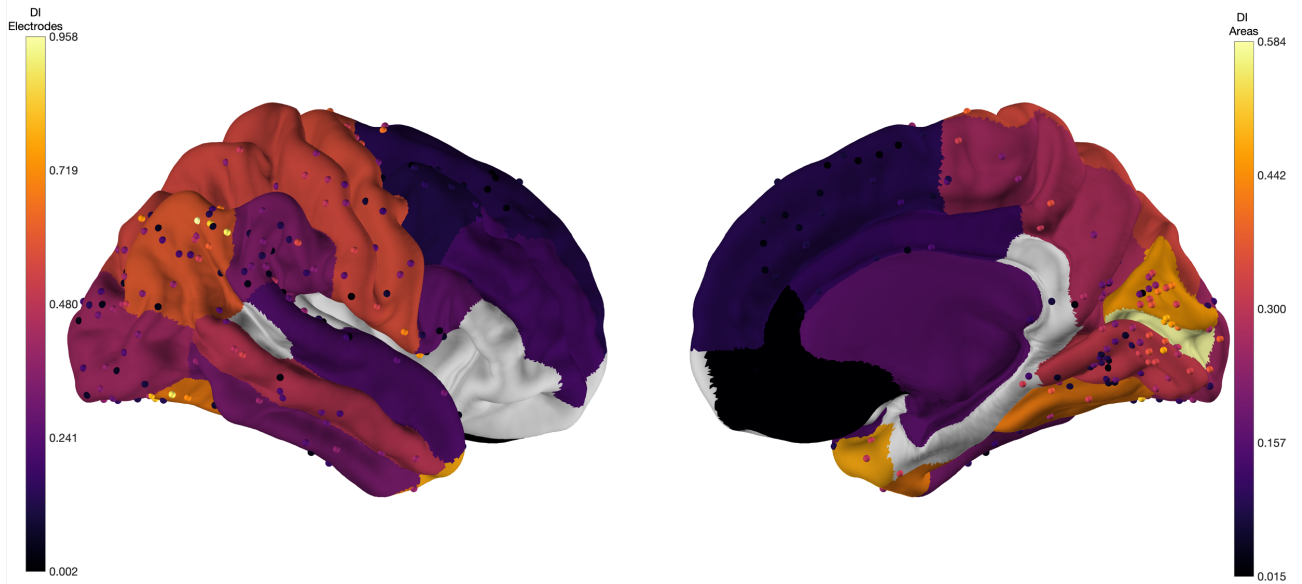
Figure 3.19 Magnitude of Discriminability Index (DI) Visualized for Three Hearing and Speaking Based Activities (Quiet, Someone is Talking, Patient is Speaking) on an Average Brain for the 280 electrodes and 36 Brain Areas. The top figure is for quiet and MIN is the feature. The middle figure is for someone is talking and the feature is RMS. The bottom figure is for patient is speaking and the RMS feature. The brain areas with at least one electrode are colored while the brain areas not covered are in gray. Each dot is an electrode and they are colored based on DI. The brain areas are also colored based on average DI. The color bar on the left is for electrodes and the color bar on the right is for brain areas.

As seen in figure 3.19, quiet, someone is talking, and patient is talking all have similar brain areas and electrodes with the highest DIs. For someone is talking and patient is talking, the highest average DI for brain area is the temporal pole while it is the middle temporal gyrus for quiet. The middle temporal gyrus is the light strip in the bottom of the left brain image for the quiet figure. The middle temporal is the light region at the bottom left of the right brain image of the someone is talking and patient speaking figures. The most informative electrodes are, however, not primarily in these locations. Instead, the inferior parietal area (area with light colored electrodes at the back of the brain) contains some of the electrodes with highest DIs across all of the three activities. In addition, for someone is talking and patient is speaking, the pars operculis (front area with one light electrode) and the supramarginal gyrus (right of the inferior parietal area) also contain electrodes with the highest DIs.

Watch TV- Beta



Video Games- HE



Sleeping- Theta

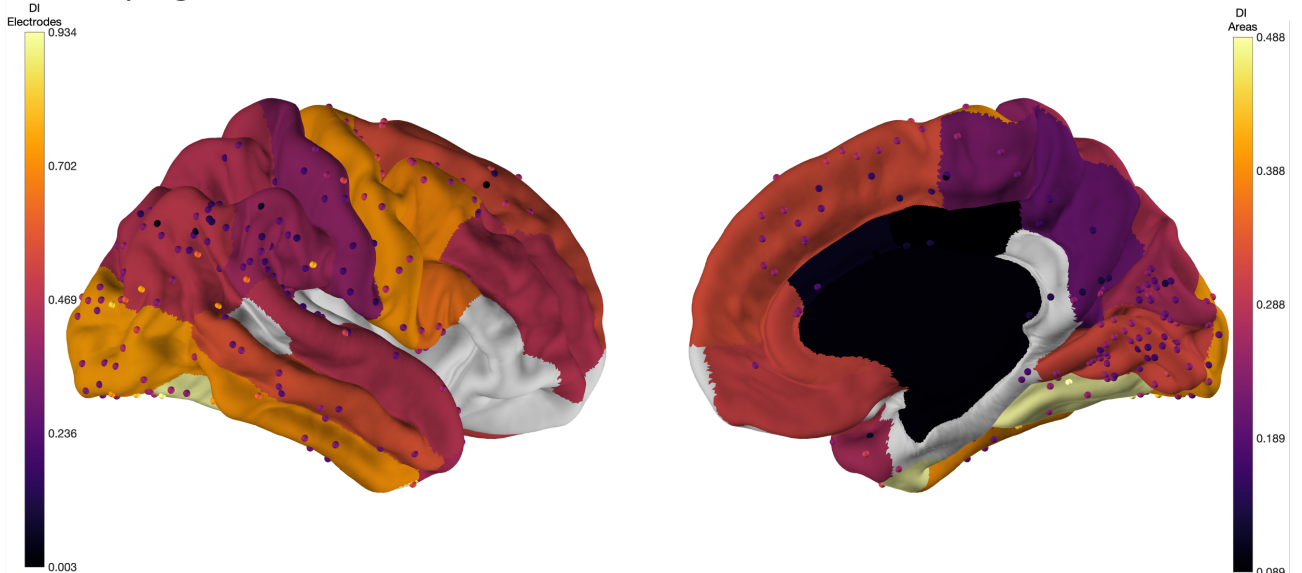


Figure 3.20 Magnitude of Discriminability Index (DI) Visualized for Three Large Scale Activities (Watching TV, Video Games, and Sleeping) on an Average Brain for the 280 electrodes and 36 Brain Areas. The top figure is for watching tv and mean beta power is the feature. The middle figure is for video games and the feature is HE. The bottom figure is for sleeping and the mean theta power feature. The brain areas with at least one electrode are colored while the brain areas not covered are in gray. Each dot is an electrode and they are colored based on DI. The brain areas are also colored based on average DI. The color bar on the left is for electrodes and the color bar on the right is for brain areas.

The most similar activities in the large scale activity visualization (figure 3.20) are video games and watching tv. In both, the pericalcarine (light area shown on the right image of the brain) has the highest average DI followed by the cuneus area and lingual area for both (also on the right image of the brain). The lingual and cuneus area contain the most important individual electrodes for watching tv. For video games, the highest DI electrodes are not in the pericalcarine, lingual, or cuneus. Instead, they are in the inferior parietal area and the fusiform gyrus. Again, for video games and watching tv, there is a large different between region and individual electrode importance shown by the very light regions and the very dark regions. For sleep, the signal is more diffuse as there are mostly light regions with only one very dark region, which represents the electrodes that have an unknown brain region. The highest average DI regions are the fusiform (bottom of the right brain figure) and lateral occipital area (back and bottom region of the left brain figure) and the most important electrodes are also located there.

3.8 Association with Brain Area Interaction

Of the six defined waves (delta, theta, alpha, beta, gamma, and broadband), I chose to focus on the theta waves and broadband waves as they both provided high DIs while also having very different region pairs as the top 5 in terms of DI. The following tables provide the top 5 electrode pairs based on DI. As in the previous section, the values in parentheses for each table indicate the DI value that is associated with the electrode in that region of the brain. A negative sign indicates that the feature had a lower value in the on state than the off state. Note that arm movement and leg movement are only for subject 1, which has only 35 choose 2 electrode pairs to compare across.

- **BODY MOVEMENT:** For body movement, the most important electrode pairs

for theta coherence (DIs are higher than those in the broadband coherence) are centered at the caudal middle frontal area (adjacent to the precentral gyrus). There is an increase in theta coherence between the caudal middle frontal area and the postcentral gyrus, pars opercularis area, and precentral gyrus. For broadband coherence, the results are more heterogenous. There is higher broadband coherence between the lateral occipital area and the inferior parietal area and the middle temporal area. In addition, there is a higher interaction between the cuneus area and the precentral gyrus.

- **CONTACT:** Again, for the contact activity, the theta coherence provides consistent results. The theta coherence is lower during contact between the inferior parietal area and the precentral gyrus, fusiform gyrus, postcentral gyrus, lateral occipital area, and the middle temporal area. The broadband coherence has a similar pattern where the broadband coherence between the inferior temporal area and the superior temporal area and middle temporal area is lower during contact.
- **EATING:** Eating has similar results as the single electrode comparisons in the previous section. For both theta and broadband coherence, the interaction between the precentral and postcentral gyrus and other areas is the most important. However, it is important to note that broadband coherence is higher and theta coherence is lower. Broadband coherence has much higher DI as well.
- **HEAD MOVEMENT:** In head movement, the interaction between the inferior parietal area and adjacent areas is the most important for identifying on and off states in the broadband frequency. The inferior parietal area interacts less with lingual, cuneus, lateral occipital areas, and itself during head movement. Instead, there is an increase between theta coherence in the precentral gyrus and surrounding areas such as the superior frontal, posterior cingulate, and precuneus.
- **PATIENT IS TALKING:** During talking, there is an increased theta coherence between the pars opercularis area and the inferior parietal area, middle temporal area, and fusiform area. Similarly, there is increased broadband coherence between pars opercularis area and the middle temporal area, postcentral area, and the inferior parietal area. In addition, there is increased broadband coherence between the precentral gyrus and the middle temporal area and the postcentral gyrus.

- **QUIET:** The coherence results for quiet were not as homogeneous as other activities. There seems to be decreased theta coherence between electrodes in the inferior parietal area and the lateral occipital area. In addition, there is decreased theta coherence between the superior parietal and supramarginal areas. In the broadband frequency, there is decreased coherence between the cuneus area and the lateral occipital area, inferior parietal area, and inferior temporal area.
- **SLEEP:** The broadband coherence increases between the different combinations of the precentral gyrus, superior temporal area, and inferior temporal area. There is an increase in theta coherence between the inferior parietal area and the inferior temporal area, postcentral gyrus, precentral gyrus, and the lingual area.
- **SOMEONE IS TALKING:** The main regions (electrode locations within the regions) that have higher broadband coherence with others while someone is talking are the middle temporal region, pars opercularis, postcentral, supramarginal, and precentral. For the theta frequency, there is increased coherence in the same regions.
- **VIDEO GAMES:** There is increased broadband coherence between electrode locations in the inferior parietal area and adjacent areas (postcentral, superior temporal, lateral occipital, and superior parietal). Conversely, there is decreased theta coherence between electrode locations in the pars opercularis and the middle temporal area and the inferior parietal area. There is also decreased theta coherence for the inferior parietal area and the lingual area.
- **WATCH TV:** There is increased broadband coherence between electrode locations in the inferior parietal area and electrodes in the same area, lateral occipital area, and cuneus area. The results are heterogeneous for the theta coherence. There is increased coherence between the superior frontal area and precentral gyrus and the supramarginal area. Also, there is decreased coherence between electrodes in the lingual area and the precuneus area and inferior parietal area.
- **ARM MOVEMENT and LEG MOVEMENT:** For these behaviors, there are not many electrodes, so the results are likely biased. Here, there is an increased theta coherence and broadband coherence between the lingual, precuneus, and cuneus areas.

3.8 Association with Brain Area Interaction

Behavior	Rank 1	Rank 2	Rank 3	Rank 4	Rank 5
BODY MOVEMENT	lateraloccipital: middletemporal (0.37)	cuneus: precentral (0.36)	precuneus: posteriorcingulate (0.36)	inferiorparietal: lateraloccipital (0.36)	precuneus: supra-marginal (0.35)
CONTACT	middletemporal: postcentral (-0.40)	superiortemporal: inferiorparietal (-0.40)	superiortemporal: inferiorparietal (-0.40)	middletemporal: inferiorparietal (-0.40)	superiortemporal: inferiorparietal (-0.40)
EATING	postcentral: postcentral (-1.28)	postcentral: precentral (-1.16)	postcentral: superiortemporal (-1.10)	superior-frontal: postcentral (-1.09)	superior-frontal: postcentral (-1.07)
HEAD MOVEMENT	lingual: inferiorparietal (-0.68)	cuneus: inferiorparietal (-0.65)	inferiorparietal: lateraloccipital (-0.62)	inferiorparietal: inferiorparietal (-0.61)	inferiorparietal: inferiorparietal (-0.58)
PATIENT IS TALKING	middletemporal: parsopercularis (0.47)	middletemporal: precentral (0.46)	parsopercularis: postcentral (0.42)	precentral: postcentral (0.41)	inferiorparietal: parsopercularis (0.38)
QUIET	cuneus: lateraloccipital (0.64)	inferiorparietal: inferiorparietal (-0.62)	cuneus: inferiorparietal (0.62)	cuneus: lateraloccipital (0.60)	cuneus: inferiortemporal (0.58)
SLEEP	superiortemporal: precentral (0.94)	inferiortemporal: precentral (0.89)	superiortemporal: inferiortemporal (0.88)	superiortemporal: inferiorparietal (0.88)	middletemporal: inferiortemporal (0.88)
SOMEONE IS TALKING	middletemporal: precentral (0.58)	middletemporal: parsopercularis (0.50)	supra-marginal: parsopercularis (0.43)	parsopercularis: postcentral (0.43)	middletemporal: postcentral (0.43)
VIDEO GAMES	unknown: lingual (-0.79)	inferiorparietal: postcentral (0.77)	superiortemporal: inferiorparietal (0.74)	lateraloccipital: inferiorparietal (0.73)	superiorparietal: inferiorparietal (0.69)
WATCH TV	inferiorparietal: inferiorparietal (0.70)	inferiorparietal: inferiorparietal (0.69)	inferiorparietal: inferiorparietal (0.68)	lateraloccipital: inferiorparietal (0.65)	cuneus: inferiorparietal (0.61)
ARM MOVEMENT	lingual: precuneus (0.27)	cuneus: lingual (0.25)	cuneus: lingual (0.24)	lingual: precuneus (0.23)	lingual: precuneus (0.23)
LEG MOVEMENT	lingual: precuneus (0.45)	lingual: cuneus (0.45)	lingual: cuneus (0.44)	cuneus: lingual (0.43)	cuneus: lingual (0.42)

Table 3.10: Broadband Coherence Top 5 Electrode Pairs Based on the Discriminability Index

3.8 Association with Brain Area Interaction

Behavior	Rank 1	Rank 2	Rank 3	Rank 4	Rank 5
BODY MOVEMENT	caudalmid- dleftfrontal: postcentral (0.52)	posteri- orcingu- late: supra- marginal (0.50)	caudalmid- dleftfrontal: parsopercu- laris (0.49)	caudalmid- dleftfrontal: parsopercu- laris (0.49)	caudalmid- dleftfrontal: precentral (0.49)
CONTACT	inferior- parietal: precentral (-0.35)	fusiform: in- feriorparietal (-0.35)	inferior- parietal: postcentral (-0.35)	lateraloccip- ital: infe- riorparietal (-0.35)	middletem- poral: infe- riorparietal (-0.35)
EATING	superior- frontal: postcentral (0.70)	postcentral: caudalmid- dleftfrontal (0.70)	postcentral: rostralmid- dleftfrontal (0.70)	postcentral: superiortem- poral (0.67)	supra- marginal: postcentral (0.63)
HEAD MOVEMENT	posteri- orcingulate: precentral (0.49)	superior- frontal: precentral (0.49)	precuneus: precentral (0.49)	precuneus: precentral (0.49)	paracentral: precentral (0.48)
PATIENT IS TALKING	inferiorpari- etal: par- sopercularis (0.78)	middletem- poral: par- sopercularis (0.73)	fusiform: par- sopercularis (0.71)	middletem- poral: par- sopercularis (0.70)	inferior- parietal: precentral (0.70)
QUIET	superiorpari- etal: supra- marginal (-0.90)	lateraloccip- ital: infe- riorparietal (-0.89)	lateraloccip- ital: infe- riorparietal (-0.89)	lateraloccip- ital: supe- riorparietal (-0.88)	superiorpari- etal: lingual (-0.88)
SLEEP	inferiorpari- etal: infe- riorparietal (0.86)	inferiorpari- etal: inferi- ortemporal (0.82)	inferior- parietal: postcentral (0.75)	inferior- parietal: precentral (0.75)	lingual: in- feriorparietal (0.73)
SOMEONE IS TALKING	inferiorpari- etal: par- sopercularis (0.96)	inferior- parietal: precentral (0.92)	inferior- parietal: postcentral (0.90)	middletem- poral: par- sopercularis (0.89)	middletem- poral: supra- marginal (0.89)
VIDEO GAMES	inferiorpari- etal: lingual (-0.80)	middletem- poral: par- sopercularis (-0.80)	middletem- poral: par- sopercularis (-0.79)	inferiorpari- etal: par- sopercularis (-0.79)	inferiorpari- etal: lingual (-0.78)
WATCH TV	superior- frontal: precentral (0.51)	precuneus: inferiorpari- etal (-0.49)	inferiorpari- etal: infe- riorparietal (0.48)	lingual: lin- gual (-0.47)	superior- frontal: supra- marginal (0.47)
ARM MOVEMENT	lingual: lin- gual (0.31)	precuneus: precuneus (0.25)	lingual: cuneus (0.24)	lingual: lin- gual (0.24)	lingual: cuneus (0.24)
LEG MOVEMENT	lingual: pre- cuneus (0.33)	lingual: cuneus (0.32)	lingual: cuneus (0.32)	lingual: pre- cuneus (0.31)	precuneus: cuneus (0.31)

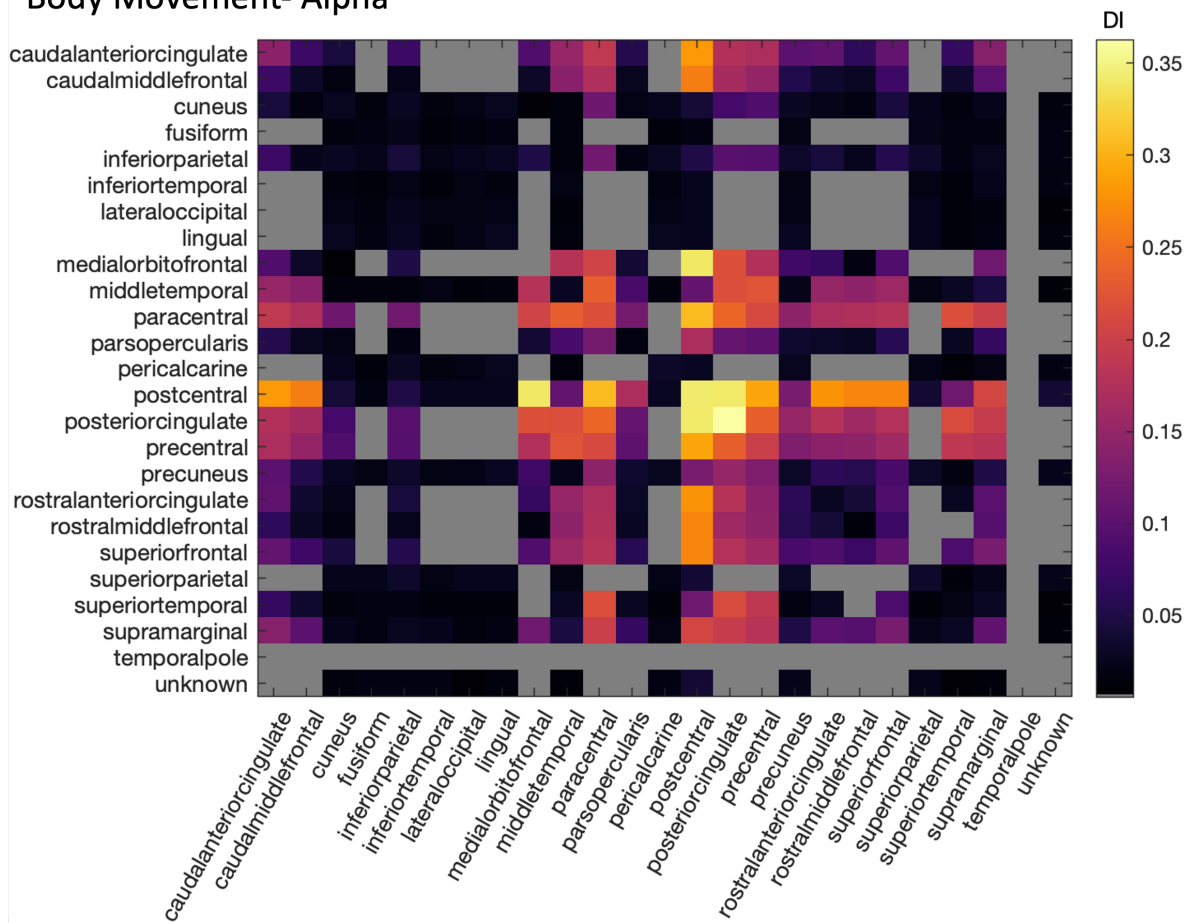
Table 3.11: Theta Coherence Top 5 Electrode Pairs Based on the Discriminability Index

3.8 Association with Brain Area Interaction

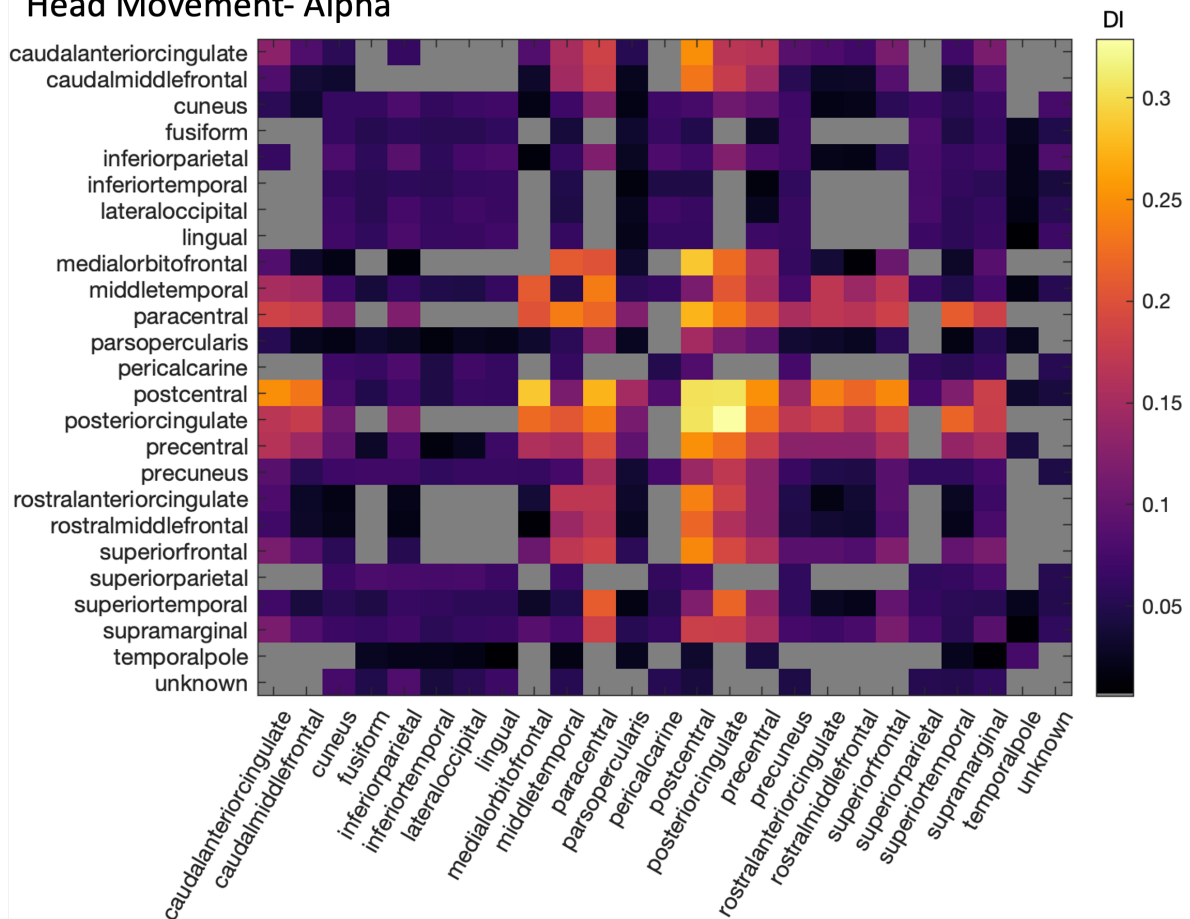
The following figures give insight into the clustering of the brain areas with coherence values that are important in distinguishing between when a behavior is happening and when it is not. The heatmaps depict the average DI for the coherence of all electrode pairs between the two areas. The specific frequency band of coherence is chosen based on the highest average DI for that activity and the activities are grouped by theme.

3.8 Association with Brain Area Interaction

Body Movement- Alpha



Head Movement- Alpha



3.8 Association with Brain Area Interaction

Figure 3.21 Magnitude of Discriminability Index (DI) Visualized for Body Movement and Head Movement Activities for the Different Pairs of Brain Regions Available for Subjects 1-3. The top figure is for Body Movement and mean alpha power is the feature. The bottom figure is for head movement and the feature is mean alpha power. The pair of brain areas with at least one electrode pair are colored while the brain area pairs that are not covered are gray. The brain area pairs are colored based on average DI.

Observing, figure 3.21 as a whole, for body movement and head movement, the average of the magnitude of DI is quite uniform for the alpha coherence. There are a lot of regions with average DIs over 0.25. The pattern of average DI is also remarkably similar between body movement and head movement. The peak of DI is at the interaction of electrodes in the posterior cingulate area. However, this may be because there is only one electrode pair in this area. The areas with a consistently high average DI when interacting with other areas are the postcentral gyrus and precentral gyrus followed by the medialorbitofrontal, middle temporal, and paracentral areas. The interaction between the postcentral area and the caudal anterior cingulate and the caudal middle frontal area also produces a high average DI.

Figure 3.22 Magnitude of Discriminability Index (DI) Visualized for Patient is Talking and Someone is Talking Activities for the Different Pairs of Brain Regions Available for Subjects 1-3. The top figure is for Someone is Talking and mean theta power is the feature. The bottom figure is for Patient is Talking and the feature is mean theta power. The pair of brain areas with at least one electrode pair are colored while the brain area pairs that are not covered are gray. The brain area pairs are colored based on average DI.

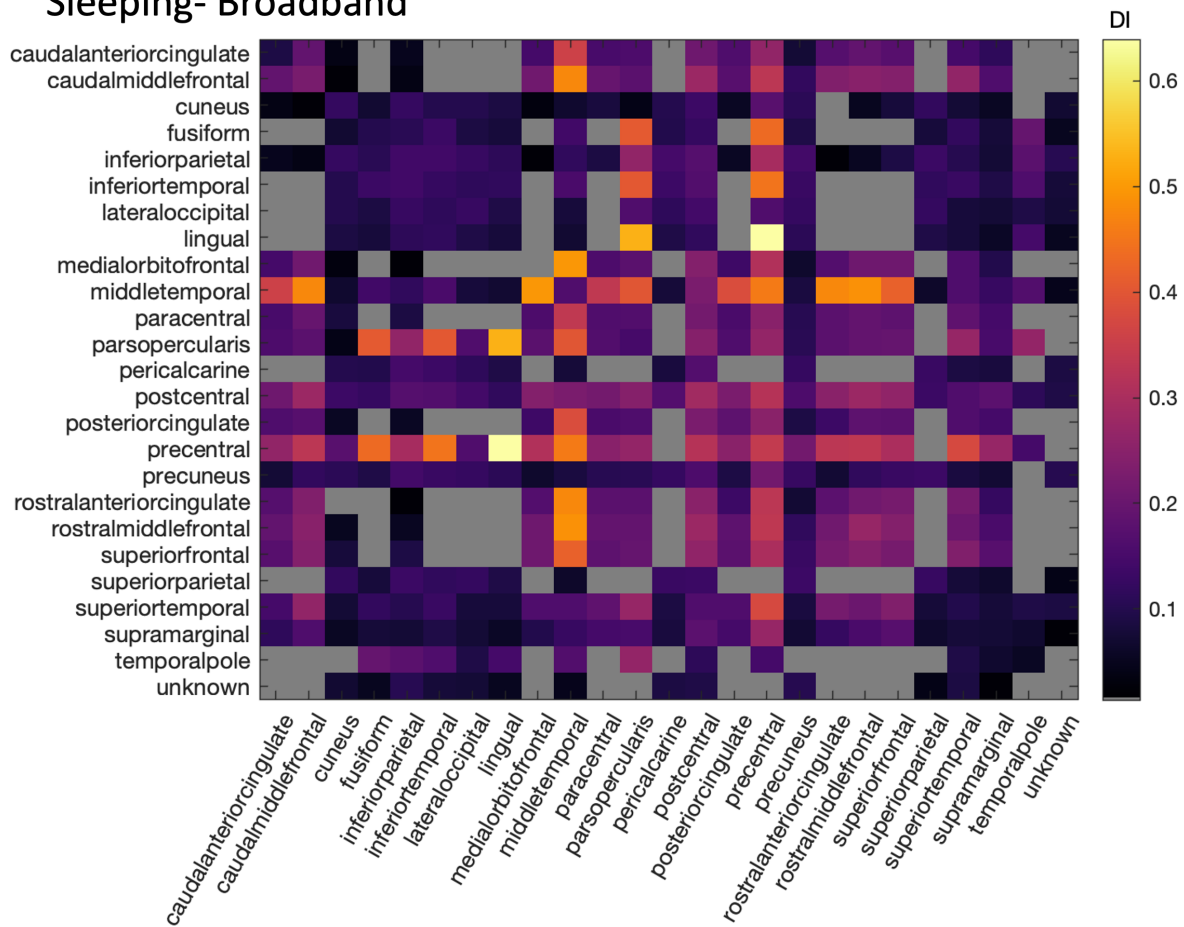
In comparison to the movement activities, there seems to be only a few brain area interactions that are the most important in distinguishing between the on and off states of the talking activities when analyzing theta coherence in figure 3.22. Again, the average magnitude of DIs are very similar across both activities. There is a particularly high average DI for the interaction between the lingual and pars opercularis areas. Again, it is important to take into account that fact there is only one electrode pair between the pars opercularis area and the lingual area. Other notable interactions are between the pars opercularis area and the inferior parietal, inferior temporal, and temporal pole areas. The theta coherence between the temporal pole and many other brain regions is also quite important in these activities as well as shown by the light colored strip on the bottom of the heatmap.

3.8 Association with Brain Area Interaction

Figure 3.23 Magnitude of Discriminability Index (DI) Visualized for Watching TV and Video Games Activities for the Different Pairs of Brain Regions Available for Subjects 1-3. The top figure is for Watching TV and mean gamma power is the feature. The bottom figure is for Video Games and the feature is mean theta power. The pair of brain areas with at least one electrode pair are colored while the brain area pairs that are not covered are gray. The brain area pairs are colored based on average DI.

As is seen in figure 3.23, the two behaviors with a significant visual component do not show the same pattern as each other. Therefore, I will analyze them separately. For watching tv, the many brain area pairs have relatively high average DI. However, there are three brain area interactions that are particularly important in distinguishing between when the patient is and is not watching tv. The interaction between middle temporal and the medial orbitofrontal area and the rostral anterior cingulate in the gamma frequency has a higher average DI. Also, the gamma coherence between the precentral gyrus and lingual area is important in watching tv. Unlike in the other activities pairs discussed thus far, the highest average DI is much higher video games than in watching tv. Overall, there are two main area interactions that are highlighted in the heatmap: lingual and pars opercularis; precentral and lingual. They both have DIs of around 0.67 while the highest DIs for watching TV are around 0.3.

Sleeping- Broadband



Eating- Gamma

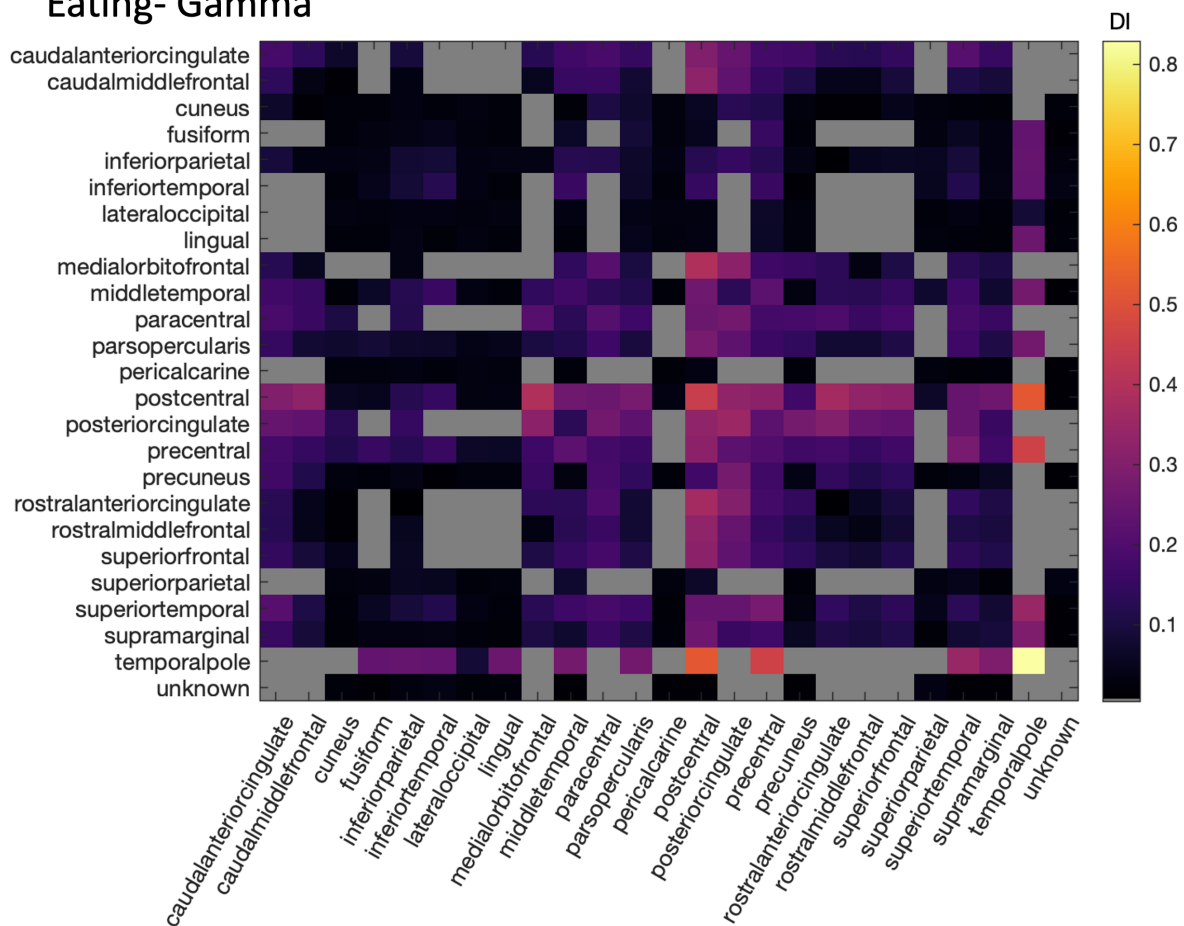


Figure 3.24 Magnitude of Discriminability Index (DI) Visualized for Sleeping and Eating Activities for the Different Pairs of Brain Regions Available for Subjects 1-3. The top figure is for Someone is Talking and mean theta power is the feature. The bottom figure is for Patient is Talking and the feature is mean theta power. The pair of brain areas with at least one electrode pair are colored while the brain area pairs that are not covered are gray. The brain area pairs are colored based on average DI.

While sleeping and eating are very different, they are grouped together here because they fulfill a physiological requirement. Although, as can be seen in figure 3.24, this point of similarity does not translate well into the cortical voltage signals. For eating, there is very high average DI for gamma coherence of electrodes within the temporal pole area. The other highest average region interaction DIs are in the range of 0.5-0.6. The gamma coherence between the postcentral gyrus and the postcentral gyrus, medial orbitofrontal area, and the temporal pole area is important in determining eating. In addition, the interaction between the precentral and the temporal pole in the gamma frequency range has high average DI. For the sleeping activity, there are many different interactions in the broadband frequency that have high average DI: lingual and precentral, lingual and pars opercularis, middle temporal and rostral middle frontal, middle temporal and rostral anterior cingulate, middle temporal and precentral, middle temporal and medial orbitofrontal, and middle temporal and caudal middle frontal.

Chapter 4

Discussion

4.1 Classification

4.2 Main Conclusions

Throughout the results section, I referenced the division between large scale activities (someone is talking, sleep, video games, and watching tv) and small scale activities (arm movement, contact, head movement, leg movement, body movement, eating, and patient is talking). This is based on the average length of the activity. In general, I am able to detect large scale activities easily and small activities poorly (relative to the large scale activities). The one exception to this is the eating activity. The reason for this pattern is likely that small scale activities (as the name implies) are associated with less of a change in overall brain activity and the specific location of the change may not have an associated electrode near it. Instead, the large activities create a more diffuse effect on the brain as there are many changes in the environment and patient activity for large scale behaviors. Therefore, it is easy to detect the difference between on and off states even if the electrodes are not in the perfect position. While eating is a relatively infrequent and short activity, it does mimic a large activity because eating requires movement, sensation, usually hunger, interactions with others, etc.

There are only a few direct comparisons between the classification performance in this study and in "unnatural" behavior (the patient is asked to do a task or make a specific movement) or in natural behavior as the behavior labels here are either not studied in an unnatural setting or the behavior labels are too general (other works study specific

types of body movement). However, there is one study that provides accuracy metrics for detecting sleep vs wake states (80%-92%) (Pahwa et al., 2015). The very high AUC is similar to the high accuracy provided in that work. Ruescher et al. does provide the sensitivity and specificity for classification of lower and upper extremity movement and speech in natural environments. While the specificity is usually high (80%-100%), the sensitivity is quite low in some patients (ranging from 0 to 70% for lower extremity movement, 43.5% to 78% for upper extremity movement and 10-27% for speech)(Ruescher et al., 2013). The AUC for movements ranged from 0.70 to 0.84 and the AUC for speech ranged from 0.73 to 0.87. Making a direct comparison is difficult but given a specific cutoff probability, the models from this study tend to outperform the ones used in Ruescher et al. for all three activities.

Overall, in this study, I show that it is possible classify many different types of continuous natural behavior in multiple patients using ECoG data.

4.2.1 Sources of Error in Classification

The lower amount of electrodes in the subject 1, particularly in the regions of the brain associated with motor movement is likely the reason why the classification AUC was relatively low for movement-based behaviors and contact. In addition, even though data from the cortical surface rather than the through a non-invasive EEG provides higher resolution, the information is still a summation over many pyramidal neurons and the signal still has to travel and can be disrupted before it reaches the electrodes. Many of the activities in question are also not fully explained by structures in the cortex (the advantages of sEEG is the ability to reach deep brain structures). Electrode placement and data collection is one of the three potential sources of low classification ability that are not related to choices of modelling.

Another type of error is caused by potential inaccuracies in the labelling. While a half-second error in the labelling of a large scale activity will be harmless as each activity can last for hours, a half-second error in a one-second long activity (leg movement) will cause issues. It is difficult to get perfect labelling accuracy for movement-based activity due to the diversity of possible movements and small movements that may not be easily detected on video. Due to the very time-intensive process of labelling, it was not possible to have multiple annotators for the same time frame. I corrected many of the explicit

errors in the annotations (such as two off labels in a row without an on label in between). However, mislabelling due to slow reaction time by the labeller or incorrect perception of the activity by the labeller was not thoroughly checked.

The last type of error is based on the heterogeneity of a particular behavior. Leg movements are very different from each other, so it would be ideal to label the specific types of leg movements. However, from videos, this is a difficult task. In addition, there are many different types of video games and TV programs. If the particular type of TV program or game is trained on but a different type is tested on, then the classification ability would drop significantly. While the first schema for classification attempted to reduce this error by randomly sampling from all time points, the drop in classification performance in the second schema highlights this source of error.

4.2.2 Training and Testing on Different Time Periods of the Day

As discussed in section 3.4.2, there is a steep drop in classification accuracy for many activities including movement, contact, quiet, someone is talking, and watching tv when the training and testing data come from distinct activity events or different times of day. The only behaviors that seem to be robust to the new setup are eating, video games, and sleeping (except in the case of subject 3). It is, of course, a harder task to learn on types of events or activities that may have not occurred before. For example, if a classifier was trained while the subject was watching the news at one time and then watching an action movie, then it may be difficult for a classifier to identify the when tv is being watched. In addition, the time of day that the movie is watched at and other environmental factors associated with the tv watching may significantly change the features that the model uses to make decisions. In future studies, it would be important to collect data and behavior labels for multiple days so that even if the classifier is trained on the first few days and tested on the last day, the training data should be fully representative of the testing data. It would also be useful to explore other models or hyperparameter search options to improve classification accuracy in this setting.

4.2.3 Time Windows

In an ideal world, behavior labels would be assigned at a higher resolution (1/10 sec) so that the precise time of movement or contact (for example) could be identified (this is less important for large scale activities such as watching tv or sleep). In this study, I had to only consider labels at the 1 second level due to human labelling capabilities. As we saw in section 3.4.4, there is an increase in AUC when moving to a higher time window, which shows that the performance of classifiers may be slightly inflated if using large time windows. On the contrary, large time windows do cause issues for classification since I defined the window based on whether the on or off state had the majority share of the time window. Therefore, each time window can have more of the opposite label time points as the time window length increases. This may be why certain activities did show an increased accuracy at the one second time window level. In addition, the boost in AUC from increasing the time window may just be because of better estimation of features. Coherence and mean power can be better estimated with more data. Overall, having higher resolution behavior labels would allow for a deeper exploration of this topic.

4.2.4 Differentiating Between Multiple Behaviors

The results provided in section 3.5 show that it is possible to differentiate between behaviors that have a physical component to them: arm movement, body movement, head movement, leg movement, talking, eating, and contact. These activities were chosen as it would be useful to know the difference between physical movements in the context of BCIs. Here, I show that the random forest classifier is useful in differentiating between five different activities while ensuring that the behaviors do not overlap in time. However, is it possible to do multi-label classification with high accuracy? There are multiple behaviors that happen at the same time such as eating and body/head movement. Ultimately, multi-label classification is the most realistic classification scenario. However, it is also worth studying in future works whether having one multi-label classifier or many classifiers dedicated to each activity would be better for this task. Overall, this study should provide the first step for multi-class and multi-label classification in the world of natural behavior.

4.2.5 Prediction of Action Initiation

Using a setup similar to the one used in Wang et al. (N. X. R. Wang et al., 2017), I showed that it is possible to detect behavior well before the initiation of the behavior using data at least from 1/250s before to 1s before (for subject 3 and subject 1 movements) and 1s to 2s before (for all subject 2 behaviors and subject 1 talking). The reason it is at least as much as the listed time ranges is because, again, the data is labelled at the one second label. As long as 50% of the time window has the behavior, then it is marked as the behavior. This means that the earlier time points of the window likely don't actually have the behavior occurring, so the lag times are greater than or equal to those listed. These results are similar to those in Wang et al. (N. X. R. Wang et al., 2017). They found that it was possible to detect (above chance) movement initiation using data from 0.8s to 1.8s before the initiation of the activity. The accuracy of prediction was around 65% (50% is chance accuracy). Another study showed above chance decoding ability for hand grasping 100msec-500msec before hand movement (Muralidharan, Chae, and Taylor, 2011) and a further study showed the ability to decode hand movement initiation using data from 0s-1s before hand movement (Z. Wang et al., 2012b). In this study, I found the AUC using data from 1/250s before to 1s before to be around 0.6-0.7 and from 1s to 2s to be around 0.55 to 0.6 (for the behaviors higher than chance).

It is plausible to believe that some of the classification performance is due to brain signals that exist before an action is performed or speech is produced. For example, the reaction time between a stimulus and a motor response is around around 200msec (Elliott, 1968). Therefore, in the 1/250s before to 1s before initiation, this information from the brain is available for classification. For the patient is talking behavior, it is also possible that brain signals related to speaking are present even one second before the production of speech. However, it is likely that classification performance is also a result of autocorrelation between the IFPs during movement and the time points before the movement. To test this theory, I calculated the autocorrelation for all single-electrode features and all subjects. Since I considered the positive samples to be x seconds before the activity was labelled and the control point to be x-1 seconds before the activity, I was interested in the difference between the autocorrelation between the two. If the positive samples have a high correlation with the activity time period and the negative samples don't, then this would indicate that autocorrelation is an important factor. The range of

the differences in autocorrelation between the first and second time point before action initiation was 0.01 to 0.18 and between the second and the third, it was 0.01 to 0.07. Since the upper range is relatively high in both cases, is likely that simple autocorrelation in the signal provided a reasonable portion of the decoding accuracy.

4.3 Implications of Classification Results

Many studies that have been discussed in the introduction have been able to decode behavior and movement with very high accuracy in a setting where the patient is consciously thinking of doing the the activity. However, natural movement or naturally doing an activity is very different. For example, picking up a pen when knowing that you have to write a reminder for yourself is different from a researcher telling you to make a specific grasping movement. The results in this study are too preliminary to be used in BCIs but further studies should attempt to replicate the design of this work. They should study natural movement or natural speech at a fine level, for example. To be fully capable and usable, BCIs must be able to decode natural behavior.

4.4 Association with Brain Areas and Interactions

The purpose of studying how the different brain areas and their interactions are associated with each activity is two-fold. One is to to discover what kind of features that the model would have learned from and if those features are biologically relevant. Secondly, many of these different activities have not been well-studied in a natural environment and the brain area interactions for these activities also have not been well-studied (both for natural and directed activities). It is important to note, however, that these descriptions must be interpreted with reference to the specific electrode locations for each subject visualized in figure 2.1. In addition, many of these interpretations are just hypotheses and much more work needs to be done to prove the associations that I am listing here.

4.4.1 Activities

- **Body Movement, Head Movement, Arm Movement, Leg Movement, Contact:** The areas of the brain that coordinate motor activity and sensory inputs

are relatively well studied. The precentral gyrus and the postcentral gyrus control movement and sensory processing of mostly touch-based information (Roux et al., 2020). The organization of both gyri are similar. In particular, the top portion of the brain is responsible for movement/sensory information for the legs and as one travels down the cortex, there are the regions that control/receive touch information for the chest, arms, hands, eyes nose, lips, tongue, and larynx/pharynx (Roux et al., 2020). The results in section 3.7 follow this pattern. In particular, the postcentral and precentral gyrus are the most important for decoding body movement, head movement, and contact. Figure 3.18 is a good visual representation of this where the precentral and postcentral gyri are highlighted while the rest of the brain is primarily purple or black for body movement. It is also particularly interesting that the electrodes that are most important for body movement are towards the top of the brain and are even in the paracentral area (associated with leg movement). While not pictured in figure 3.18, for HE, the same overall pattern is seen with the most important electrodes located towards the bottom of the gyrus. Even in the figure showing MAV, the most important electrode in the postcentral gyrus is the bottom-most one. A possible reason that there are important electrodes in the superior parietal area is because it is associated with attention and visual processing (Johns, 2014). The subject would likely move their head in response to some sort of visual stimuli, which is being processed in the superior parietal area. Finally, a hypothesis as to why even for these movement activities, there is stronger signal in the sensory area is possibly because movements are generally associated with a subsequent touch or it is possible that there is imperfect mapping. Regarding the brain area interaction results, overall, the precentral and postcentral gyri are important in identifying movement. For body movement, the interaction between the caudal middle frontal area and the precentral and postcentral gyri in theta frequency is increased. The caudal middle frontal area is responsible for controlling saccadic eye movements for searching a scene (El-Baba and Schury, 2020). It may be that visual information is guiding body movement. In addition, there is increased broadband coherence between the cuneus and precentral areas. The cuneus area is responsible for basic visual processing (Johns, 2014) so the previous explanation of response to visual stimuli is bolstered. Other brain region interactions in the broad-

band frequency associated with body movement are the lateral occipital area and the middle temporal area, which, among other things, are broadly responsible for object recognition (Grill-Spector, Kourtzi, and Kanwisher, 2001) and facial recognition/visual emotion recognition (Pourtois et al., 2005) respectively. This again hints at the idea that visual information is associated with movement. For head movement, the same broadband coherence patterns are observed except broadband coherence decreases when head movement occurs. In the most important interaction, the lingual area is included, which like the others also is involved in visual processing (face recognition, word processing, visual memory, etc.) (Bogousslavsky et al., 1987). In theta frequency band, the precentral gyrus is the main structure involved in the important interactions with the visual areas.

While one would expect signals in the postcentral area to primarily be associated with contact, only a few of the top ranked electrodes in terms of DI are located there. Instead, many of the visual areas mentioned previously have lower RMS and gamma power. In addition, the inferior parietal area has an increased RMS and decreased gamma power. The inferior parietal area has been associated with many different functions including attention, language comprehension, face recognition, and social cognition (Numssen, Bzdok, and Hartwigsen, 2021) It is possible to interpret contact as a social activity so this may be the reason the inferior parietal area is useful here. In broadband coherence, there is decreased broadband and theta coherence between the electrodes in many of the visual areas and the inferior parietal region and the precentral and postcentral gyri, which follows the single-electrode results.

As mentioned in section 3.7 and 3.8, because the electrodes for subject 1 are primarily not located in the postcentral and precentral gyrus, there are a lot of brain area interactions and brain areas that may not normally be considered important in movement. However, the one electrode in the postcentral area is one of the top electrodes for arm movement and many of the most important electrodes according to mean gamma power and HE are in regions adjacent to the two gyri (superior temporal and supramarginal).

- **Eating:** Eating has similar patterns as the head and body movement. This is likely

because the primary component of eating is movement (especially of the mouth, tongue, and pharynx). As discussed before, movements and sensory information from these regions are associated with the bottom of the precentral and postcentral gyri. In figure 3.18, it shows there is increased gamma activity in the postcentral gyrus at a location that is below the most important electrodes for body movement. When considering brain area interactions, the increased theta coherence and decreased broadband coherence within the precentral and postcentral gyrus is associated with eating. In addition, the same increase and decrease in theta coherence and broadband coherence is seen between these gyri and the superior frontal area and the caudal middle frontal area. Again, the caudal middle frontal area could be involved due to the visual component of eating (need to see the food to eat). However, the function of the superior frontal area is less known. One study did conclude that the region is involved in appetite control (Tuulari et al., 2015) after seeing food.

- **Patient is Talking and Someone is Talking:** The areas of the brain associated with these two activities are very similar. This is likely because when a patient is talking, someone else is talking immediately after, before, or even during. In addition, the areas responsible for processing speech are also closely involved in speech production (Binder, 2015). There is a drop in RMS, HE, and gamma power in the pars opercularis area when the patient is talking. The pars opercularis is the primary location of speech production in the brain (Petrides, 2013). The precentral and postcentral gyri are also associated with talking. In figure 3.19, we also see that only one of the bottom-most electrodes is important (likely related to mouth movement). Another notable area is the inferior parietal area, which also has lower RMS, HE, and gamma power during talking. Geranmayeh et al. describes the significant involvement that inferior parietal area has in speech (Geranmayeh et al., 2012). In addition, while someone is talking, the inferior parietal area has relatively large decrease in RMS and HE. A large area of the brain is responsible for speech comprehension and it includes the inferior parietal area (Binder, 2015; Bareham et al., 2018). Another relevant region in decoding the hearing of speech is the supramarginal gyrus, which has been shown to be important in phonological processing (Deschamps, Baum, and Gracco, 2014). Considering brain area interactions

for speech production, there is increased broadband coherence and theta coherence between the pars opercularis area and many of the other areas discussed in this section (inferior parietal, postcentral, precentral) in addition to new ones (middle temporal and fusiform). The fusiform is primarily associated with facial recognition, and its importance here is likely just because talking usually requires looking at someone's face. While the middle temporal area is involved in visual processing, it is also involved in phonological processing (Ashtari et al., 2004). Although I am discussing speech comprehension here rather than speech production, as mentioned earlier, speech production usually requires comprehension and vice versa. For speech comprehension, there is an increased theta and broadband coherence with other brain areas already mentioned in this section (inferior parietal, pars opercularis, precentral, postcentral, and middle temporal). Overall, it is remarkable that there is such a strong functional connection between the speech comprehension areas and speech production areas. It is curious, however, that the superior temporal gyrus is not very useful in discriminating between when someone is talking and when they are not as it is considered one of the primary locations of the auditory processing (Muñoz-López et al., 2015).

- **Quiet:** Considering the RMS feature, the most informative electrodes show a higher RMS during quiet and all of these electrodes are located in the inferior parietal area. When analyzing the someone is talking, I mentioned the importance of the brain area in language comprehension, so it follows that quiet would also be associated with this area. There is also increased HE and decreased gamma activity in the inferior temporal area off the brain. A lesion study conducted by Bonilha et al. showed that damage to the inferior temporal area is implicated in issues with language comprehension, so it would make sense that it would be associated with quiet here in this study (Bonilha et al., 2017). The information from coherence (brain area interaction) has the similar structures involved in addition to the middle temporal area, supramarginal gyrus, and many of those generally included in speech production (pars opercularis, precentral, postcentral). As mentioned previously, the supramarginal gyrus is deeply involved in phonological processing. In addition, the middle temporal area, similar to the inferior temporal area is also important in language processing (Bonilha et al., 2017). Overall, theta coherence decreases and

broadband coherence increases between these regions.

Recently, there has also been a lot of research and interest in the brain network while a person is resting (Default Network) but is still conscious (not sleeping). There are many different hypotheses regarding its purpose but one leading theory is that it allows for internal thought processes during rest (Buckner, 2013). Two of the primary regions that are active during this process are the inferior parietal area and the middle/inferior temporal gyri in addition to structures in the frontal lobe (Buckner, 2013). While much of the evidence in this study points towards these structures having lower activity (low gamma content), the functional interaction in the broadband frequency range (table 3.11) within the inferior parietal area is lower during quiet. This is the opposite pattern from what is seen in the other entries of the table for quiet. It is possible that this decoupling of brain signals in the broadband frequency is related to the Default Network. Of course this is only a preliminary hypothesis and more should be studied regarding the default network and between and within brain area interactions.

- **Video Games and Watching TV:** These are both visual-based activities (in addition to audio as in the last two examples). For both watching tv and video games, there is high gamma activity, HE, and RMS in the lingual and fusiform gyri (table 3.7 and 3.8). Both the lingual and fusiform gyri are involved in visual processing, visual memory, face recognition, and reading (Machielsen et al., 2000; Mechelli et al., 2000). When playing video games and watching TV, there are reading components (instructions of closed captions) as well as facial recognition. In addition, as shown in figure 3.20, the pericalcarine area has the highest average importance. The pericalcarine area is where much of the primary visual cortex is, which is responsible for basic visual processing (Johns, 2014; Tootell et al., 1998). Interestingly, there is lower RMS in the precentral gyrus while watching tv. This may be because actively watching tv usually means that the person is fixated on one spot (tv) and is not moving much. In addition, while playing video games, there is decreased RMS and higher gamma content in the inferior parietal area. As listed before, the inferior parietal area is involved language comprehension, and this matches with my findings here because of the language components to video games (both normal video games and those given to these patients by researchers).

For broadband coherence, there is increased interaction within the inferior parietal area and between it and the lateral occipital and cuneus areas. These two areas are primary involved in visual processing while the inferior parietal area is involved in many different activities including language comprehension. It could be that the visual information from the occipital lobe is being transferred to the inferior parietal lobe along the dorsal visual pathway so that the patient can react to the information on the television (Hebart and Hesselmann, 2012). However, given just coherence, it is not possible to know the direction of information flow. Therefore, this is just a preliminary hypothesis. Another possibility is that the interaction between these regions represents the combination of visual information and auditory information from the television. There are similar important interactions for video games in addition to interactions with the superior temporal area, the pars opercularis, and the middle temporal area (lower theta coherence and higher broadband coherence). The superior temporal and middle temporal area are involved in audio processing, which would be important during video games. However, it is interesting that the pars opercularis is included as its primary responsibility is speech production. It may be because the patient sometimes responds verbally during the researcher-given video games. Considering the highest average importance based on DI in watching TV (figure 3.23), there are a few regions in the frontal lobe that have high gamma coherence with the middle temporal gyrus (medial orbitofrontal, rostral anterior cingulate, superior frontal, rostral middle frontal). These structures are generally involved in memory, emotion, and sensory integration (Boisgueheneuc et al., 2006; W. Tang et al., 2019; Kringelbach, 2005).

- **Sleep:** Sleeping is a unique activity in which the brain signals associated with it are not localized to a specific region. Instead, as shown in figure 3.20, the important electrodes and brain areas are somewhat uniformly distributed throughout the brain. As a result, the type of brain waves and features are more important to analyze in sleep. Sleep is divided broadly into two major types: Non-Rapid Eye Movement (NREM) sleep and Rapid Eye Movement Sleep (REM) (Purves et al., 2019). NREM is further divided into four stages in which the amplitude of waves increases and the frequency of waves decreases. In REM sleep, brain waves mimic those of awake brain waves (higher frequency and lower amplitude than NREM

waves). In table 3.7, during sleep, the RMS feature is higher, which indicates high amplitude waves as expected. The HE is also higher during sleep, which follows the prior information as higher HEs generally indicate less inversions of the brain voltage, which is associated with low frequency activity. In addition, there is less gamma frequency content during sleep (table 3.10) and more delta wave content (data not explicitly included here). Regarding the functional connectivity of brain areas during sleep, the results are not as clear. There is generally a higher broad-band, theta, and gamma coherence during sleep (table 3.11 and 3.10) while there is lower delta, alpha, and beta coherence during sleep. Each of these trends are also quite strong based on the discriminability index. Nguyen et al. studied functional connectivity in the brain and found that there was a difference in the connections based on the stages of sleep, so it is possible that a clear picture can only be created when labelling the different stages of sleep (T. Nguyen et al., 2018).

4.4.2 Interpretation of Features

In the previous section, I only hinted at the meaning of each feature in relation to the behaviors. However, here, I will analyze the features explicitly. Generally, higher HE, RMS, entropy, and more slower wave content (delta, theta, and alpha waves) represent a lack of activity in the particular area of the brain. For example, as shown in tables 3.7-3.9, in the movement activities and eating, there is lower RMS and HE but greater gamma power in the motor and sensory areas. This is evidence of this trend. In addition, during sleep and quiet (passive activities), there is lower gamma power and higher RMS and HE. During video games and watching tv, there is increased gamma activity and lower RMS and HE in visual and auditory areas. Of course, these are general trends and there are exceptions to this rule (low gamma activity in pars opercularis during speech). While RMS is a proxy for the amplitude of the waves and higher amplitudes means a greater number of neurons are creating the signal, this does not mean there is greater activity. In fact, it usually means there is lower activity since larger amplitude waves can actually replace the high activity signals represented by low amplitude beta or gamma waves (Jia and Kohn, 2011). In other words, more neurons synchronously firing at a low frequency means lower activity but less neurons with higher frequency means higher activity.

The coherence in each frequency band is much more difficult to understand. The coherence between regions in high frequency bands cannot be viewed as the activation of a particular network or circuit. Instead, generally, high coherence in the theta and delta frequency correlates with an activity. This is because of the positive values of DI in body movement, eating, head movement, patient is talking, and someone is talking activities. However, it is interesting that watching tv has multiple signs of DI and video games primarily has negative signs of DI in theta for areas implicated in visual and auditory processing. As expected, there is decreased coherence during quiet between regions which are responsible for auditory processing. For sleeping, theta coherence increases (which would again break the pattern), but sleeping may have to be treated separately because of the unique brain waves that are associated with it (theta and delta waves). On the other hand, the broadband and gamma coherence seem to be highly correlated and produce results that are quite heterogeneous. Overall, the use of coherence in studies is still quite new and how it should be interpreted is still not full clear (Bowyer, 2016). Because of this, it may be best to do coherence studies in controlled environments rather than in natural environments like this one.

4.5 Future Directions

There are many different ways to iterate on this work to increase the usefulness of these results and also improve classification ability. The methods of improvement generally fall in the following categories: patient data, behavior labels, change of the classifier type, comparison of results with those from non-natural behaviors.

4.5.1 Patient Data

To consider the generalizability of these results to different patients, it is necessary to collect more behavior labels from more patients with a wide variety of demographic characteristics including age, race/ethnicity, sex, handedness, etc. This would allow for better estimates of the importance of different regions of the brain as the number of electrodes increase when combining patient data. In addition, we will then have a better idea of the inter-patient variability in classification performance. The ultimate goal would be to combine data across patients for training and testing. This would require the exact

same placement of electrodes across patients. While this is theoretically possible, the requirements of epilepsy monitoring make this unfeasible.

4.5.2 Behavior Labels

Patient labels should be made at a higher resolution and with greater accuracy to improve the reliability of these results. However, the limitation is the quality of videos of the patients and the amount of time available to label the videos. If a labeller could watch the videos at 1/25th speed, they could detect activities at a high resolution. However, this would make for very long videos. In addition, to ensure accuracy, multiple labellers should be assigned to one video and the difference in labels should be examined.

As discussed in section 4.1.1, the labels used in this study are quite general. For a proof-of-concept study for decoding natural behaviors, this is okay. However, in follow-up studies it would be important to get more precise labels especially for movement. Body movement is obviously very general. Even arm movement, leg movement, and head movement are very general as they still encompass many different types of movement. Ideally, the patient would be wearing sensors that both records the type of movement and also the time of movement initiation. This would also for a more precise understanding of the ability to predict future behaviors as now I am only able to define periods of one second.

Finally, having accurate behavior labels for multiple days of activity would allow for a more realistic scenario where training of a classifier is done for multiple days and the implementation of the classifier is done on the last few days (and the classifier is tuned at the beginning of each testing day to account for day-to-day variation).

4.5.3 Change to the Classifier Type

As I hinted at in the introduction section, the time series nature of the data is not well-accounted for in this study. What is happening before (both the data and the labels) are not used in future time points. Simple recurrent neural networks (RNN), which account for the time ordering of data, have been used in BCIs for classification of movement and speech (Willett et al., 2021). Other articles that analyze EEG and iEEG data use more complex versions of RNNs such as Long Term Short Term Memory Networks (LSTM)(Moses et al., 2021; Du et al., 2018; Bresch, Großekathöfer, and Garcia-Molina,

2018; Xu et al., 2020) or gated recurrent unit networks (GRU) (S. Lee et al., 2021; Chen, Jiang, and Y. Zhang, 2019). Finally, a more simple model to train that could also account for the time series nature of the data is a Hidden Markov Model (HMM). The observed states would be the voltage data for each electrode or the features for each electrode while the hidden states would be the behavior labels (M. Lee, Ryu, and Kim, 2020). These are all feasible alternatives given the problem set up.

Another point of model improvement is related to the spatial information from the electrodes. The relationship between the electrodes and their positions are not explicitly taken into account in the current classifiers. One method for accounting for spatial data is through the use of a CNN where one dimension of the input layer is the number electrodes. This method has been shown to have higher classification performance for distinguishing between Parkinson’s Disease patients and healthy controls using EEG data (S. Lee et al., 2021). Another approach is described in Wang et al. (Z. Wang et al., 2012b) in which a Modified Time-Varying Dynamic Bayesian network (MTVDBN) was used, which is more sophisticated version of Naive Bayes. It models the dependencies of time and location for each input feature and electrode combination.

4.5.4 Comparison of Results with Those from Non-Natural Behaviors

The primary claim of this work is that it is very different and likely a more difficult task to decode behaviors in a natural setting rather than in a research setting. However, it would be ideal if the differences between decoding behavior in both environments could be compared for a subject. Future experiments should ask patients to make explicit movements and for those same patients (at a different time), natural movements should be labelled. Then, the decoding ability and characterization of brain signals should be done for both situations and finally compared.

References

- Aguiar Neto, Fernando Soares de and João Luis Garcia Rosa (2019). “Depression biomarkers using non-invasive EEG: A review”. In: *Neuroscience & Biobehavioral Reviews* 105, pp. 83–93.
- Akwei-Sekyere, Samuel (2015). “Powerline noise elimination in biomedical signals via blind source separation and wavelet analysis”. In: *PeerJ* 3, e1086.
- Angrick, Miguel et al. (2019). “Speech synthesis from ECoG using densely connected 3D convolutional neural networks”. In: *Journal of neural engineering* 16.3, p. 036019.
- Armitage, Roseanne (1995). “The distribution of EEG frequencies in REM and NREM sleep stages in healthy young adults”. In: *Sleep* 18.5, pp. 334–341.
- Ashtari, Manzar et al. (2004). “Left middle temporal gyrus activation during a phonemic discrimination task”. In: *Neuroreport* 15.3, pp. 389–393.
- Astolfi, Laura et al. (2009). “The track of brain activity during the observation of tv commercials with the high-resolution eeg technology”. In: *Computational intelligence and neuroscience* 2009.
- Astrand, Elaine, Claire Wardak, and Suliann Ben Hamed (2014). “Selective visual attention to drive cognitive brain–machine interfaces: from concepts to neurofeedback and rehabilitation applications”. In: *Frontiers in systems neuroscience* 8, p. 144.
- Atagün, Murat İlhan (2016). “Brain oscillations in bipolar disorder and lithium-induced changes”. In: *Neuropsychiatric disease and treatment* 12, p. 589.
- Avanzini, Pietro et al. (2012). “The dynamics of sensorimotor cortical oscillations during the observation of hand movements: an EEG study”. In: *PLoS One* 7.5, e37534.
- El-Baba, Rami M and Mark P Schury (2020). “Neuroanatomy, frontal cortex”. In.
- Bagnall, A et al. (n.d.). “The great time series classification bake off: An experimental evaluation of recently proposed algorithms. Extended version. arXiv 2016”. In: *arXiv preprint arXiv:1602.01711* ().

- Bansal, Arjun K et al. (2014). “Neural dynamics underlying target detection in the human brain”. In: *Journal of Neuroscience* 34.8, pp. 3042–3055.
- Bareham, Corinne A et al. (2018). “Role of the right inferior parietal cortex in auditory selective attention: An rTMS study”. In: *Cortex* 99, pp. 30–38.
- Binder, Jeffrey R (2015). “The Wernicke area: Modern evidence and a reinterpretation”. In: *Neurology* 85.24, pp. 2170–2175.
- Bleichner, Martin G et al. (2016). “Give me a sign: decoding four complex hand gestures based on high-density ECoG”. In: *Brain Structure and Function* 221.1, pp. 203–216.
- Bogousslavsky, Julien et al. (1987). “Lingual and fusiform gyri in visual processing: a clinico-pathologic study of superior altitudinal hemianopia.” In: *Journal of Neurology, Neurosurgery & Psychiatry* 50.5, pp. 607–614.
- Boisgueheneuc, Foucaud du et al. (2006). “Functions of the left superior frontal gyrus in humans: a lesion study”. In: *Brain* 129.12, pp. 3315–3328.
- Bonilha, Leonardo et al. (2017). “Temporal lobe networks supporting the comprehension of spoken words”. In: *Brain* 140.9, pp. 2370–2380.
- Boonyakitanont, Poomipat et al. (2020). “A review of feature extraction and performance evaluation in epileptic seizure detection using EEG”. In: *Biomedical Signal Processing and Control* 57, p. 101702.
- Bowyer, Susan M (2016). “Coherence a measure of the brain networks: past and present”. In: *Neuropsychiatric Electrophysiology* 2.1, pp. 1–12.
- brain-lobes.html 49_15CerebralCortex-L.jpg* (2021). URL: <https://www.bio1152.nicerweb.com/Locked/media/ch49/brain-lobes.html> (visited on November 30, 2021).
- Bresch, Erik, Ulf Großekathöfer, and Gary Garcia-Molina (2018). “Recurrent deep neural networks for real-time sleep stage classification from single channel EEG”. In: *Frontiers in computational neuroscience*, p. 85.
- Buckner, Randy L (2013). “The brain’s default network: origins and implications for the study of psychosis”. In: *Dialogues in clinical neuroscience* 15.3, p. 351.
- Bui, Toai and J Nguyen (2019). “Neuroanatomy, cerebral hemisphere”. In.
- Burkhalter, Andreas and Kerry L Bernardo (1989). “Organization of corticocortical connections in human visual cortex”. In: *Proceedings of the National Academy of Sciences* 86.3, pp. 1071–1075.

- Burle, Boris et al. (2015). “Spatial and temporal resolutions of EEG: Is it really black and white? A scalp current density view”. In: *International Journal of Psychophysiology* 97.3, pp. 210–220.
- Buskila, Yossi, Alba Bellot-Saez, and John W Morley (2019). “Generating brain waves, the power of astrocytes”. In: *Frontiers in neuroscience* 13, p. 1125.
- Carus-Cadavieco, Marta et al. (2017). “Gamma oscillations organize top-down signalling to hypothalamus and enable food seeking”. In: *Nature* 542.7640, pp. 232–236.
- Chen, JX, DM Jiang, and YN Zhang (2019). “A hierarchical bidirectional GRU model with attention for EEG-based emotion classification”. In: *IEEE Access* 7, pp. 118530–118540.
- Chestek, Cynthia A et al. (2013). “Hand posture classification using electrocorticography signals in the gamma band over human sensorimotor brain areas”. In: *Journal of neural engineering* 10.2, p. 026002.
- Chin, César Márquez et al. (2007). “Identification of arm movements using correlation of electrocorticographic spectral components and kinematic recordings”. In: *Journal of neural engineering* 4.2, p. 146.
- Dale, Anders M, Bruce Fischl, and Martin I Sereno (1999). “Cortical surface-based analysis: I. Segmentation and surface reconstruction”. In: *Neuroimage* 9.2, pp. 179–194.
- Del Río, Jahaziel Molina et al. (2019). “EEG correlation during the solving of simple and complex logical–mathematical problems”. In: *Cognitive, Affective, & Behavioral Neuroscience* 19.4, pp. 1036–1046.
- Derix, Johanna et al. (2014). “From speech to thought: the neuronal basis of cognitive units in non-experimental, real-life communication investigated using ECoG”. In: *Frontiers in human neuroscience* 8, p. 383.
- Deschamps, Isabelle, Shari R Baum, and Vincent L Gracco (2014). “On the role of the supramarginal gyrus in phonological processing and verbal working memory: evidence from rTMS studies”. In: *Neuropsychologia* 53, pp. 39–46.
- Destrieux, Christophe et al. (2010). “Automatic parcellation of human cortical gyri and sulci using standard anatomical nomenclature”. In: *Neuroimage* 53.1, pp. 1–15.
- Dong, Debo et al. (2021). “The Association between Body Mass Index and Intra-Cortical Myelin: Findings from the Human Connectome Project”. In: *Nutrients* 13.9, p. 3221.

- Du, Anming et al. (2018). “Decoding ECoG signal with deep learning model based on LSTM”. In: pp. 0430–0435.
- Elliott, Rogers (1968). “Simple visual and simple auditory reaction time: A comparison”. In: *Psychonomic Science* 10.10, pp. 335–336.
- Fauchon, Camille et al. (2020). “The Modular Organization of Pain Brain Networks: An fMRI Graph Analysis Informed by Intracranial EEG”. In: *Cerebral Cortex Communications* 1.1, tgaa088.
- Gärtner, Matti and Malek Bajbouj (February 2014). “Encoding-related EEG oscillations during memory formation are modulated by mood state”. In: *Social Cognitive and Affective Neuroscience* 9.12, pp. 1934–1941. ISSN: 1749-5016. DOI: 10.1093/scan/nst184. URL: <https://doi.org/10.1093/scan/nst184>.
- Geranmayeh, Fatemeh et al. (2012). “The contribution of the inferior parietal cortex to spoken language production”. In: *Brain and language* 121.1, pp. 47–57.
- Graf, M et al. (1984). “Electrocorticography: information derived from intraoperative recordings during seizure surgery”. In: *Clinical Electroencephalography* 15.2, pp. 83–91.
- Grill-Spector, Kalanit, Zoe Kourtzi, and Nancy Kanwisher (2001). “The lateral occipital complex and its role in object recognition”. In: *Vision research* 41.10-11, pp. 1409–1422.
- Guo, Ning et al. (2021). “Speech frequency-following response in human auditory cortex is more than a simple tracking”. In: *NeuroImage* 226, p. 117545.
- Halgren, Eric et al. (1980). “Endogenous potentials generated in the human hippocampal formation and amygdala by infrequent events”. In: *Science* 210.4471, pp. 803–805.
- Harmony, Thaha (2013). “The functional significance of delta oscillations in cognitive processing”. In: *Frontiers in integrative neuroscience* 7, p. 83.
- Hebart, Martin N and Guido Hesselmann (2012). “What visual information is processed in the human dorsal stream?” In: *Journal of Neuroscience* 32.24, pp. 8107–8109.
- Hill, N Jeremy et al. (2012). “Recording human electrocorticographic (ECoG) signals for neuroscientific research and real-time functional cortical mapping”. In: *JoVE (Journal of Visualized Experiments)* 64, e3993.

- Hotson, Guy et al. (2016). “Individual finger control of a modular prosthetic limb using high-density electrocorticography in a human subject”. In: *Journal of neural engineering* 13.2, p. 026017.
- Iaselli, Eleonora (2018). “A review of feature extraction and performance evaluation in epileptic seizure detection using EEG”. In: “iELVis: An open source MATLAB toolbox for localizing and visualizing human intracranial electrode data” (2017). In: *Journal of Neuroscience Methods* 281, pp. 40–48. ISSN: 0165-0270. DOI: <https://doi.org/10.1016/j.jneumeth.2017.01.022>.
- Jáuregui-Lobera, Ignacio (2012). “Electroencephalography in eating disorders”. In: *Neuropsychiatric disease and treatment* 8, p. 1.
- Jia, Xiaoxuan and Adam Kohn (2011). “Gamma rhythms in the brain”. In: *PLoS biology* 9.4, e1001045.
- Johns, Paul (2014). *Clinical Neuroscience E-Book*. Elsevier Health Sciences.
- Johnson, Elizabeth L et al. (2019). “Spectral imprints of working memory for everyday associations in the frontoparietal network”. In: *Frontiers in systems neuroscience* 12, p. 65.
- Kawase, Tetsuaki et al. (2005). “Recruitment of fusiform face area associated with listening to degraded speech sounds in auditory–visual speech perception: A PET study”. In: *Neuroscience letters* 382.3, pp. 254–258.
- Kennedy, PR and KD Adams (2003). “A decision tree for brain-computer interface devices”. In: *IEEE Transactions on Neural Systems and Rehabilitation Engineering* 11.2, pp. 148–150.
- Khursheed, Faraz et al. (2011). “Frequency-specific electrocorticographic correlates of working memory delay period fMRI activity”. In: *Neuroimage* 56.3, pp. 1773–1782.
- Kisley, Michael A and Zoe M Cornwell (2006). “Gamma and beta neural activity evoked during a sensory gating paradigm: effects of auditory, somatosensory and cross-modal stimulation”. In: *Clinical neurophysiology* 117.11, pp. 2549–2563.
- Klimesch, Wolfgang (1999). “EEG alpha and theta oscillations reflect cognitive and memory performance: a review and analysis”. In: *Brain Research Reviews* 29.2, pp. 169–195. ISSN: 0165-0173. DOI: [https://doi.org/10.1016/S0165-0173\(98\)00056-3](https://doi.org/10.1016/S0165-0173(98)00056-3). URL: <https://www.sciencedirect.com/science/article/pii/S0165017398000563>.

- Klimesch, Wolfgang (2012). “Alpha-band oscillations, attention, and controlled access to stored information”. In: *Trends in cognitive sciences* 16.12, pp. 606–617.
- Kringelbach, Morten L (2005). “The human orbitofrontal cortex: linking reward to hedonic experience”. In: *Nature reviews neuroscience* 6.9, pp. 691–702.
- Lalo, Elodie et al. (2007). “Phasic increases in cortical beta activity are associated with alterations in sensory processing in the human”. In: *Experimental brain research* 177.1, pp. 137–145.
- Lee, Miran, Jaehwan Ryu, and Deok-Hwan Kim (2020). “Automated epileptic seizure waveform detection method based on the feature of the mean slope of wavelet coefficient counts using a hidden Markov model and EEG signals”. In: *ETRI Journal* 42.2, pp. 217–229.
- Lee, Soojin et al. (2021). “A convolutional-recurrent neural network approach to resting-state EEG classification in Parkinson’s disease”. In: *Journal of neuroscience methods* 361, p. 109282.
- Li, Yue et al. (2017). “Gesture decoding using ECoG signals from human sensorimotor cortex: a pilot study”. In: *Behavioural neurology* 2017.
- Little, Simon et al. (2013). “Adaptive deep brain stimulation in advanced Parkinson disease”. In: *Annals of neurology* 74.3, pp. 449–457.
- Liu, Dong et al. (2018). “EEG-Based Lower-Limb Movement Onset Decoding: Continuous Classification and Asynchronous Detection”. In: *IEEE Transactions on Neural Systems and Rehabilitation Engineering* 26.8, pp. 1626–1635. DOI: 10.1109/TNSRE.2018.2855053.
- Machielsen, Willem CM et al. (2000). “fMRI of visual encoding: reproducibility of activation”. In: *Human brain mapping* 9.3, pp. 156–164.
- Mak, Joseph N and Jonathan R Wolpaw (2009). “Clinical applications of brain-computer interfaces: current state and future prospects”. In: *IEEE reviews in biomedical engineering* 2, pp. 187–199.
- Marjaninejad, Ali, Babak Taherian, and Francisco J Valero-Cuevas (2017). “Finger movements are mainly represented by a linear transformation of energy in band-specific ECoG signals”. In: *2017 39th Annual International Conference of the IEEE Engineering in Medicine and Biology Society (EMBC)*. IEEE, pp. 986–989.

- Mazher, Moona et al. (2015). “A comparison of brain regions based on EEG during multimedia learning cognitive activity”. In: pp. 31–35. DOI: 10.1109/ISSBES.2015.7435888.
- Mechelli, Andrea et al. (2000). “Differential effects of word length and visual contrast in the fusiform and lingual gyri during”. In: *Proceedings of the Royal Society of London. Series B: Biological Sciences* 267.1455, pp. 1909–1913.
- Miller, Kai J, Kurt E Weaver, and Jeffrey G Ojemann (2009). “Direct electrophysiological measurement of human default network areas”. In: *Proceedings of the National Academy of Sciences* 106.29, pp. 12174–12177.
- Moses, David A et al. (2021). “Neuroprosthesis for decoding speech in a paralyzed person with anarthria”. In: *New England Journal of Medicine* 385.3, pp. 217–227.
- Muñoz-López, M et al. (2015). “Anatomical pathways for auditory memory II: information from rostral superior temporal gyrus to dorsolateral temporal pole and medial temporal cortex”. In: *Frontiers in Neuroscience* 9, p. 158.
- Muralidharan, A, J Chae, and DM Taylor (2011). “Early detection of hand movements from electroencephalograms for stroke therapy applications”. In: *Journal of neural engineering* 8.4, p. 046003.
- Nakanishi, Yasuhiko et al. (2013). “Prediction of three-dimensional arm trajectories based on ECoG signals recorded from human sensorimotor cortex”. In: *PloS one* 8.8, e72085.
- Nguyen, Thien et al. (2018). “Exploring brain functional connectivity in rest and sleep states: a fNIRS study”. In: *Scientific reports* 8.1, pp. 1–10.
- Numssen, Ole, Danilo Bzdok, and Gesa Hartwigsen (2021). “Functional specialization within the inferior parietal lobes across cognitive domains”. In: *Elife* 10, e63591.
- Osipova, Daria et al. (2006). “Theta and Gamma Oscillations Predict Encoding and Retrieval of Declarative Memory”. In: *Journal of Neuroscience* 26.28, pp. 7523–7531. ISSN: 0270-6474. DOI: 10.1523/JNEUROSCI.1948-06.2006. eprint: <https://www.jneurosci.org/content/26/28/7523.full.pdf>. URL: <https://www.jneurosci.org/content/26/28/7523>.
- Pahwa, Mrinal et al. (2015). “Optimizing the detection of wakeful and sleep-like states for future electrocorticographic brain computer interface applications”. In: *PloS one* 10.11, e0142947.

- Parvizi, Josef and Sabine Kastner (2018). “Human intracranial EEG: promises and limitations”. In: *Nature neuroscience* 21.4, p. 474.
- Petrides, Michael (2013). *Neuroanatomy of language regions of the human brain*. Academic Press.
- Pistohl, Tobias et al. (2012). “Decoding natural grasp types from human ECoG”. In: *Neuroimage* 59.1, pp. 248–260.
- Posada-Quintero, Hugo F et al. (2019). “Brain activity correlates with cognitive performance deterioration during sleep deprivation”. In: *Frontiers in neuroscience* 13, p. 1001.
- Pourtois, Gilles et al. (2005). “Perception of facial expressions and voices and of their combination in the human brain”. In: *Cortex* 41.1, pp. 49–59.
- Purves, Dale et al. (2019). *Neurosciences*. De Boeck Supérieur.
- Rayi, Appaji and Najib Murr (2021). “Electroencephalogram”. In: *StatPearls [Internet]*.
- Roux, Franck-Emmanuel et al. (2020). “Functional architecture of the motor homunculus detected by electrostimulation”. In: *The Journal of Physiology* 598.23, pp. 5487–5504.
- Ruescher, Johanna et al. (2013). “Somatotopic mapping of natural upper-and lower-extremity movements and speech production with high gamma electrocorticography”. In: *Neuroimage* 81, pp. 164–177.
- Rutkove, Seward B (2007). *Introduction to volume conduction*. Springer, pp. 43–53.
- Ryun, Seokyun et al. (2014). “Movement type prediction before its onset using signals from prefrontal area: an electrocorticography study”. In: *BioMed research international* 2014.
- Satow, Takeshi et al. (2003). “Distinct cortical areas for motor preparation and execution in human identified by Bereitschaftspotential recording and ECoG-EMG coherence analysis”. In: *Clinical neurophysiology* 114.7, pp. 1259–1264.
- Schalk, Gerwin (2010). “Can electrocorticography (ECoG) support robust and powerful brain-computer interfaces?” In: *Frontiers in neuroengineering* 3, p. 9.
- Seeber, Martin, Reinhold Scherer, and Gernot R. Müller-Putz (2016). “EEG Oscillations Are Modulated in Different Behavior-Related Networks during Rhythmic Finger Movements”. In: *Journal of Neuroscience* 36.46, pp. 11671–11681. ISSN: 0270-6474. DOI: 10.1523/JNEUROSCI.1739-16.2016. eprint: <https://www.jneurosci.org/>

- content/36/46/11671.full.pdf. URL: <https://www.jneurosci.org/content/36/46/11671>.
- Shirhatti, Vinay, Ayon Borthakur, and Supratim Ray (2016). “Effect of reference scheme on power and phase of the local field potential”. In: *Neural computation* 28.5, pp. 882–913.
- Smith, Elliot H et al. (2022). “Human interictal epileptiform discharges are bidirectional traveling waves echoing ictal discharges”. In: *Elife* 11, e73541.
- Smith, S J M (2005). “EEG in the diagnosis, classification, and management of patients with epilepsy”. In: *Journal of Neurology, Neurosurgery & Psychiatry* 76.suppl 2, pp. ii2–ii7. ISSN: 0022-3050. DOI: 10.1136/jnnp.2005.069245. eprint: https://jnnp.bmj.com/content/76/suppl_2/ii2.full.pdf. URL: https://jnnp.bmj.com/content/76/suppl_2/ii2.
- Sparks, D Larry et al. (2000). “Neural tract tracing using Di-I: a review and a new method to make fast Di-I faster in human brain”. In: *Journal of neuroscience methods* 103.1, pp. 3–10.
- Tang, Hanlin et al. (2014). “Spatiotemporal dynamics underlying object completion in human ventral visual cortex”. In: *Neuron* 83.3, pp. 736–748.
- Tang, Wei et al. (2019). “A connectional hub in the rostral anterior cingulate cortex links areas of emotion and cognitive control”. In: *Elife* 8, e43761.
- Tootell, Roger BH et al. (1998). “Functional analysis of primary visual cortex (V1) in humans”. In: *Proceedings of the National Academy of Sciences* 95.3, pp. 811–817.
- Tsuchiya, Naotsugu et al. (2008). “Decoding face information in time, frequency and space from direct intracranial recordings of the human brain”. In: *PloS one* 3.12, e3892.
- Tuulari, Jetro J et al. (2015). “Neural circuits for cognitive appetite control in healthy and obese individuals: an fMRI study”. In: *PloS one* 10.2, e0116640.
- Voorhies, Jason M and Aaron Cohen-Gadol (2013). “Techniques for placement of grid and strip electrodes for intracranial epilepsy surgery monitoring: pearls and pitfalls”. In: *Surgical neurology international* 4.
- Wang, Jiarui et al. (2021). “Mesoscopic physiological interactions in the human brain reveal small-world properties”. In: *Cell reports* 36.8, p. 109585.

- Wang, Nancy Xin Ru et al. (2017). “AJILE Movement Prediction: Multimodal Deep Learning for Natural Human Neural Recordings and Video”. In: *CoRR* abs/1709.05939. arXiv: 1709.05939. URL: <http://arxiv.org/abs/1709.05939>.
- Wang, Nancy XR et al. (2016). “Unsupervised decoding of long-term, naturalistic human neural recordings with automated video and audio annotations”. In: *Frontiers in human neuroscience* 10, p. 165.
- Wang, Zuoguan et al. (2012a). “Decoding onset and direction of movements using electrocorticographic (ECoG) signals in humans”. In: *Frontiers in neuroengineering* 5, p. 15.
- (2012b). “Decoding onset and direction of movements using electrocorticographic (ECoG) signals in humans”. In: *Frontiers in neuroengineering* 5, p. 15.
- Weiss, Sabine and Peter Rappelsberger (2000). “Long-range EEG synchronization during word encoding correlates with successful memory performance”. In: *Cognitive Brain Research* 9.3, pp. 299–312. ISSN: 0926-6410. DOI: [https://doi.org/10.1016/S0926-6410\(00\)00011-2](https://doi.org/10.1016/S0926-6410(00)00011-2). URL: <https://www.sciencedirect.com/science/article/pii/S0926641000000112>.
- Willett, Francis R et al. (2021). “High-performance brain-to-text communication via handwriting”. In: *Nature* 593.7858, pp. 249–254.
- Wolpaw, Jonathan R et al. (2002). “Brain–computer interfaces for communication and control”. In: *Clinical neurophysiology* 113.6, pp. 767–791.
- Xu, Gaowei et al. (2020). “A one-dimensional cnn-lstm model for epileptic seizure recognition using eeg signal analysis”. In: *Frontiers in Neuroscience* 14, p. 1253.
- Yanagisawa, Takufumi et al. (2011). “Real-time control of a prosthetic hand using human electrocorticography signals”. In: *Journal of neurosurgery* 114.6, pp. 1715–1722.
- Zhang, Honghui and Joshua Jacobs (2015). “Traveling theta waves in the human hippocampus”. In: *Journal of Neuroscience* 35.36, pp. 12477–12487.
- Zilles, Karl and Katrin Amunts (2010). “Centenary of Brodmann’s map—conception and fate”. In: *Nature Reviews Neuroscience* 11.2, pp. 139–145.